

STIF

November 1977

78-10056

LANDSAT

FOLLOW-ON INVESTIGATION PROGRAM

APPROVED INVESTIGATION NO 28990

# INVESTIGATION OF ENVIRONMENTAL CHANGE PATTERN IN JAPAN

(E78-10056) INVESTIGATION OF ENVIRONMENTAL  
CHANGE PATTERN IN JAPAN Final Report  
(Science Univ. of Tokyo (Japan) -) 180 p  
HC A09/MF A01

N78-17429

CSSL 04B

Unclas

G3/43

00056

## FINAL REPORT

Prepared for

The National Aeronautics and Space Administration

Goddard Space Flight Center

Greenbelt, Maryland 20771

U.S.A.

Submitted by

Takakazu MARUYASU

Prof. Science University of Tokyo



STIF

November 1977

98-10056

LANDSAT

FOLLOW-ON INVESTIGATION PROGRAM

APPROVED INVESTIGATION NO. 28990

# INVESTIGATION OF ENVIRONMENTAL CHANGE PATTERN IN JAPAN

(E78-10056) INVESTIGATION OF ENVIRONMENTAL  
CHANGE PATTERN IN JAPAN Final Report  
(Science Univ. of Tokyo (Japan).) 180 p  
HC A09/MF A01

N78-17429

CSCI 04B

Unclas

G3/43

00056

## FINAL REPORT

Prepared for

The National Aeronautics and Space Administration

Goddard Space Flight Center

Greenbelt, Maryland 20771

U.S.A.

Submitted by

Takakazu MARUYASU

Prof. Science University of Tokyo

November 1977

LANDSAT

FOLLOW-ON INVESTIGATION PROGRAM  
APPROVED INVESTIGATION NO. 28990

# INVESTIGATION OF ENVIRONMENTAL CHANGE PATTERN IN JAPAN

FINAL REPORT

Original photography may be purchased from:  
EROS Data Center

Sioux Falls, SD

Prepared for

The National Aeronautics and Space Administration

Goddard Space Flight Center

Greenbelt, Maryland 20771

U. S. A.

**ORIGINAL CONTAINS  
COLOR ILLUSTRATIONS**

Submitted by

Takakazu MARUYASU

Prof. Science University of Tokyo

RECEIVED

JAN 25 1978

SIS/902.6

## Preface

Continued from Landsat-1, a group of specialists in Japan participated in Landsat-2 Follow-On Investigation Program under the theme of "Investigation of Environmental Change Pattern in Japan".

Twelve co-investigators were in charge of research work in each special field, and could drive remarkable results as follows.

Details of each investigation will be represented in following reports.

### Abstract of papers

#### 1. Agriculture

Dr. Hayashi, a specialist of agricultural field, ascertained how the Landsat data can be used to identify existing and changing state of agricultural land use in Hokkaido, where the scale of agriculture is comparatively large in Japan. He has got the results to make the identification of species and ages of grass in pasture and the classification of soil into several types possible. It means Landsat data will be effectively used for the cultivation, reclamation or management of agricultural land from now on.

#### 2. Forestry

Dr. I. Nakajima, engaged in the investigation of forestry, tried to identify how many species the forest trees can be classified by Landsat-data. And, as another topic, he examined the function of forest for maintaining natural environment. In Japan, this function increasingly important in addition to its fundamental function of <sup>Su</sup> applying lumber.

Based on the results of these investigation, he proposed his new idea for the reasonable method of "Forest Preservation Plan".



### 3. Land-use

Dr. S. Murai developed the technique of classification and checked its accuracy. His study deals with a mathematical model for estimating vegetation cover of Tokyo District. Two types of model, multi-regression analysis and parametric model, were tested for the geographically corrected test area. The results obtained conclude that vegetation cover can be well estimated from Landsat MSS data with accuracy of not less than 80 percent.

### 4. Classification of Shoreline

In this study the method of classification of shoreline at the reclaimed land, Ria and sand beach were examined.

Dr. D. Shoji, a specialist of hydrography, had an interest in the detection of the indication of minor environmental changes along the shoreline. He confirmed that Landsat MSS data is more effectively used for this purpose than the observing the topographic map.

### 5. Oceanography

Dr. D. Shoji analyzed the variation in Kuroshio Oceanic Current using Landsat MSS data. Interpreted Data from Landsat MSS data were compared with the oceanographic data directly obtained at the area concerned at that time. It became clear that the Band 4 and 5 can be effectively used to obtain the information as to the sea surface, such as spreading of effluent water, eddy like motion on the boundary zone of oceanic current. He analyzed the eddy pattern offshore Shionomisaki using Landsat MSS data.

### 6. Meteorology and Land-use Classification

Based on the MSS data taken in early autumn by Landsat-1 and 2, Dr. K. Tsuchiya and Mr. Ochiai studied on the environmental change pattern in Central Japan. They confirmed that, at the process of digital analysis of MSS data, the effect of thin cirrus is to be carefully taken into account. In this case, thin cirrus often is hard to recognize visually, but is clearly found in band 4 imagery.

Through these investigations, it was clearly recognized that, for making land-use map effectively with Landsat data, careful correction for atmospheric effects is always unavoidable.

#### 7. Environment of Coastal area

Dr. K. Watanabe, a specialist of oceanography, and Mr. Ochiai, a specialist of data acquisition technology, made a feasibility study for the monitoring of water pollution of sea surface. According to their studies, spreading pattern of effluent, and red tide can be clearly analyzed with Landsat data. Mr. H. Ochiai has studied the change of environmental features about three years. As objects of study, red tide, river effluent, coastal process are included.

Dr. K. Tsuchiya, Messrs. K. Takeda and H. Ochiai studied the change of sea surface condition in Seto Inland Sea and its coastal region, based on Landsat MSS data of three years time lapse.

This study was successfully done by a simple manual photographic method "Equi Density Slicing Method".

#### 8. Fishery

This report elucidates how MSS data is utilizable for fishery on the basis of analysis of same imageries of MSS-4 and 5. This study was conducted by Dr. T. Watanabe, a specialist of fisheries, and its results are most prospective at present in Japan.

This report include two topics. One is concerned with the spawning and nursing area of anchovy, and another is about sardine fishing location.

MSS data provide us with extensive informations about marine environmental condition, and these are closely related with the movement of a school of fish.



## Recommendation

From these investigations, we recommend following items.

(1) Landsat data can be effectively used in the monitoring of environmental change which is intensively concerned with field of industry, agriculture, fishery, forestry etc.

Therefore, it is very desirable these projects to be followed continuously in future.


(2) For the landuse unit in Japan, it is desirable the resolution of MSS data is improved to about one half of present status.

(3) This Follow-On project provided many valuable informations. Through many feasibility studies their useful results were widely demonstrated in Japan.

The construction of ground receiving station is now going on. After the completion of this station, we will be able to use more valuable informations, and apply them more actively to various fields.

## Acknowledgement

It is very grateful for participating these useful projects. Our activity was greatly promoted in this field. I would like to represent my sincere appreciation to NASA and its staffs.



TAKAKAZU MARUYASU

Principal Investigator

Professor Science University of Tokyo

List of Investigators

Principal Investigator: Takakazu MARUYASU  
Science University of Tokyo

Co-Investigator: Hiroaki OCHIAI  
Toba National Merchant Marine College

Yasuhiro SUGIMORI  
National Research Center for Disaster Protection,  
Science and Technology Agency

Daitiro SHOJI  
Hydrographic department, Marine Safety Agency,  
Ministry of Transportation

Kaname TAKEDA  
National Institute of Resources,  
Science and Technology Agency

Kiyoshi TSUCHIYA  
National Space Department Agency of Japan

Iwao NAKAJIMA  
Forest Experiment Station, Forest Agency,  
Ministry of Agriculture and Forestry

Takamasa NAKANO  
Tokyo Metropolitan University

Shigechika HAYASHI  
Hokkaido National Agricultural Experiment Station,  
Forest Agency;  
Ministry of Agriculture and Forestry

Seiji HORIKAWA  
University of Tokyo

Shunji MURAI  
University of Tokyo

Kantaro WATANABE  
Tokai University

Taisuke WATANABE  
Fisheries Agency,  
Ministry of Agriculture and Forestry



Index of papers

	Author	Theme
Agriculture	Dr. Hayashi	Observation of Present State of Agricultural Land-Use by Analysing Landsat data ..... 1
Forestry	Dr. Nakajima	Investigation of the Ecological Environment Index from Observation of the Regional Vegetation cover and their Growing Condition .....15
Landuse	Dr. Murai	An Analysis on Vegetation cover by using Landsat MSS data .....49
Classification of Shorelines	Dr. Shoji	Classification of Shorelines .....61
Oceanography	Dr. Shoji	Investigation of Variations in the Prominent Oceanic Current, Kuroshio..69
Meteorology and Landuse Classification	Dr. Tsuchiya and Mr. Ochiai	Environmental Change Pattern in Central Japan as revealed by Landsat Data .....91
Environment of Coastal Area	Dr. K. Watanabe	General Pattern of the Turbid Water in the Seto-Inland Sea extracted from Multispectral Imageries by the Landsat-1 and -2 .....101
	Mr. Ochiai	Significant Applications of Landsat -2 MSS Data to Marine Environment ..121
	Mr. Ochiai Dr. Tsuchiya and Mr. Takeda	Application of Landsat MSS Data to the Study of Oceanographical Environment .....143
Fishery	Dr. T. Watanabe	Utilization of Landsat-2 Data for Fisheries .....157

OBSERVATION OF PRESENT STATE OF AGRICULTURAL LAND-USE  
BY ANALYSING LANDSAT DATA

'INVESTIGATION OF ENVIRONMENTAL CHANGE PATTERN IN JAPAN'  
(28990)

by

Shigechika Hayashi  
Upland Farming Division,  
National Agricultural Experiment Station,  
Memuro, Hokkaido, 082, JAPAN

## 1. Introduction

In Hokkaido where the scale of agricultural field is comparatively large, wide area observation by LANDSAT has great possibility of effective use for analysing real state and changes of agricultural land.

In this study authors investigated the method of applying LANDSAT data for observing agricultural land in Hokkaido as a part of 'Investgation of Environmental Change Pattern in JAPAN' (28990).

This study was performed by following members: Shigechika Hayashi and Michikazu Fukuhara of Upland Farming Division, Hokkaido National Agricultural Experiment Station; Yoshizumi Yasuda and Yasubumi Emori of Institute of Color Technology Faculty of Engineering, Chiba University; Joji Iisaka of Scientific Center of JAPAN IBM.

## 11. Techniques

From LANDSAT data of agricultural field in Tokachi District:

(1). Ratio image were made by photographic treatment. (2). Digital analysis was performed using the computer. And the results were compared with ground truth data.

### 1. Data used (figure 1)

24 May, 1973, 'Kushiro' (LANDSAT-1), 70 mm B & W film.

11 June 1975, 'Onihiro' (LANDSAT -2), 70 mm B & W film and CCT.

### 2. Channel used and wave length ( m)

4 (0.5 - 0.6), 5 (0.6 - 0.7), 6 (0.7 - 0.8), 7 (0.8 - 1.1).

3. Area used for analysis was overlapped part of both (1) and (2), and this part corresponds to Tokachi District (figure 2).



#### 4. Preparation of ratio images by photographic treatment.

B & W bulk position of 4, 5, 7 bands in the two scenes of LANDSAT data, the one 'Kushiro' (1973) and the other 'Obihiro' (1975), were enlarged to 1:200,000 scale, then the ratio images of 1975/1973 of each band were made.

These images were analysed using slicing instrument (GRAFI-COLOR 905) and difference between two years was extracted.

Process of making ratio images is illustrated in figure 3.

#### 5. Digital analysis using computer.

Digital analysis of CCT of 'Obihiro' (1975) by computer was performed using LARSYS IBM-DCS version program. LARSYS analysis flow is illustrated in figure 4. Results of interpretation were color-displayed finally.

### 1.1. Accomplishment

1. In the season when the data were obtained, the crops planted in Tokachi fields having not grown so much except winter wheat and grasses, authors chose grasses and soils as an object of analysis. Density distribution pattern in the B & W bulk positives of three upland fields, belonging to different soil types, are shown in figure 5.

In this figure; (1). Seasonal difference between May and June is recognized. (2). The order of reflectance intensity among soil types did not change.

2. To extract the change pattern of agricultural fields which occurred in process of time, ratio images were made. Change patterns obtained from ratio images were classified into 5 types as follows:

(1). Changes of land management and use during two years.

(2). Seasonal change of plant growth.

(3). Apparent change produced by difference of relative densities among the subjects in the images.

(4). Influences of looking angle.

(5). And influences of noises, clouds and etc...

The bare-ground produced by reclamation practice was recognized remarkably in the ratio image of band 7 (figure 6 - 8).

3. Digital analysis using computer was performed on the area near Nakaotofuke and Nishishihoro, where the results of ratio image analysis showed remarkable changes of land use.

This area has been markedly changed to bare ground owing to the renovation and establishment of grassland based on the agricultural land reclamation plan.

After clustering analysis a training field was chosen among run-data on the MIS(CCT) tapes, and then statistical values were obtained concerning this region (figure 9). By this treatment 13 classes were identified in this training field: 4 bare ground (A - D), 6 grasslands (E - J), wheat field (K), range (L), Woods (W).

On these statistical values maximum likelihood method was applied and then classification map was made (figure 10).

According to these results, it was considered that in this reclaimed land the main coverage was timothy which had been showed 4 years before and the productivity is not high, because of the infertile soil (A, C) poor in organic matter, and that there were also unreclaimed area.

4. According to the ground truth data, it was proved that in the reclaimed grassland of this area, timothy was dominant coverage and the fertility was poor because of the shallowness of gravel stratum and of deficiency of organic matter.

The plan of application of waste water from the potato starch factory is being realized in this area to enrich the soil fertility.

Unidentified area in the classification map dominantly consisted of unreclaimed land, where the soil surface was covered with mixture of grass and woods.

#### IV. Significant Results

Significant results of this study are as follows:

1. In the Plains of Tokachi, where the scale of agricultural field is comparatively large in JAPAN, LANDSAT data with its accuracy has proved to be useful enough to observe the actual condition of agricultural land-use and changes more accurately than the present methods.
2. Authors could identify the species and ages of grasses in pasture and classify the soils into several types, using LANDSAT data. Therefore, LANDSAT data feasible in the application to wide area planning of cultivation, reclamation or management on agricultural land.

#### V. Publications

M. Fukuoka, S. Hayashi, Y. Yasuda and Y. Emori: Multitemporal Analysis of Agricultural Land using LANDSAT Data, Proceedings of the 1977 Meeting, JAPAN SOCIETY OF PHOTOGRAMMETRY, May 1977, pp. 73 - 74.

#### VI. Problems

For practical use, following problems should be solved:

1. Periodical data acquisition suitable to special climatic condition in JAPAN.
2. Resolution suitable for the scale of agricultural field in JAPAN.
3. Reducing the time of data acquisition.

4. Establishment of techniques for analysis and application suitable for agriculture, which has various local characteristics.
5. Accumulation of analytical case studies on agriculture.

#### VII. Data Quality and Delivery

No.

#### VIII. Recommendations

No.

#### IX. Conclusions

From the results of the analysis, LANDSAT data proved to be feasible to detect the actual condition of land use, namely, the changes of agricultural lands, grassland management and etc... When timely information is available, LANDSAT data will be useful for remote sensing to study such large scale agricultural fields as in Hokkaido from the wide viewpoint.

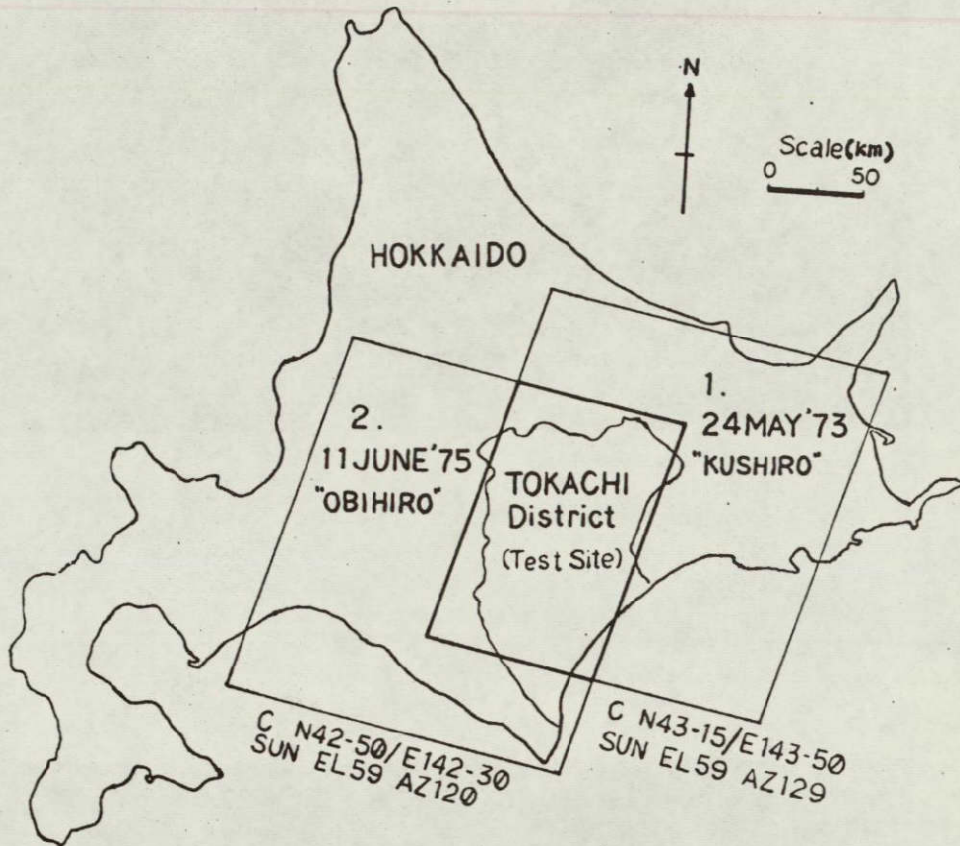


Figure 1. Observed area in the seanes used.



Figure 2. Photographs of analysed area (Tokachi District).



(1). 24 May 1973, 'Kushiro', band 7 image.

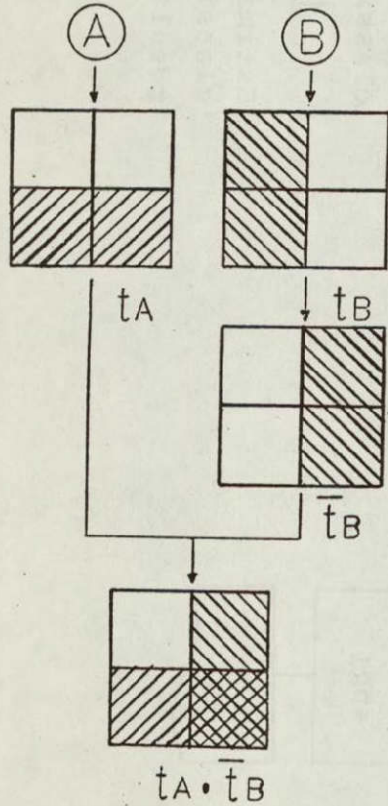


(2). 11 June 1975, 'Obihiro', band 7 image.

ORIGINAL PAGE IS  
OF POOR QUALITY



Figure 3. Process of preparing ratio images.



Let the negative density of image A, B be  $D_A$ ,  $D_B$ , respectively, and let the positive density of B be  $D_B^*$ . Density of superimposed image of negative A on positive B, i.e.  $D_{AB}$ , becomes

$$D_{AB}^{\gamma} = D_A + D_B^* = D_0 + D_A - \gamma D_B \quad \dots\dots\dots(1)$$

where  $D$  is density of constant level.

When

$$\gamma = 1$$

$$D_{AB} = D_A - D_B \quad \dots\dots\dots(2)$$

then

$$D_A = -\log(\bar{r}H)_A^{\gamma A} \quad \dots\dots\dots(3)$$

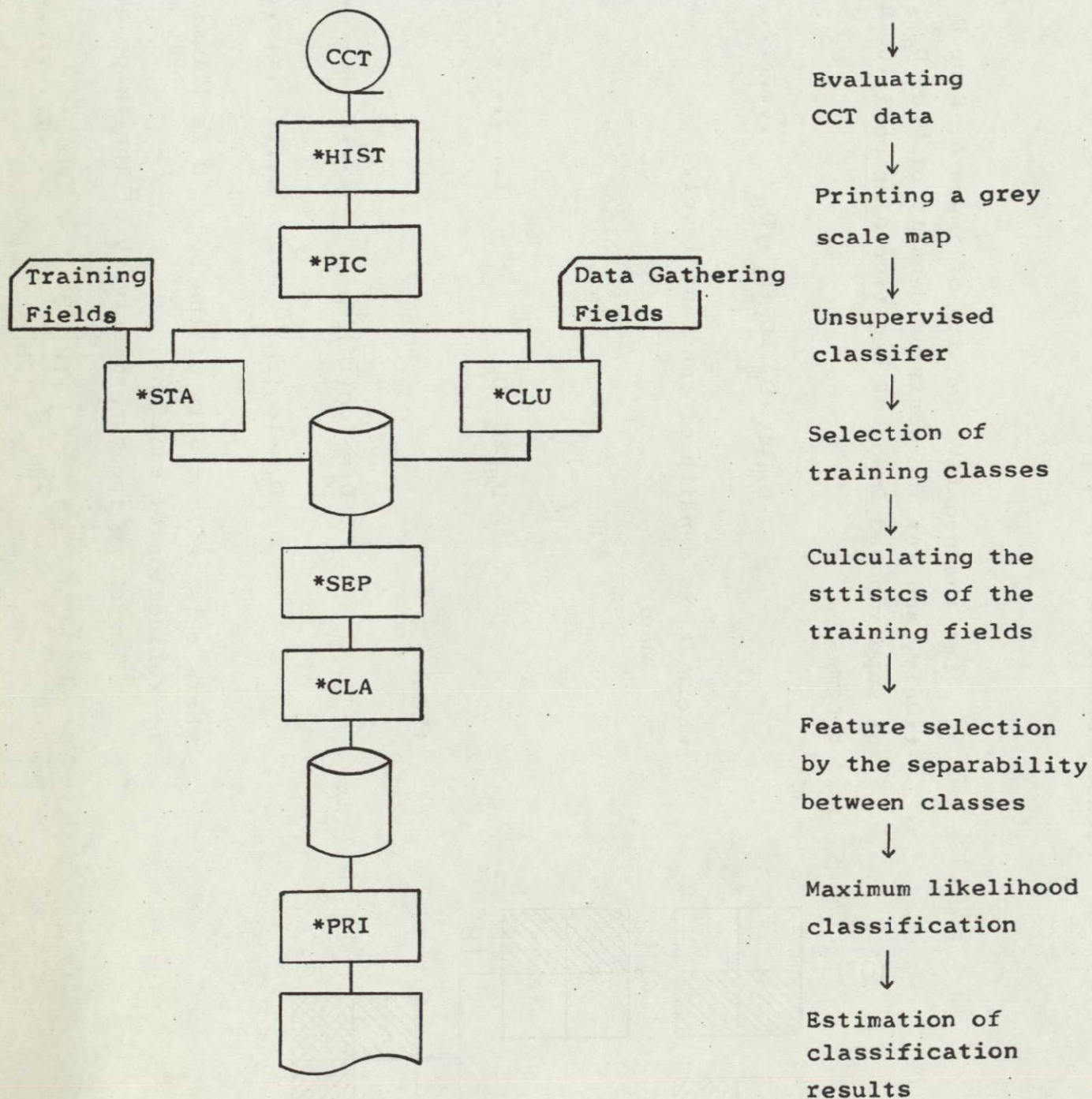
$$D_B = -\log(\bar{r}H)_B^{\gamma B} \quad \dots\dots\dots(4)$$

where  $r$  is reflectivity of the body,  $H$  is illumination intensity of reflection of sunlight.

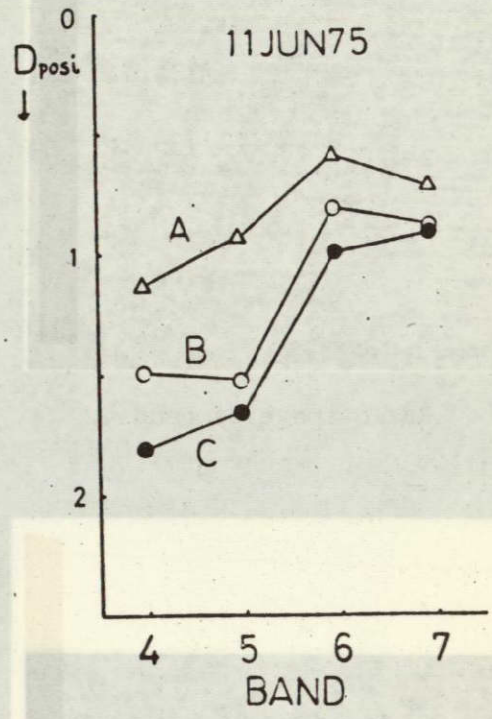
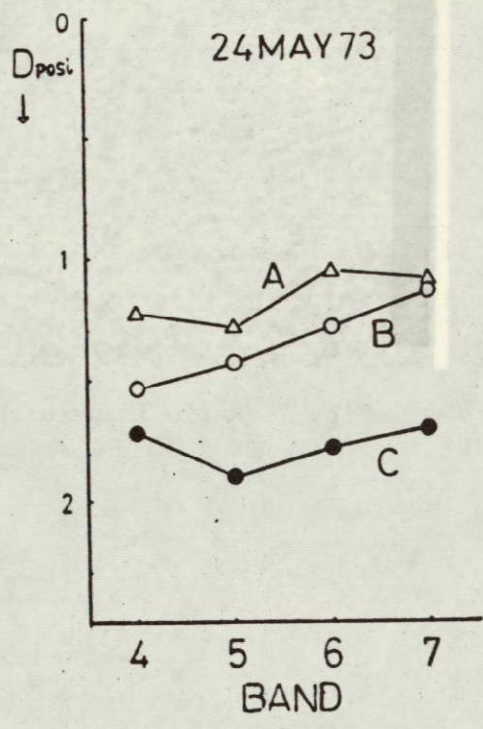
Therefore the transmissivity of the image obtained is

$$T_{AB} = \gamma \frac{[\bar{r}H]_B^{\gamma B}}{[\bar{r}H]_A^{\gamma A}} \quad \dots\dots\dots(5)$$

Figure 4. Digital analysis flow.







ORIGINAL PAGE IS  
OF POOR QUALITY

Figure 5. Density distribution patterns of different soils determined by B & W positives. (1973, 'Kushiro', 1975, 'Obihiro')





Fig. 6 Ratio image of band 4.

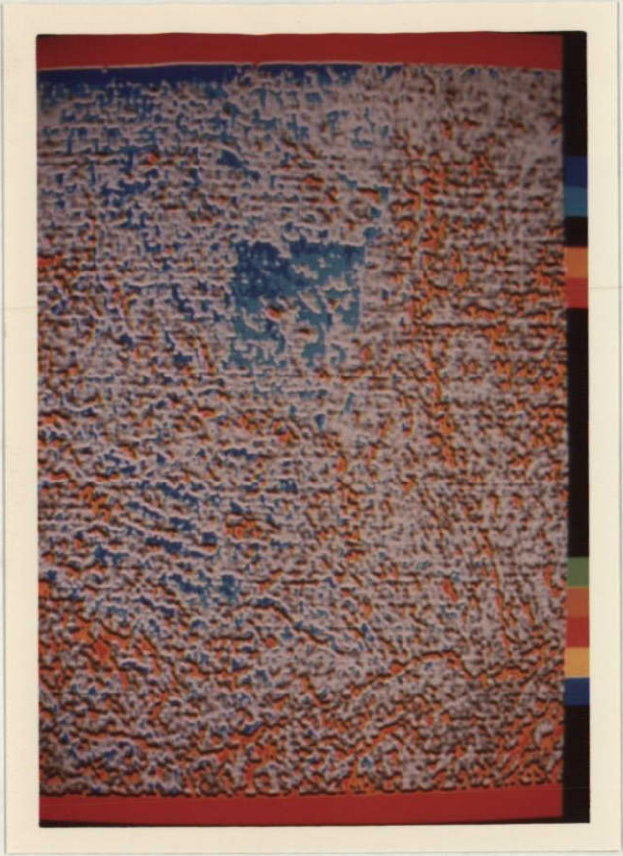


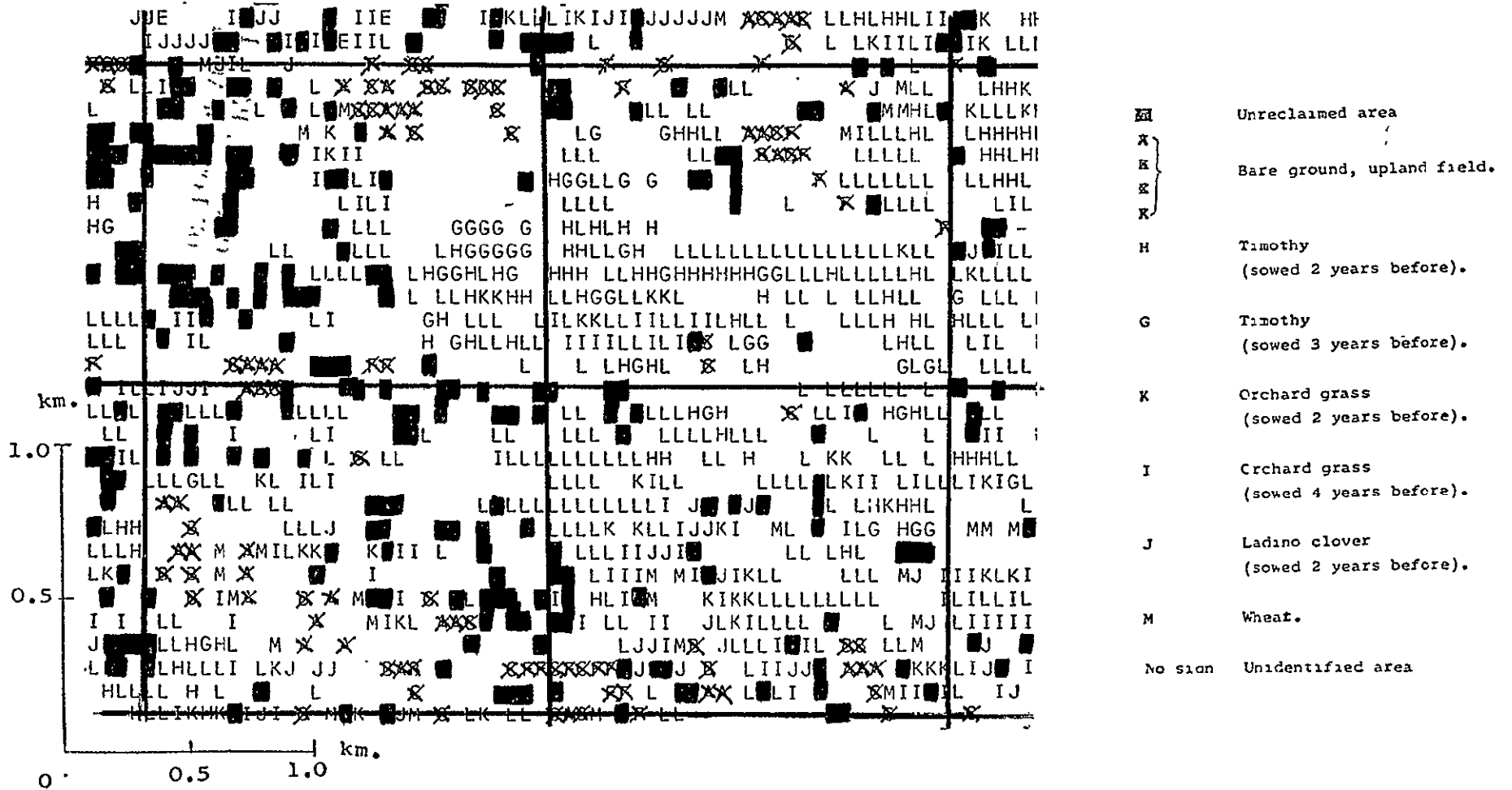
Fig. 7 Ratio image of band 5.



Fig. 8 Ratio image of band 7.

ORIGINAL PAGE IS  
OF POOR QUALITY

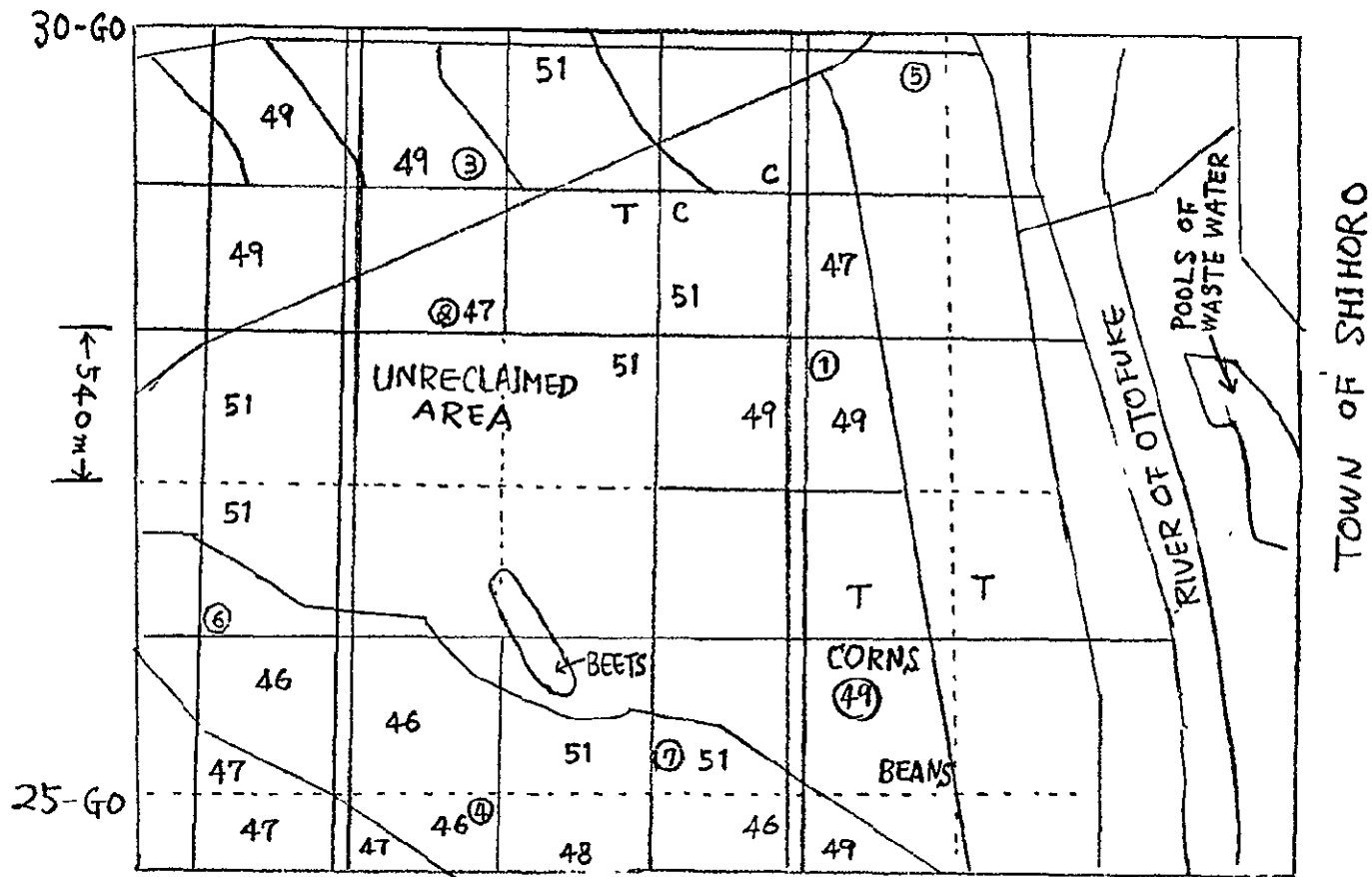
Figure 10. A part of classification map of reclaimed land used as a test field. (Discrimination rate of training field is 87.5 % as a whole.)



ORIGINAL PAGE IS OF POOR QUALITY



Figure 11. Ground truth data.



C.....Red clover.

T.....Timothy.

46-51....Years when timothy was sowed.

1 - 7 ...Experimental fields on applying potato-starch's  
waste water by YOSHICKA et al..

Investigation of the Ecological Environment Index from  
Observation of the Regional Vegetation Cover and their  
Growing Condition

Dr. Iwao Nakajima

Government Forest Experiment Station  
Ministry of Agriculture and Forestry

I. Introduction

The purpose of this study is to confirm that LANDSAT data can be effectively used as the fundamental information source of the regional exploitation and conservation planning. As the first step of this work, the tests of the land cover and land use discrimination using LANDSAT data were executed.

This report include some significant results of this study:

1. Determination of discrimination level of the land cover and land use using LANDSAT data in Japan.
2. The use of the theme extraction map of the vegetation growth and land use type for natural environment survey.
3. The effective use of the digital categorization for the actual vegetation map making.
4. The natural conservation planning of the north Kanto area(1500 km<sup>2</sup>) using LANDSAT data.

The respective advantages of the survey techniques depending on the LANDSAT data, air-borne data and the field survey were made clear through the research. And also the system of the inventory and survey for environmental quality were basically examined. From these works, we realized that LANDSAT data will become to play the leading part in the environmental survey work in future. This research is continuing for the aim of the operational use.

**PRECEDING PAGE BLANK NOT FILMED.**

14  
**PRECEDING PAGE BLANK NOT FILMED.**

## II. Techniques

### II-1. Research for basic acknowledgement of the environmental information.

"Plate 1" shows the whole view of Japan Island composed of 65 different imageries of LANDSAT-1 and -2. These were chosen from the imageries of least cloud/snow covers. The infrared color composition and the mosaic work were done by the Photogrammetry Laboratory of Forest Experiment Station. The color tone of each plain or forest area is not uniform because of the seasonal difference.

The image shows that Japan Island is covered by the mountainous forest up to about 70%, also flat areas are cultivated intensively, and in each flat plain many dense urban areas can be seen as blue color tone. The urban occupies about 2% of the whole area of Japan. However, more than 60% of the total population gathers in these limited parts.

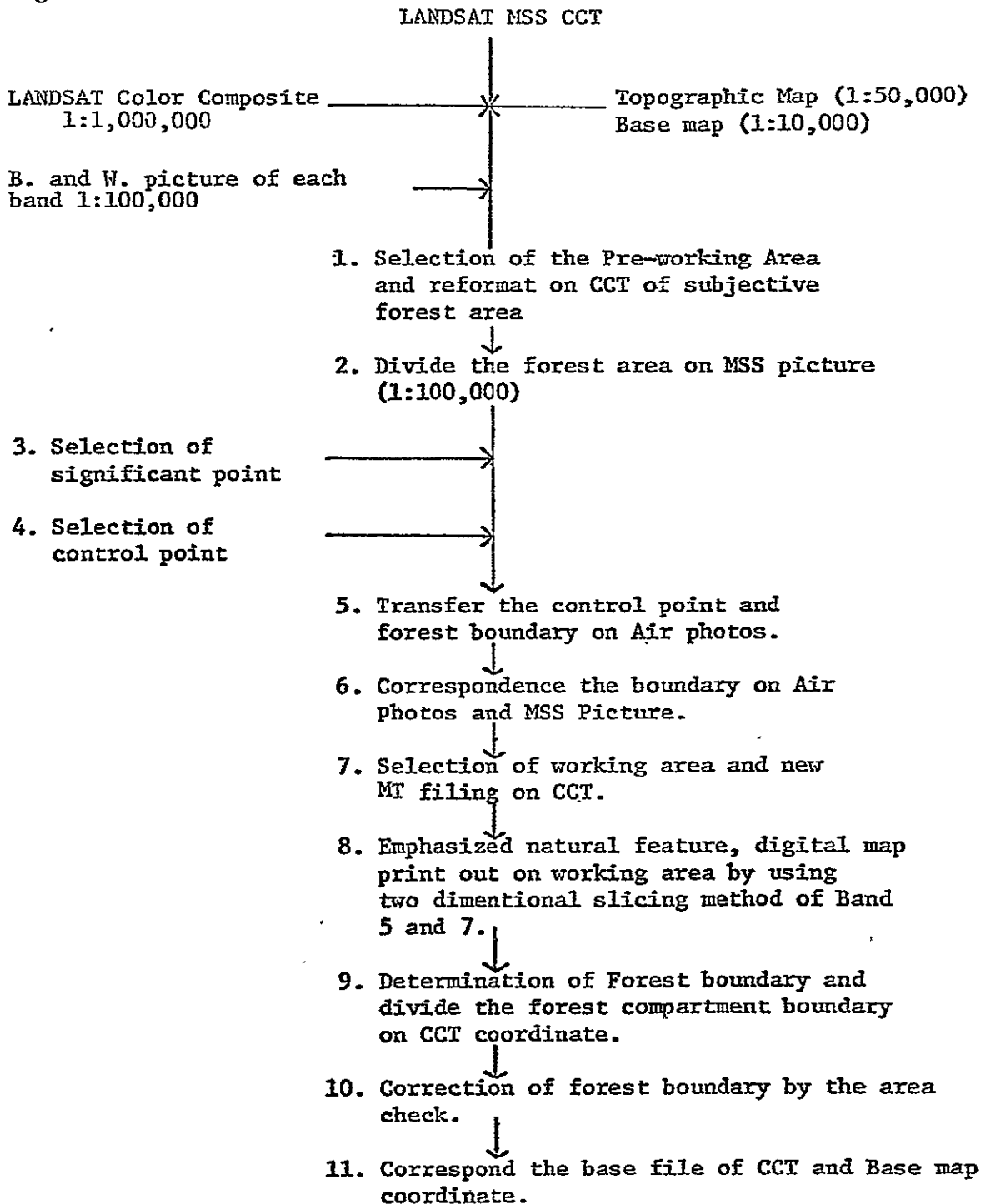
On the enlarged picture, it can be seen that the coastal zone near large cities is covered completely by the artificially constructed area. Many whitish dots representing bare soil where new construction work is going scatter in the mountain foot zone. The rapid change of pattern of the natural environmental condition of Japan Island is a good example which explains the fact that the ecological environmental quality can be evaluated by the rate of artificial change of natural landcover.

The environmental information can be obtained through the analysis of change pattern of.....

1. The physical condition.
2. The coverage pattern.
3. The human activity.

The physical condition of item 1 is mainly composed of topography, geography and climate. These factors are quantitative. In Japan the information of these items can be easily obtained from various kinds of map and other data. The coverage pattern of item 2 is represented by rather qualitative factors such as forest type, grass land type, bare soil ratio, residential cover and other natural and artificial land surface type. The LANDSAT data are the most effective information sources for this item.

Fig. 1



The human activity pattern of item 3 can be partly interpreted by the land cover. But the sociological information such as national or local census data which are also important for evaluating these items must be secured from other sources.

The following techniques were applied to these LANDSAT data analysis...

1. Photogrammetric interpretation of the mono-chrome and color-composite pictures of LANDSAT-1, 2.
2. Making of the theme map of the vegetation types and the land use by the photographic procedure.
3. Digital classification by man-machine system (M-das, Image 100 and others)

The multi-altitude air borne data by air camera and MSS and also the field survey data were widely used for the purpose of accumulating the training data and checking the results of LANDSAT data analysis.

## II-2. Classification

The results of the LANDSAT data classification of land cover were checked at the following 5 different type test area, i.e. suburb of large city, agricultural land, forestry national park, eroded mountain and industrial area. The results of classification were compared with the interpretation results of airphoto and the conventional vegetation type maps.

In these cases, each LANDSAT-CCT was transformed to map after geometric coordinate registration was done by three dimensional formula with the accuracy of one pixel.

Through this work it was ascertained that a procedure shown in Fig 1 could be effectively applied and to keep the correspondence between LANDSAT -CCT data and the map for narrow forest area of the test site.

For this transformation 32 control point were selected in accordance with following condition.....



Table 1. Accuracy of Coordinate Transformation

Map(X,Y)			MSS CCT(X,Y)	
$X = \sum_{i=0}^{nm} a_{ij} x^i y^j$			$x = \sum_{i=0}^{nm} A_{ij} X^i Y^j$	
$Y = \sum_{i=0}^{nm} b_{ij} x^i y^j$			$y = \sum_{i=0}^{nm} B_{ij} X^i Y^j$	
n = 1, 2, 3, 4,				
Order	M <sub>x</sub>	Max <sub>x</sub>	M <sub>y</sub>	Max <sub>y</sub>
1	47.2 <sup>m</sup>	123.2 <sup>m</sup>	36.6 <sup>m</sup>	73.4 <sup>m</sup>
2	42.7	95.7	37.9	80.0
3	43.7	91.9	36.0	81.1
4	46.1	84.3	38.8	73.1
Order	m <sub>x</sub>	max <sub>x</sub>	m <sub>y</sub>	max <sub>y</sub>
1	0.77	2.30	0.48	1.08
2	0.68	1.29	0.50	1.14
3	0.67	1.25	0.50	1.17
4	0.67	1.06	0.56	1.03

1. Mountain peak where clearly changed from dark to light.
2. Boundary of the bare soil and vegetation coverage, that is, the clear edge of cutting forest stand, farm field.
3. The artificial marks in the forest.
4. The clear points in the river bed.

Table 1. shows an example of the accuracy of the map coordinate transformation in the forest area. From this, only applying the 1st. order transformation gives good results for practical use if we can use sufficient number of control point, as in this case.

The linear function classification method, maximum likelihood method and Maharanovis distance method were applied for the vegetation pattern categorization.

The histogram of the 4 MSS bands of the training area were used to find the basic classification patterns. Then the spectral signature of each band was obtained as their average vector of their spectral groups. Also

the cords of classifications obtained from the land use survey were combined. The spectral signature of each class is composed of a set of 4 values of the individual materials on the ground. The similar spectral signature of each class joins together. Then results of the pattern categorization were coincide satisfactorilly in wide view point but many differences exist in detail if it were compared with the surface truth.

Table 2. A Example of the Test Results of Pattern Identifications by total 437 Systematic check points.

Conventional Survey	1	2	3	4	5	6	7	8	9	10	% Coincide	
LANDSAT												
Soft Wood F.	1	60	20	1	1	0	0	0	0	82	73.2	
Hard Wood F.	2	18	29	2	2	0	0	1	0	3	52.7	
Orchard.	3	11	3	21	8	0	1	1	1	3	42.9	
Farm.	4	3	5	6	33	8	9	2	0	10	76	43.4
Residential.	5	5	4	4	20	22	17	3	0	6	81	27.1
Dense Urban.	6	1	3	0	6	5	25	1	2	14	57	43.9
Park.	7	2	5	0	1	1	1	4	0	3	17	23.5
Under Const.	8	0	0	1	1	0	2	1	0	1	6	0.0
Others.	9	3	2	1	1	0	5	1	0	1	14	7.1
Total	10	103	71	36	73	36	60	14	3	41	437	
% Coinside		58.3	40.8	58.3	45.2	61.1	41.7	28.6	0.0	2.4		

Table 2. shows an example of the accuracy of classification in case the maxmum likelihood method was simply applied at the city suburb area. In this table we can see the accuracy of the classification to surface survey becomes only 43.7% on the average. The classification was done 9 items as soft wood forest, hard wood forest, orchard, agricultural land, residential area, densely build-up area, park, the area under construction and others. The best results is only 60% coincide in the category of soft wood forest. This is probably due to the fact that those classes having similar signature

of the land cover or the land use are grouping to the main categories such as forest, farm or densely build-up urban area.

The classification error is mainly due to the following reasons.....

- (1) The incorrect recognition of several tens pixels in a uniform.
- (2) Classification of area composed of more than 2 classes in the pixel unit, especially in such a case of residential area more than 30% of which is covered by vegetation or the park area.
- (3) Classification of the area covered by similar land cover with the several pixels.

These errors occur mainly from following cases.

Error 1: From the miss recognition by shadow influence caused by topographic feature.

Error 2: From the difference of the size between a classification unit area and the corresponding pixel. These errors will decrease by adding the air-borne data for reference.

Error 3: Mis-classification of the area which were composed of special surface condition such as the under construction area containing bare soil, grassland, swampy bush, river bed etc. In those cases, more conventional survey will be needed.

Another example can be shown as the accuracy of the categorization. It becomes clear that only 3 forest types inside the sunny side are classified well even in the most complicated area. This is confirmed by comparing the analyzed groups with the truth acquired by ground survey for 10 groups of spectral signature on each training area. The rest was classified as the threshold of the shadow influences.

It is understood that in order to improve the accuracy of categorization, the research for the shadow effect and the selection of classification category is most important especially in the mountaneous area.

From above studies, it can be said that the accuracy of categorization will be uprised more than 50% if the topographic data are well taken in account in the classification process.

### II-3. Land cover and land use discrimination level using LANDSAT data

LANDSAT data basically inform us of the land cover information by means of the electro magnetic reflectance. And in some cases, we need not only the informations of the actual land use but their future changes in each areas which will be resulted from potentiality, human activity and the ecological and bio-environmental condition. Even if LANDSAT data can not catch these information directly, we can assume the major part of them from their physical and geographical characteristics.

To obtain the actual information of the land use in more detail, it is desirable to combine the other kinds of information, like as bio-environmental condition and air photos etc, especially in case of intensively complicated land use area as in Japan.

Table 3 shows the detail of Work Step to classify land cover using LANDSAT data and ground survey data.

Level 1-4 are the groups which can be automatically classified by LANDSAT data only.

Level 5 is the groups which are recognized by combining LANDSAT data with air photos data.

Level 6 is the group basically depending on conventional information besides air photo data and some seasonal informations.

In other words, "Level 1-4" are the levels to be recognized with use of the spectral classification technique. "Level 5" is the level combining LANDSAT data with photographic data. "Level 6" is the level combining the results of direct observation with LANDSAT data.

In our case land use classification work was done using 3 different stages shown in Table 4 according to data size resolution.

Therefore, for the area which is composed by small unit of land use like Japan, it must be carefully considered that information obtained from LANDSAT data is not the pure data, but the composite one of the same area. But this method is very effective because of rapid and correct preparation of statistical data, especially when we ask for general aspect of wide region.

Table 4. Relationship between unit area size and resolution

Level	Unit area size	Use
I	1000-500 m mesh (Resolution 100 <sub>m</sub> - 50 <sub>m</sub> )	Regional planning Vegetation naturality etc...
II	400-200 m mesh (Resolution 50 <sub>m</sub> - 20 <sub>m</sub> )	Forest inventory. Basic management plan Land faculty survey
III	100-50 m mesh (Resolution 20 <sub>m</sub> - 10 <sub>m</sub> )	Agriculture productivity. Forest management. Road construction. Ecological survey, Vegetation growth and damage, etc.

Land use level in Japan are as Table 5. In this table, LANDSAT data offers effectively the information with the accuracy of 90% in case of "Level I" and from case of "Level II" from 70% to 80%.

#### II-4 Theme Extraction Map Making

"Plate 2" shows the land cover interpretation by LANDSAT color composite picture of Dec. 15, 1972, of Mt. Fuji area. That was classified in 9 classes that is, 4 coniferous forest, deciduous forest, field, farm or range, bare soil and water surface.

Some data were interpreted from the LANDSAT color composite of Feb. 25, 1972. Unfortunately we could not get better images of LANDSAT-2 in same area. "Plate 3" shows a example of theme map of that area. This was made from the 4 bands negative and positive films of two sceneries, by means of slicing to 10 steps density by the photographic procedure. Each class was extracted according to the pre-determined spectro signature of 4 bands of one scenery. The theme extraction map was separately printed on the seven transparent films.

The percentage of coverage was used as the classification index of category.

1. Vegetation coverage over 70% :..... Forest, Grassland, range
2. from 70 to 40% :..... Agricultural area
3. less 40% :..... Residential, Urban, bare soil



Table 3. Land Cover Identification Level by LANDSAT

Condition A : A.D.P.(Spectral)  
 " B : + Air photos(Graphical)  
 " C : + Other information

Vegetation, Water	Dry Wet	Object	Land Cover Condition A:	Land Cover and Use Condition B:	Land Use Condition C:
Level 1(A)	2(A)	3(A)	4(A)	5(A+B)	6(C)
Vegetation	Dry	Grass (Grass Land)	Dark Light Tall Low	Farm Crop. Vegetable. Range Lawn Wild grass	Range City park Cemetery Cutting area Ground Rest farm Garden Reclamation River bed
		Tree (Forest)	Dark Coniferous Light Evergreen Deciduous Mixed Bamboo	Planted Forest Natural Forest Orchard	Forest type
		Grass and Tree	Dark Light Tall Low	Natural Farm Planted Farm Bush Shurub	Range Reclamation Tea Cutting area Sabanna Mulbery Rest farm Park Nursery Garden
	Wet	Grass (Wet Grass Land)	Dark(Dense) Light(Poor)	Water grass Paddy Farm Wet land	Peat Fish pond Low Land Lotus Horse radish Seed bed
		Tree (Forest)	Dark Light	Mangrove forest	
		Grass, tree	Dark Light		

Non Vegetation	Dry	Construction (Artificial)	Urban area(Dense) (Open)	Building Dike Road Air port Rail way Pavement Bridge Harbor	Residential Dike House Factory Parking Park Ground Dam site
		Natural	Bare soil Gravel Dry grass	Reclamation Sand hill Dike Paddy field Road Farm "	Reclamation Cliff Ground River bed Dam
	Wet	Construction (Artificial)		Culture raft	Habor Culture raft Mole
		Natural	Bare soil Gravel Dry grass	Sea shore Paddy field	River bed
	Water		Water Clear Impure	Lake Flood Pond Sea River Harbor	Drainage
	Others		Snow Ice Cloud		

Table 5. Land Use Identification Level from Remote Sensing Data.

LANDSAT Resolution : 60m x 70m Mesh : 500m Map scale : 1/200,000	LANDSAT High Altitude Air Craft Resolution : 25m x 25m Mesh : 200m Map scale : 1/50,000	High and Low Altitude Air Craft Resolution : < 5 m Mesh : 50m Map scale : 1/25,000 to 1/10,000
Level I	Level II	Level III
Town (Artificial construction)	Residential	High Density Town Low Density Town Residential Construction Village Others (School etc.)
	Factory	Factory
	Special equip	Athletic field Others (Tank, Green house etc.)
	Road	Auto road Main road Other road
Agriculture	Paddy field	Paddy field
	Farm	Farm Others (Tee Mubel Nusery etc.)
	Grass Land	Range Lawn Wild grass Shrub Wet grass
Forest	Coniferous	Artificial forest Natural coniferous
	Hard Wood	Ever green forest Deciduous forest
	Mixed	Mixed forest
	Others	Orchard Other forest

	Rock	Lava Stone factory Rock
bare surface	Gravel	Volcanic ash Gravel Other sandy
	Soil surface	Reclamation Under construction Open area
	Others	Dry grass Wet land
Water	River, Drainage	River, Drainage Lake, Pond Artificial pond, pool
	Sea	Sea
Snow	Snow	Snow
Ice	Ice	Ice
Cloud		
Shadow		

The density difference of the band 4 and 5 was effectively used in case of classifying the artificial constructions and bare soil area.

Volcanic rock area such as Mt. Fuji and water surface were extracted as the infrared absorbing area. The snow cover area has very strong reflectance in every 4 bands. The vegetation cover area difference between autumn and winter can be used as the index of the detail identification of the coniferous and the deciduous forest types, grass land and farm field also the fir (*Abies*) and spruce (*Picea*) tree series in the coniferous forest. "Plate 4" is a same example of land use theme extraction map made from 4 season LANDSAT images in Toyama prefecture (located in north side of middle part of Japan). (illustrated on Plate 1).

Seasonal change of the color image were as follows : .....

- 1) Deciduous forest, grass and farm field changed their tone time to time by their seasonal vegetation growth mainly affected by water contents of land surface. Especially remarkable difference was recognized between May 10 and May 25 scaneries.
- 2) The farm field expressed their seasonal change according to their cultivation works.
- 3) The infrared reflection values of the new leaves in the spring was extremely high and difficult to classify the forest types. By deducting the coniferous forest area classified on the winter images from the spring images with all vegetation cover the grass and deciduous forest area was extracted.
- 4) The distribution of the paddy field was clearly extracted as the water surface cover area using the imageries of the early planting season.
- 5) The artificial construction and urban area was classified as the area having the larger reflection difference in band 5 and 7 in the imageries of fall and winter.

The average value of density in band 5 and 7 for some categories is shown by Table 6.

Theme extraction work was carried out with referring the displayed

images on multi-data color system 4200. This method was very economical and practical as compared with the digital processing way.

Table 6 Average density of the different seasons  
(Band 5 and 7)

Date	73.5.10		73.5.25.		72.10.5.		72.12.6.	
Band	5	7	5	7	5	7	5	7
Forest	1.0	4.55	1.03	8.33	0.74	3.23	0.84	2.22
Paddy	1.67	0.52	1.49	0.57	0.81		1.00	0.73
City	1.05	0.40	0.95	0.39	0.78	0.29	0.85	0.58

### III. Accomplishment

#### III-1. The natural environment condition of Mt. Fuji area.

Mt. Fuji srea is located in national park zone and is expected to be kept in strict conservation of the natural ecological conditions.

Each class of the land cover was measured as Table 7 from the theme extraction map.

Table 7 Land cover percentage of Mt. Fuji

Conifer	Deciduous	Wild	Low grass	Bare soil	Water	Shadow
46.6%	11.8%	4.3%	20.5%	5.8%	2.1%	8.9%

It was estimated from this results that about 69% of the whole area is the area where is keeping the natural environmental condition as agriculture, industry, urbanization etc, and about 46 % is the coniferous forest zone. Fortunately, it was confirmed that fir (Abies), spruce (Picea) and pine forest are keeping their natural environment in specially high degree.

Judging from the detail, it can be said that south west side of Mt. Fuji is covered about 60% by natural coniferous forest and about 40% by artificial larch plantation and wild grass. And north east side is covered by low grass as the bush vegetation zone appears among pine forest, and

there bushes gives undesirable effects on ecological condition of the wild forest of hemlock (*Tuga diversifolia* Masy.) at Aokigahara.

Changes of the environmental condition have been caused by road construction work. Natural environment of the low grass zone was also heavily disturbed by the road construction.

From the whole view of the land cover classification by space data, it was found that the 46% of this area is now exposing against the future environmental destruction and about 25% is too heavily destroyed to recover the native environmental quality by itself.

These results were reported to the Natural Environment Conservation Committee of the Environment Agency in March 1971.

III-2. The actual vegetation map making by the digital classification

"Plate 5" shows the vegetation classification display of north side area of Mt. Fuji. By using the training data on the color composite and also by the field checking the identification of 26 classes was made by M-das.

The boundaries of the actual vegetation map made by the conventional method were over-laid for correcting. Table 8 shows color allocation for the classes. "Plate 6" shows the enlargement of a part of the above image representating classification of the pine forest and fir forest (*Abies firma*). The IR air photograph is attached for refference (Plate 7).

The LANDSAT data was very useful for improving the accuracy of the conventional mapping results. It was expected that the boundaries and the locations of the vegetation classes were to be in some extent.

The application of LANDSAT data will reduce considerably the cost and time for vegetation map making with higher accuracy.

III-3. The natural conservation planning with LANDSAT data in North Kanto.

In Japan, forest has an important function for maintaining natural environment in addition to its fundamental function of supplying lumber resources. However this function is decreasing at present. Therefore it has become necessary to take every effective procedure to maintain and increase this function of a forest.

Table 8 Legend of the classification

4	Fir	(Dark green)
5	Hemlock	(Green)
6	Alder	(Reddish)
9	Beech	(Brown)
14	Red pine	(Light green)
20	Oak (34)	(Yellow)
21	Birch	(Dark yellow)
22	High grass	(Blue)
23	Lawn	(light blue)
40	Sugi	(Dark green)
41	Lach	(Copper green)
44	Orchard	(Light yellow)
47	Farm	
49	Paddy field	(Red)
51	City	
52	Water	(Dark blue)
53	Bare soil	(White)
	Snow cover	(Black)

In the function of maintaining natural environment there exist many factors. Each factor has complicated relation to human life. Therefore when we consider the function of forest, we must take account of a relationship between social status and a forest in each area.

The main object of this research is to make a plan to distribute a forest more properly not only for the purpose of maintaining the function of forest, but also for increasing the function of a forest through combination of social factors with its detailed information.



(1) Procedure

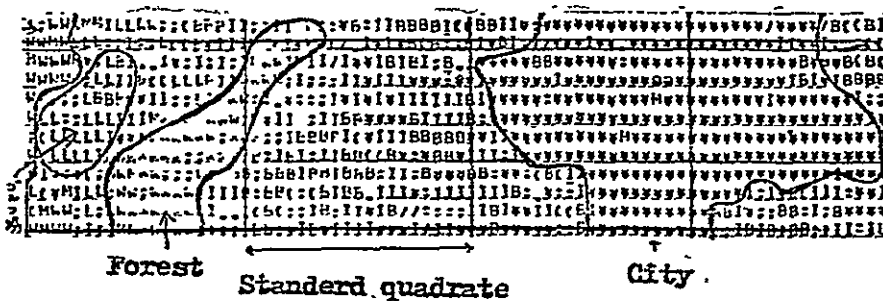
The work of analysis was done by following procedures.

- 1) The area of North Kanto having about 7,500 km<sup>2</sup> was selected as a training area. (illustrated on Plate 1). The whole area was divided into about 2 km rectangle mesh. Based on the LANDSAT data the percentage of wooded area was computed. In this case, as wooded area and grass land can be clearly classified, grass land was executed.
- 2) The census data were used as the data of population in each mesh. Topographical map was further used to decide whether the mesh belongs to mountainous region or not.

(2) Basic network and analytical data sources

The total number of the quadrates was determined as 1972. Each quadrate has 2.25 km x 1.85 km square and contains 4 geometric standards in it. By the digital information of LANDSAT CCT, the types of land use were recognized in 14 classes as Table 9 dividing the standard quadrate into 1/20 x 1/20 quadrate. These result was printed out by 4 bands spectro signature for the classified categories as Fig 2.

Fig. 2 An example of the LANDSAT data out put



The 14 classes was adjusted to items as Table 10. Mainly the air photos were used for the confirmation and the correction of these recognition. The other reference data are also shown in Table 10.

Table 10 Pattern recognition class by LANDSAT-CCT of North Kanto

1	Water(1)		Clear
2	Water(2)		Muddy
3	Forest		
4	City		
5	Bare soil		
6	Grass		Lawn
7	Farm(1)	} ———	Paddy
8	Farm(2)		
9	Farm(3)	} ———	Corn
10	Farm(4)		
11	Farm(5)	} ———	Vegetable
12	Farm(6)		
13	Farm(7)		
14	Others		

Table 11 Quadrate information

1	x coordinate	Vegetation map	16	Population	Census
2	y coordinate		17	Dynamic Po.	
3	Artificial F.		18	1st Indust. Po.	
4	Natural F.		19	2nd Indust. Po.	
5	Orchard		20	3rd Indust. Po.	
6	Grass		21	Forest labor	
7	City green		22	Agrical. labor	
8	City		23	Agrical Family	
9	Forest	LANDSAT	24	Terrain	Map
10	Artificial Ve.		25	Elevation	
11	Urban		26	Valley density	
12	Non Vegetation		27	} Regional plan	
13	Lawn		28		
14	Water		29		
15	Others		30		

(3) The results of the data recognition and analysis of the area

1) Present condition of vegetation growth in North Kanto.

North Kanto area is covered by 38% of the forest class, 50% of the other vegetation growth area.

But the distribution pattern of the forest and the population is not uniform. The land use analyzing work into 3 categories such as forestry, agricultural and urban was done by the computation of linear function method in order to make the relationship between land use and vegetation growth clear. The classification function are determined using selected 243 samples quadrate data of LANDSAT. As the variants of this calculation, following 12 items such as forest, artificial grass cover, population, dynamic population, 1st, 2nd and 3rd industrial employment population ratio, agricultural population, families, terrain feature elevation and vally density were used for each sample quadrate.

The correctability of this zoning was 98.8% in forestry and agricultural area and 97.6% in urban area. According to this result, the zoning map was drawn and the area was measured 42% as forestry, 45% as agricultural and 13% as urban area.

From this zoning results, it was found that 65% of the urban zone has only less than 5% of forest coverage.

It means the forest area is remarkably decreasing in the flat area of North Kanto.

2) The evaluation of the land resource functions.

The erosion danger grade was classified in 4 stages by the settled 9 categories within the forest cover percentage and type, topographic feature and the population as shown in Fig, 3 and mapped as Fig. 4.

Using the samely technique the flood danger grade map and the water shade potentiality map were drawn.

Fig. 3 Erosion danger grade classification

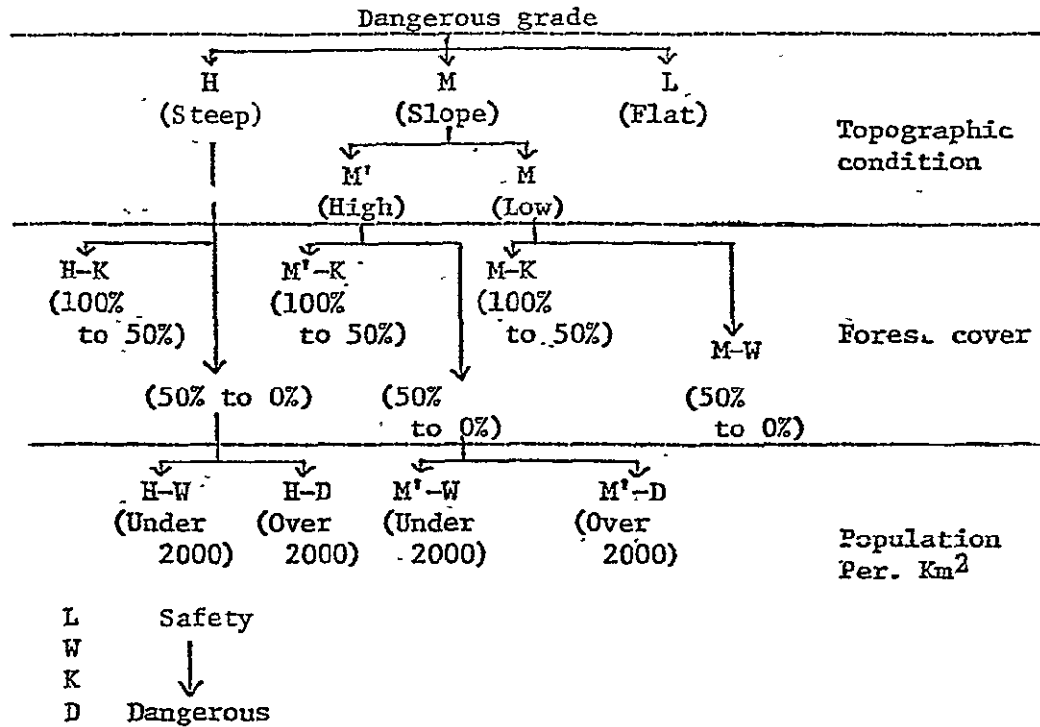


Fig. 5 Timber productivity classification

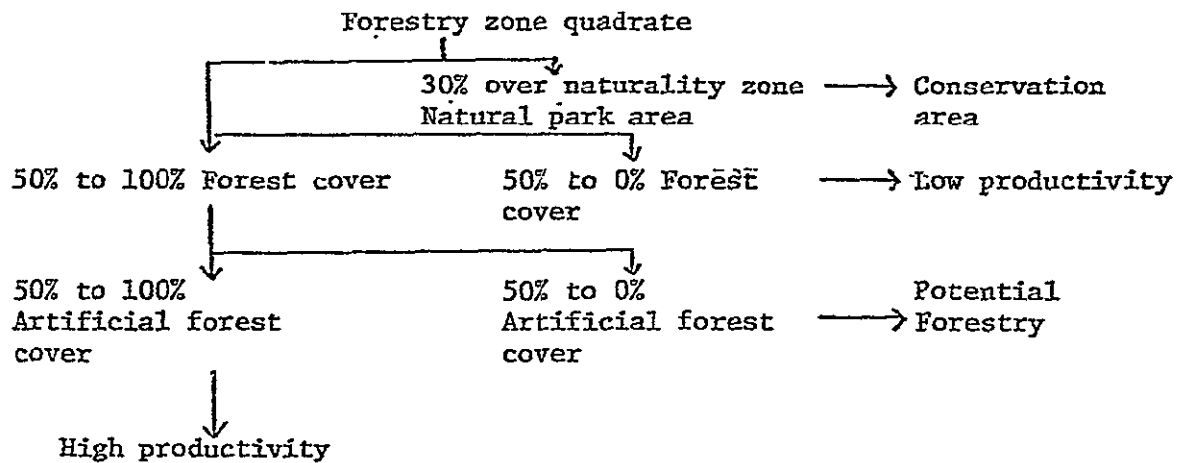
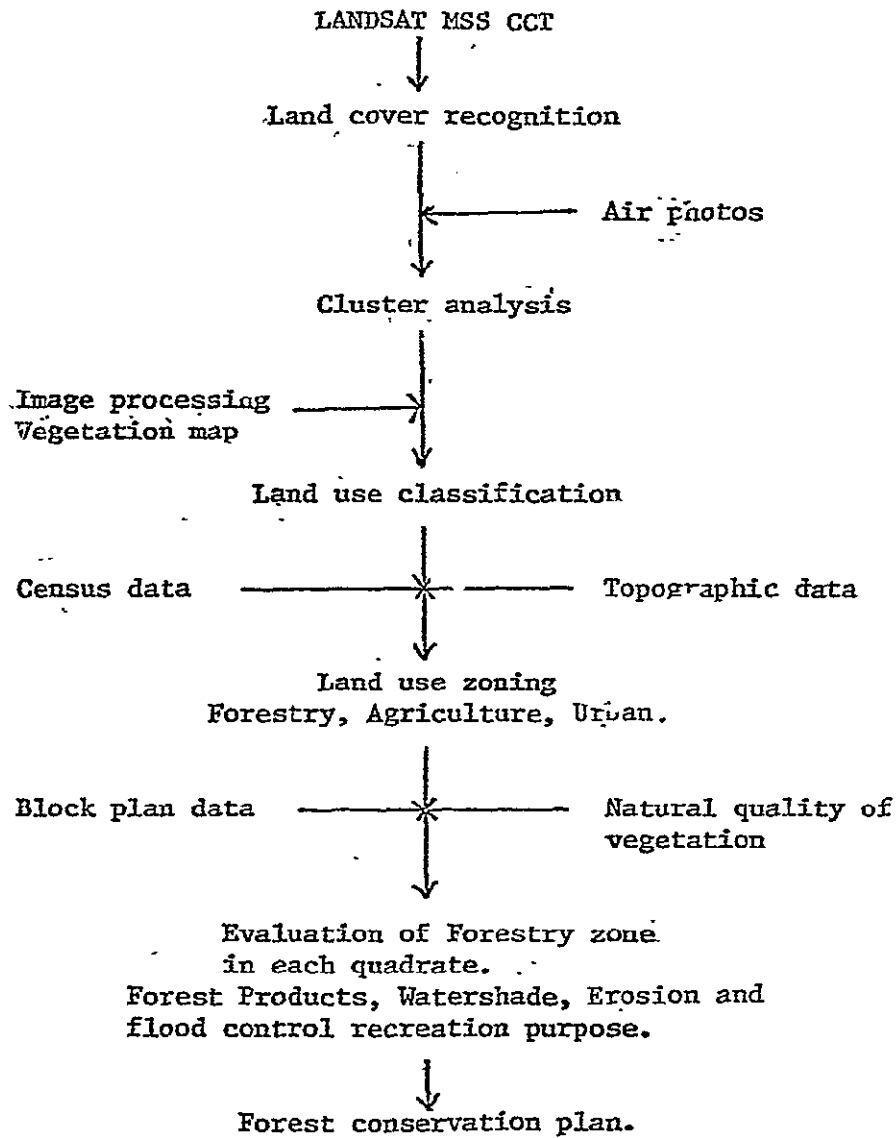


Fig. 7 LANDSAT data application diagraph for Forest conservation plan.



The forest productivity map was drawn as shown in Fig.5 evaluating timber productivities of each quadrate by combining those data of the forest type, cutting and planting labor force, topographic condition, vegetation naturarity and regional park plan.

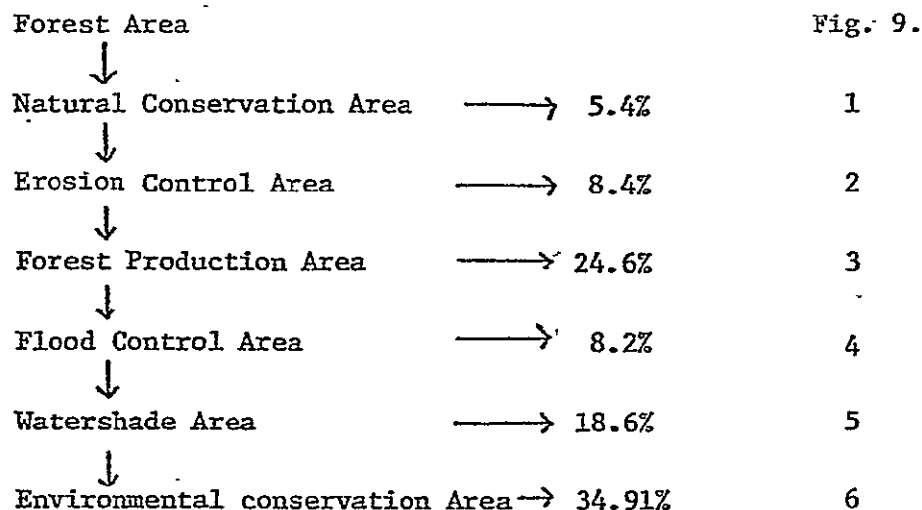
The faculties of the recreating the environmental condition of each quadrate were evaluated by the analysis of the forest cover percentage and the distance factor connecting with the population distribution and were mapped by 5 grades of the common recreation supply ability as Fig. 6.

The whole procedure regarding above works is shown in Fig. 7.

3) The forest conservation plan mapping.

the north Kanto forest conservation plan was schemed under the use of the evaluation of the forest function, the procedure of which was flow-charted as Fig. 8. Finally the map of the forest conservation planning was drawn as Fig. 9.

Fig. 8 Forest exploitation and conservation plan of North Kanto area





As the result of this work, the 53% of the forest in this area must be treated as sustained the area of regular forest faculty besides the timber production management. These show the typical types of the conservation of natural environmental condition for the region surrounding the populated area as Kanto.

These results were reported to the National Land Agency through Forest Agency in March 1976.

#### IV. Significant Results.

The actual land cover condition of Japan is highly fractionated and changing rapidly with the laps of time. Although LANDSAT data is regarded as the rough information for the land use management of the ecological environment survey. It has remarkable ability for the preraration of the initial information of the whole aspect or for the collection of statistical data of the wide region, that is very difficult by the conventional survey method limited by the time and labor of today.

Also LANDSAT data can be used to produce economically detailed and practical report for regional planning with the combination of the other various survey informations.

The significant results of this research are especially as follows :

- (1) The actual land cover and ecological environment are remarkably changeable at the rapidly industrialized area by the urbanization in the flat plane also by the forest works and road construction in the mountainous area. Therefore the adjustment or the correction of the formal vegetation or the land use map is practically impossible even spending 5 years, if only the conventional survey method is employed.

The practical use of the recognition results by the LANDSAT data is proved as the base map of the field survey or the retouching work of the vegetation and land use. The effective benefit to cut down the cost, labor and time to the grade of more than 10% or lower of the conventional method is certified.

- (2) The correct and detailed vegetation map is prepared by the combined interpretation of the repetition data of LANDSAT of the different seasons at the warm and temperate forest in Japan.
- (3) The basic land use zoning map for the exploitation and conservation planning of the wide area is prepared effectively by LANDSAT data for the use of the intensive country.
- (4) LANDSAT data forms the basic frame for gathering other kind of information in a total analytical system of the country.
- (5) LANDSAT data offers basic information from the wide point of view for the other narrow survey method and makes it possible to use efficiently the air borne or surface survey results.

#### VI. Publications.

1. Iwao Nakajima : Environmental Quality pattern Mapping from Space Data. The 11th International Symposium on Space Technology and Science. June 1975, Tokyo.
2. Iwao Nakajima : Degradation of the Vegetation Cover with Urbanization and its Influence on the Flow of Polluted Air. The 10th International Symposium on Remote Sensing of Environment Oct. 1975, Michigan.
3. Iwao Nakajima : The Kinki district observation from LANDSAT data. History and Geography (66) pp.1-13. 1975. 7.
4. Iwao Nakajima : The data processing in Remote Sensing. Application Physics : Vol. 44. No. 11. pp.45-55. 1975, 11.
5. Iwao Nakajima : Forest Survey by Cosmic Photograph, Farming Japan, Vol. 9. 1975. 7.
6. Iwao Nakajima : The Research for the Interpretation and Analysis of the Forest, the Analysis of the Digital Display Images. The Exploitation of the Remote Sensing Application : Science and Technology Agency. 1976, 3.
7. Iwao Nakajima : The Vegetation Survey by Remote Sensing. Environment Agency : 1976, 3.
8. Iwao Nakajima : The Forest and Land Surface Mensuration by Remote Sensing. The JAPAN Electric Science Society. 1976, 4.
9. Iwao Nakajima : Air-Borne and LANDSAT data Processing for Environment Study. US-Japan Seminar on Image Processing in Remote Sensing. Maryland 1976, No. V.
10. Iwao Nakajima : Remote Sensing for Agriculture and Forestry. RESTEC Vol. I 1976, 12.
11. Iwao Nakajima : The Forest Conservation Planning of North Kanto by LANDSAT data. Report of the Japan Society of Photogrammetry 1976, 5.
12. Iwao Nakajima : Remote Sensing : Manual of Photographic Techniques: 1977, 6.

#### VII. Data Quality and Delivery

The data quality is very satisfactory. But it was very unfortunate that repetition of the coverage to Japan by LANDSAT-2 was very few.

#### VIII. Recommendation

Especially the stereoscopic data acquisition would be more helpful for these study.

#### IX. Conclusion

The investigation of LANDSAT data application is continueing. It is certain that more effective results will be obtained in near future.

ORIGINAL PAGE IS  
OF POOR QUALITY

ORIGINAL PAGE IS  
OF POOR QUALITY

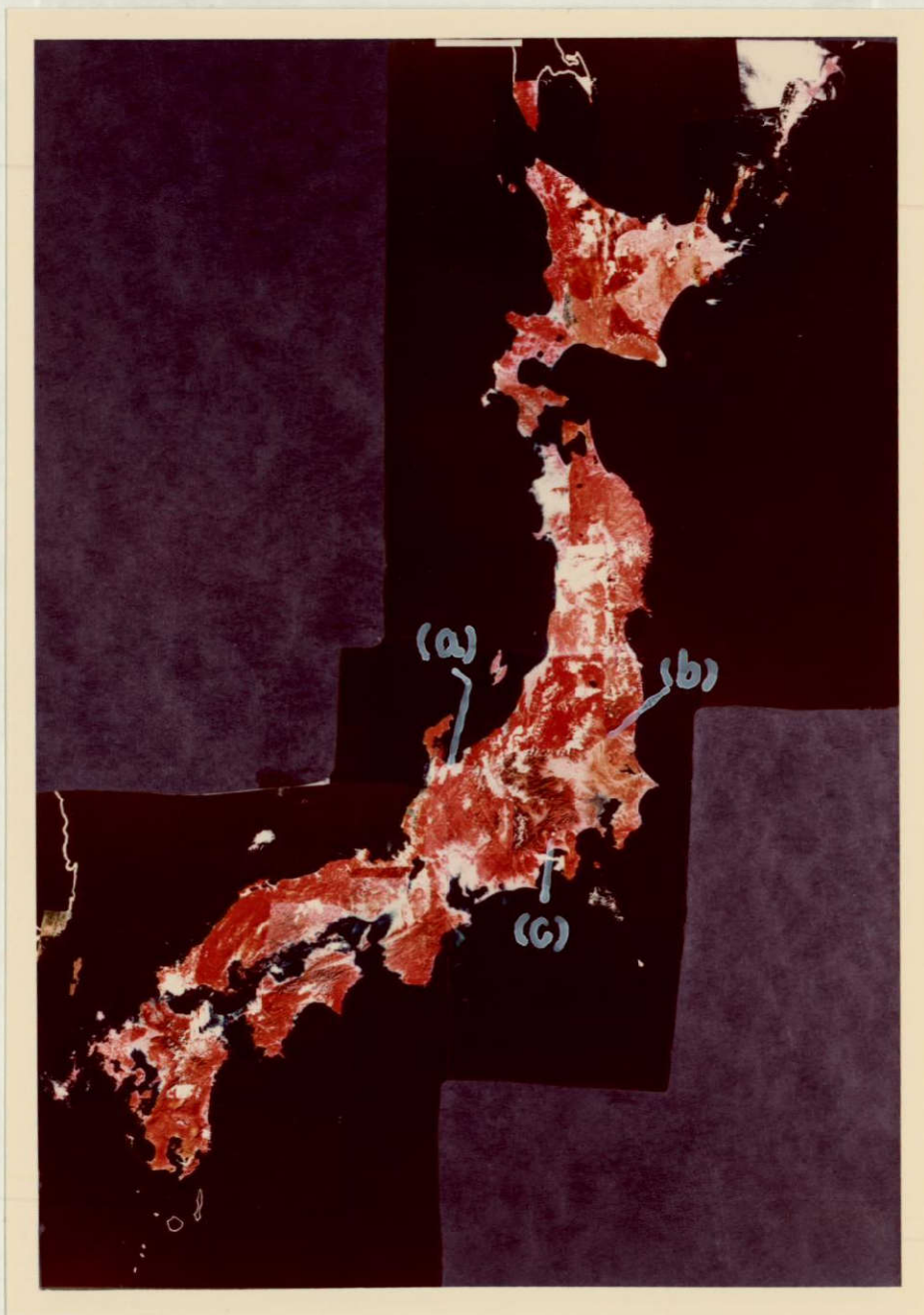


Plate 1 Whole view of Japan Island

- (a) Toyama area
- (b) North Kanto area
- (c) Mt. Fuji



ORIGINAL PAGE IS  
OF POOR QUALITY

ORIGINAL PAGE IS  
OF POOR QUALITY

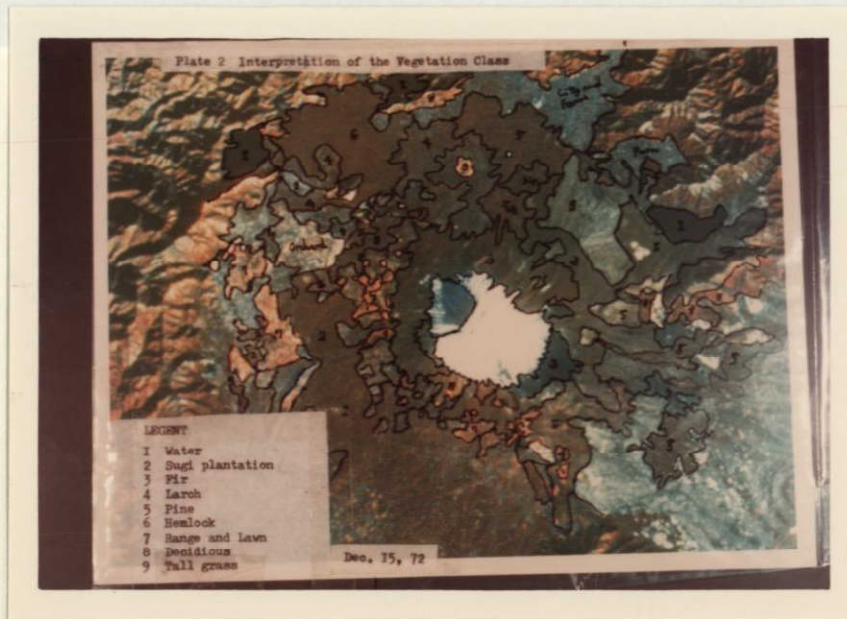


Plate 2

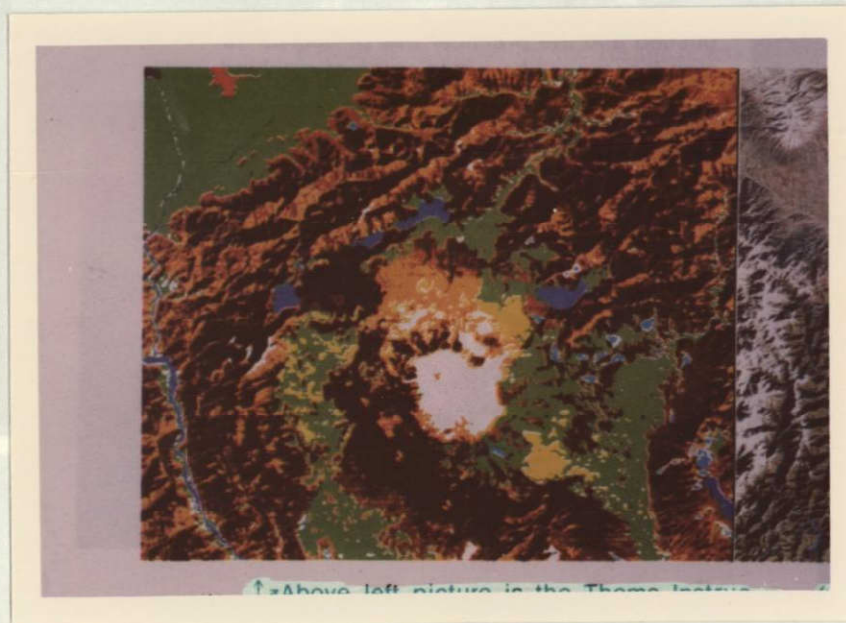


Plate 3

ORIGINAL PAGE IS  
OF POOR QUALITY

ORIGINAL PAGE IS  
OF POOR QUALITY



Plate 4



Plate 5



ORIGINAL PAGE IS  
OF POOR QUALITY

ORIGINAL PAGE IS  
OF POOR QUALITY

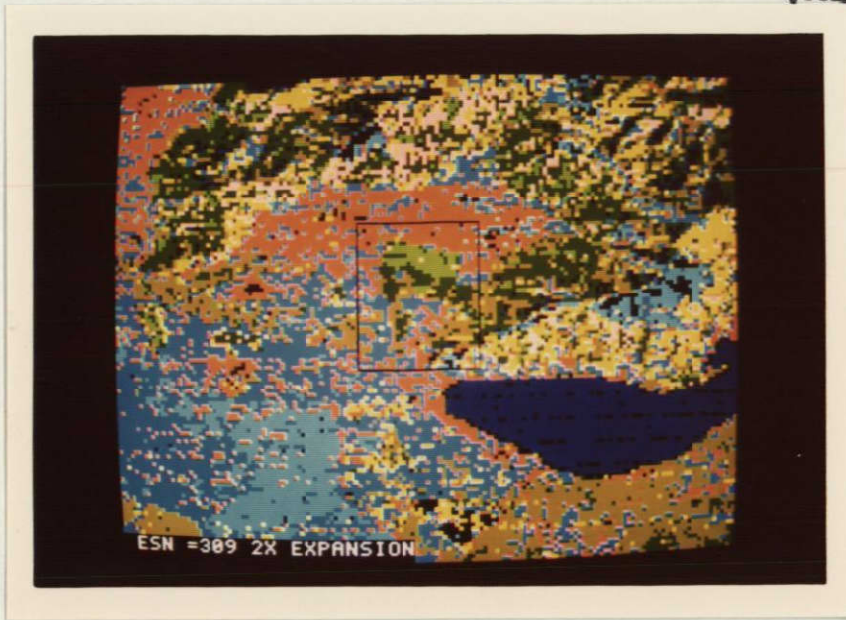


Plate 6

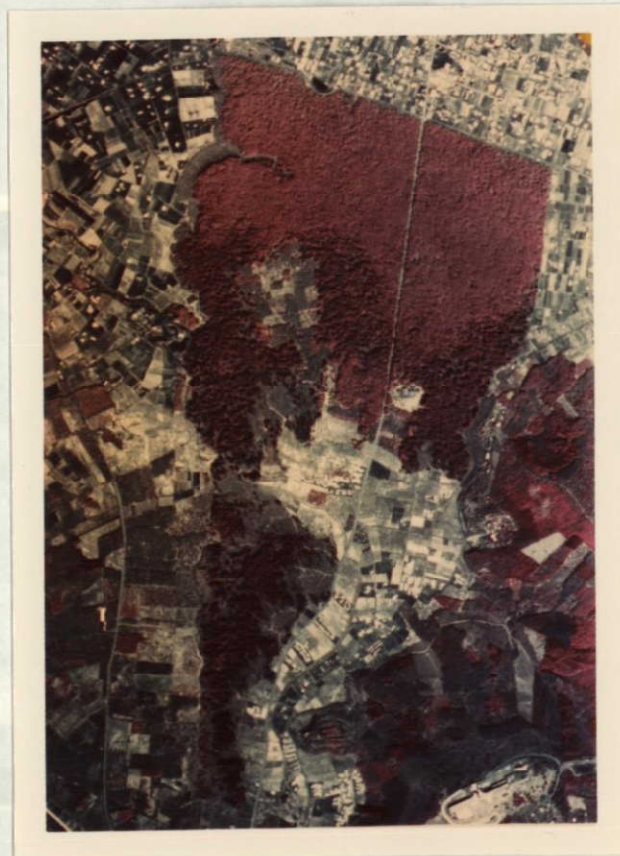
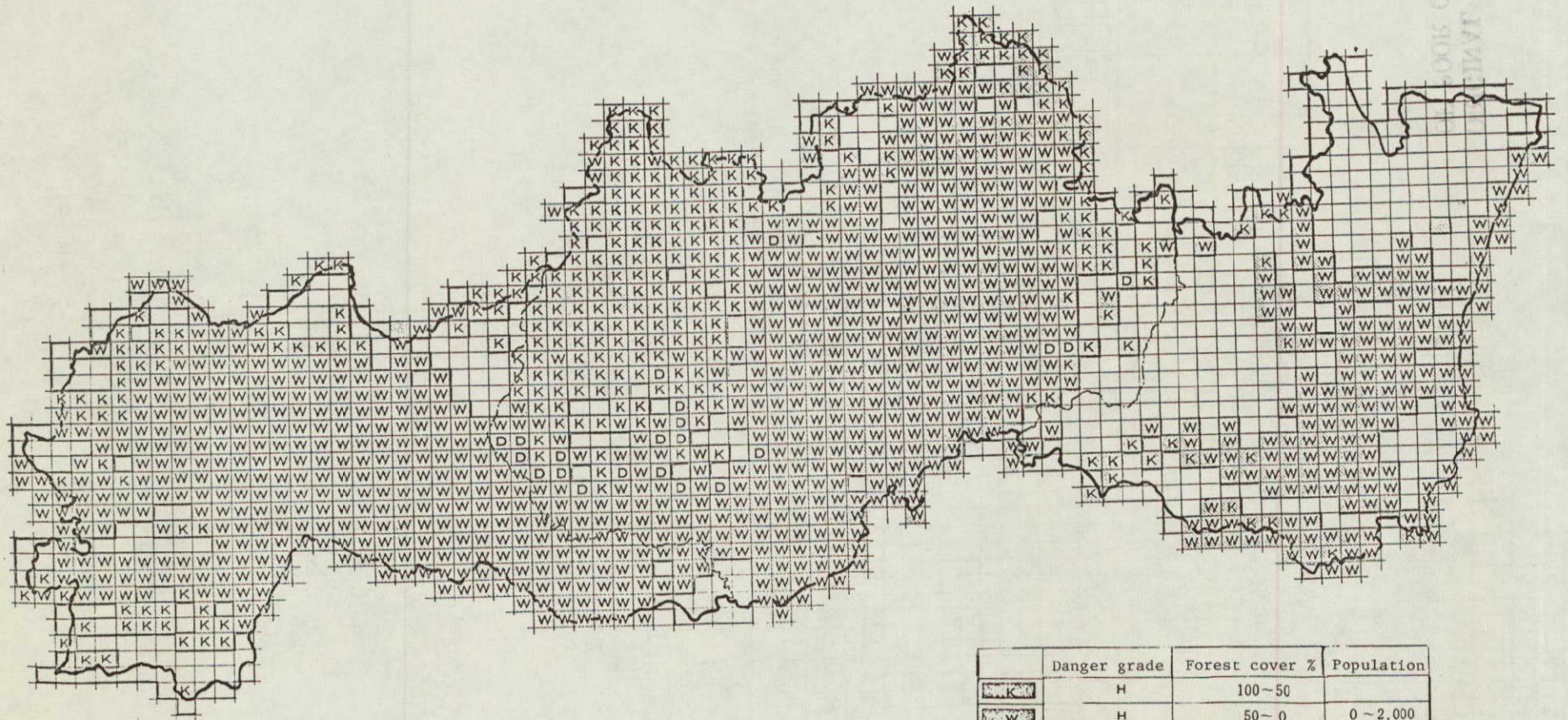


Plate 7



FIG. 4 EROSION DANGER GRADE



-45-

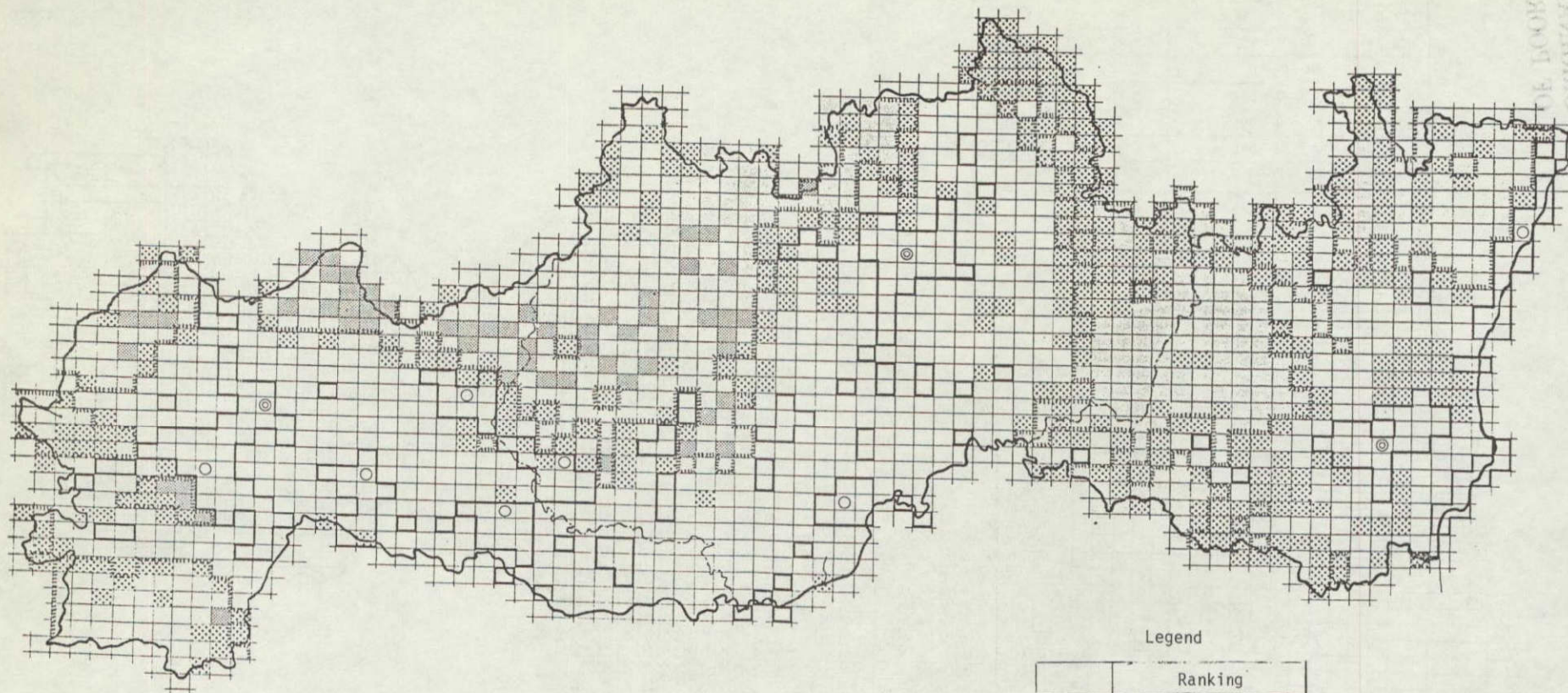
	Danger grade	Forest cover %	Population
	H	100-50	
	H	50-0	0-2,000
	H	50-0	over 2,000
	M	100-50	
	M	50-0	0-2,000
	M	50-0	over 2,000
	M	100-50	
	M	50-0	
	L		

ORIGINAL PAGE IS  
OF POOR QUALITY

COLE CASTILLA  
PLATE IV 12



FIG. 6 COMMON RECREATION SUPPLY ABILITY



Legend

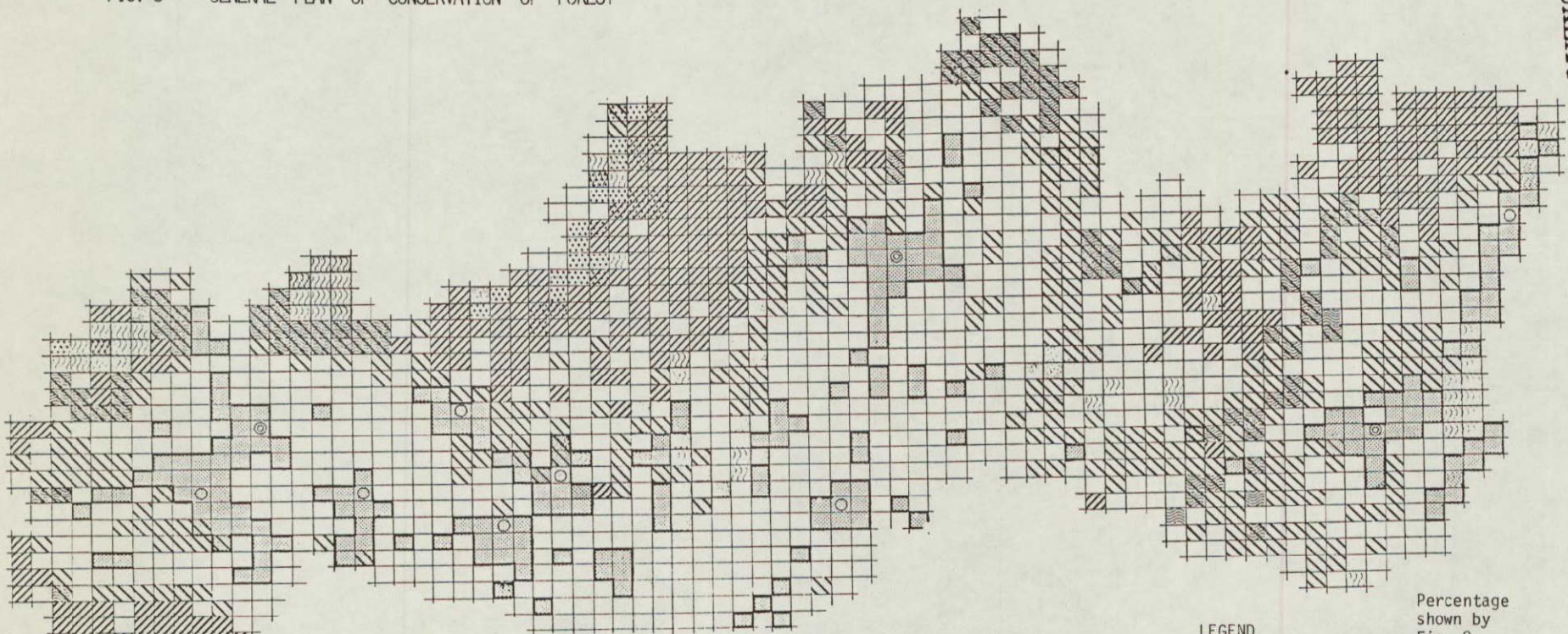
Ranking	
	6
	5
	4
	3 2 1
	Urban area
	Agricultural area

ORIGINAL PAGE IS  
OF POOR QUALITY

U.S. GEOLOGICAL SURVEY  
WATER RESOURCES DIVISION  
WASHINGTON, D.C. 20506



FIG. 9 GENERAL PLAN OF CONSERVATION OF FOREST



-47-

LEGEND

	Urban area		
	Erosion Control Area	→ 8.4%	2
	Flood Control Area	→ 8.2%	4
	Watershade Area	→ 18.6%	5
	Forest Production Area	→ 24.6%	3
	Potential Forest Production Area		
	Natural Conservation Area	→ 5.4%	1
	Environmental Conservation Area	→ 34.91%	6

Percentage shown by Fig. 8



ORIGINAL PAGE IS  
OF POOR QUALITY

AN ANALYSIS ON VEGETATION COVER  
BY USING LANDSAT MSS DATA

by

PRECEDING PAGE BLANK NOT FILMED

Shunji MURAI  
Dr. Eng. Associate Professor  
Institute of Industrial Science  
University of Tokyo  
Roppongi 7-22, Minatoku  
Tokyo JAPAN

ABSTRACT

The study deals with a mathematical model for estimating vegetation cover in Tokyo Districts by using LANDSAT MSS data. Two types of model, multi-regression analysis and parametric model, were tested for the geographically corrected test area with 45 kilometers by 18 kilometers in Tokyo Districts, where the ground survey for vegetation cover and classification was carried out by the Ministry of Construction, the Government of Japan in 1973.

The results obtained from the study conclude that vegetation cover can be well estimated from LANDSAT MSS data with the accuracy of not less than 80 per cent.

INTRODUCTION

Vegetation cover can be defined as the ratio of the area with vegetation cover to the unit area. However, recognition of vegetation varies depending on the definition of vegetation. In 1973, the Ministry of Construction carried out the ground survey associated with multi-band camera aerial photographs for mapping the vegetation and land use in Tokyo Districts within 50 kilometers radius on the base of 500 meters mesh data.

Data for the unit area were digitized with respect to sixteen classes of vegetation and land use, which are utilized as the ground truth data in the study.

SELECTION OF TEST AREA

Test area was selected where Tokyo down town, suburb and hill are properly included as shown in Fig. 1. The test area corresponds to two frames of national base map, 1:50,000, namely ' HACHIOJI ' and ' TOKYO SEINANBU ' of which area makes about 800 square kilometers with 45 km in east-west direction by 18 km in north-south direction. Since so-called 500 meters mesh is made by deviding a frame of the base map of 1:50,000 into 40 grids in both direction of longitude and latitude, the test area involves 3200 mesh data.

48  
PRECEDING PAGE BLANK NOT FILMED



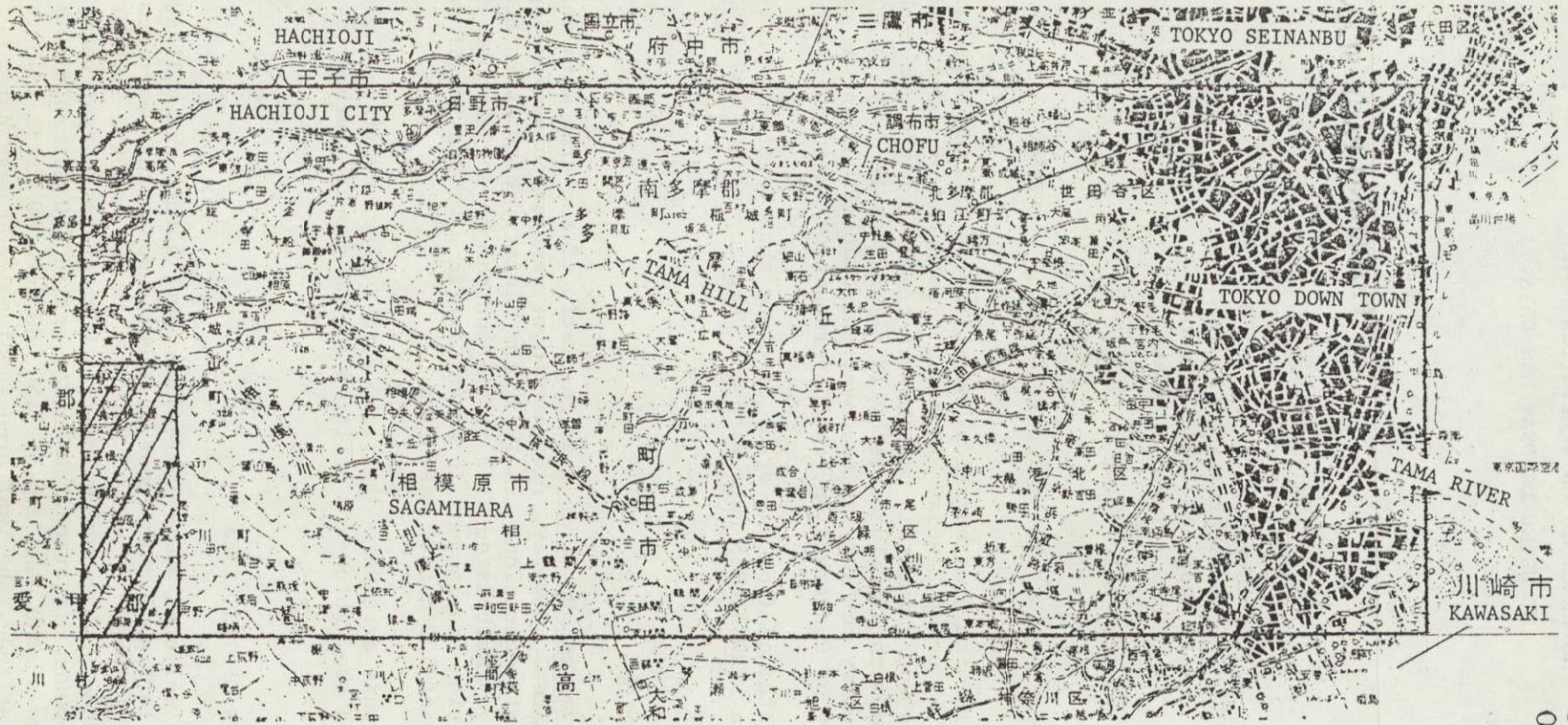


Fig. 1 Test Area

ORIGINAL PAGE IS  
OF POOR QUALITY



## MATHEMATICAL MODEL

The following two models were tested for estimating vegetation cover from LANDSAT MSS data.

### (1) Multi-regression model

Average LANDSAT data with four bands,  $X$  ( $x_1, x_2, x_3, x_4$ ) in a unit 500 meters mesh data and the corresponding vegetation cover,  $y$  is correlated by the multi-regression model as indicated as follows.

$$y = f(X) = a_1x_1 + a_2x_2 + a_3x_3 + a_4x_4 + a_0$$

Unknown parameters,  $a_0$  to  $a_4$  are estimated by the multi-regression analysis.

### (2) Parametric Model

When variable  $X$ , which is derived from LANDSAT MSS data amounts  $m$  in the unit 500 meters mesh area, let  $n$  of  $m$  be subject to the condition that variable  $X$  exceeds parameter  $k$ . Supposed that vegetation cover can be estimated as  $n/m$ , parameter  $k$  should be determined so as to minimize the standard deviation of residuals between observed vegetation cover  $G$  and estimated vegetation cover  $n/m$ .

Eight variables were examined in the parametric model.

$$X_1 = x_3 / x_1$$

$$X_2 = x_4 / x_1$$

$$X_3 = x_3 / x_2$$

$$X_4 = x_4 / x_2$$

$$X_5 = (x_3 + x_4) / (x_1 + x_2)$$

$$X_6 = (x_1 + x_2 - x_3 - x_4) / (x_1 + x_2 + x_3 + x_4)$$

$$X_7 = a_1x_1 + a_2x_2 + a_3x_3 + a_4x_4 + a_0$$

(determined by multi-regression model)

$$X_8 = b_1x_1^* + b_2x_2^* + b_3x_3^* + b_4x_4^*$$

(second principals determined by principal component analysis)

Where

$$x^* = (x - \bar{x}) / \sigma$$

## ESTIMATION OF VEGETATION COVER BY MULTI REGRESSION ANALYSIS

Multi-regression analysis was applied to 3080 500 meters mesh data with three cases of ground truth data. Table 2 summarizes the result of the analysis including coefficients  $a_0$  to  $a_4$  and accuracy of estimation represented by multi correlation coefficient and standard deviation. Coefficients in the lower column represent those for normalized data.

Best result was obtained for the case 3, in which multi-correlation coefficient  $\gamma$  is 0.871 and the standard deviation  $\sigma$  is +15.53 per cent.

Table 2 Result of Multi-regression Analysis

	Coefficient					Accuracy	
	$a_1$	$a_2$	$a_3$	$a_4$	$a_0$	$\gamma$	$\sigma(\%)$
Case 1 : $G_1$	-3.844	-4.839	3.697	6.002	81.368	0.845	17.82
	-0.242	-0.378	0.331	0.377			
Case 2 : $G_2$	-3.722	-5.140	3.874	5.781	85.638	0.856	16.92
	-0.237	-0.406	0.351	0.367			
Case 3 : $G_3$	-3.340	-5.229	3.241	6.338	83.417	0.871	15.53
	-0.220	-0.428	0.304	0.417			

Fig. 2 shows comparison between observed vegetation cover and estimated vegetation cover for the cross section lines no. 10 , and no. 25 . Fig. 3 shows the computer generated map for observed vegetation cover and estimated vegetation cover.

## ESTIMATION OF VEGETATION COVER BY PARAMETRIC MODEL

Most probable parameter  $k$ , which would be considered as an criterion to decide whether vegetation or not, was determined for each of eight cases of variables as mentioned before, so as to minimize the standard deviation between observation and estimation.

Table 3 summarizes the result of estimation by parametric model. Best estimation was obtained from the variable  $X_3 = x_3 / x_2$  that is the ratio of MSS 6 to MSS 5. The standard deviation for this case was +15.36% for the most probable parameter  $k=1.14$ . This result is of great importance from the view point of radiance, that is, since radiances for full scale of CCT data in MSS 5 and MSS 6 band correspond to 1.76 and 2.00  $mW/cm^2 \cdot sr$  respectively, the criterion  $X_3 = x_3/x_2 \geq k=1.14$  coincides with the criterion that the ratio of radiances between the two bands,  $1.76 x_3 / 2.00 x_2 \geq 1$ , or  $x_3/x_2 \geq 2.00/1.76=1.14$ . Therefore, if a slope for the ratio of MSS 6 to MSS 5 with respect to radiance is positive, it could be concluded that the corresponding data represents vegetation cover.

Table 3 Result of Estimation of Vegetation Cover  
by Parametric Model

Variable	Case 1:G <sub>1</sub>		Case 2:G <sub>2</sub>		Case 3:G <sub>3</sub>	
	k	σ	k	σ	k	σ
$X_1 = x_3/x_1$	0.93	20.61	0.90	21.43	0.94	20.05
$X_2 = x_4/x_1$	0.46	18.97	0.44	18.99	0.45	18.13
$X_3 = x_3/x_2$	1.16	17.27	1.14	16.74	1.14	15.36
$X_4 = x_4/x_2$	0.57	17.80	0.55	17.23	0.58	16.12
$X_5 = (x_3+x_4)/(x_1+x_2)$	0.76	17.90	0.75	17.88	0.76	16.66
$X_6 = (x_1+x_2-x_3-x_4)/(x_1+x_2+x_3+x_4)$	0.14	17.93	0.15	17.86	0.14	16.75
$X_7 = a_1x_1+a_2x_2+a_3x_3+a_4x_4+a_0$	49	17.58	47	17.36	48	16.08
$X_8 = b_1x_1+b_2x_2+b_3x_3+b_4x_4$	-0.1	17.85	-0.2	17.69	-0.1	16.58

Where  $X_7$  : multi-regression model  
 $X_8$  : second principal component

#### COMPARISON BETWEEN MULTI-REGRESSION MODEL AND PARAMETRIC MODEL

The following comparison between multi-regression model and parametric model can be pointed out.

- (1) Multi-regression model utilizes the average data from the stand point of statistic, while parametric model accumulates point by point data.
- (2) Parametric model results in a little better estimation, although the both model have less remarkable difference. Tendencies for error distribution in the two models look alike.
- (3) Computing time is much more needed for parametric model, while flexibility could be expected more in the parametric model.

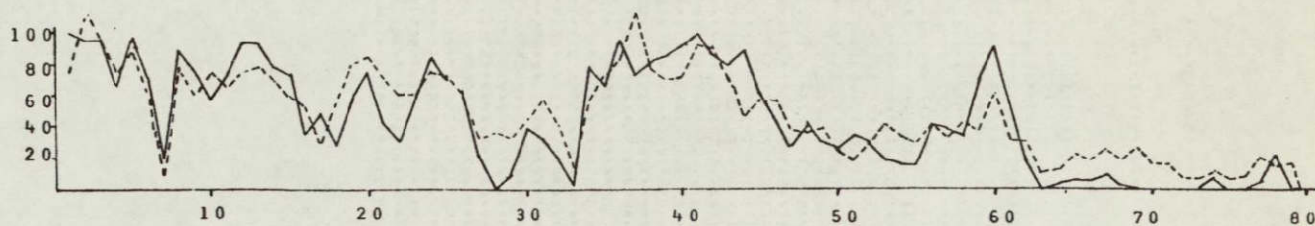
#### CONCLUSION

- (1) Vegetation cover in Tokyo Districts could be well estimated by both of multi-regression model and parametric model. Multi-correlation coefficient between observed value and estimated value was 0.87 and standard deviation was +15%.
- (2) Vegetation cover in Tokyo Districts was mapped into five levels with equal intervals of 20 per cent.

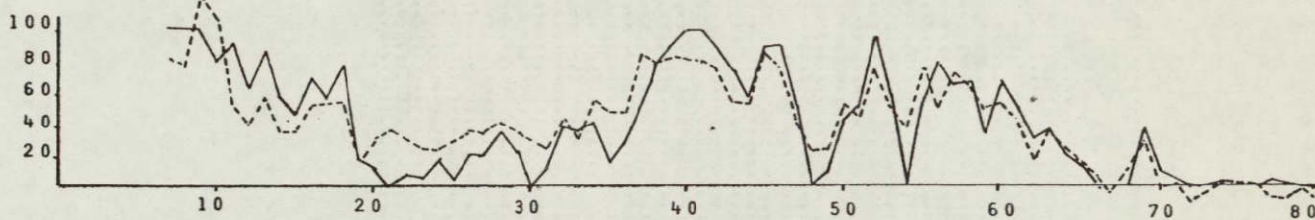
(3) Definition of vegetation should be further studied, although the parametric model concluded that the decision rule to define vegetation should be whether the slope of ratio MSS 6/MSS 5 in the radiance unit is positive or not.

(4) With detail check for the result of estimation obtained from LANDSAT data, actual vegetation cover could be much more represented in the estimated map than the ground-surveyed map.

Line No. 10



Line No. 25



— observed value  
- - - estimated value

Fig. 2 Cross Sections of Vegetation Cover for Comparison between Observed Value and Estimated Value



\*1\*2\*3\*4\*5\*6\*7\*8\*9\*0\*1\*2\*3\*4\*5\*6\*7\*8\*9\*0\*1\*2\*3\*4\*5\*6\*7\*8\*9\*0\*1\*2\*3\*4\*5\*6\*7\*8\*9\*0\*1\*2\*3\*4\*5\*6\*7\*8\*9\*0

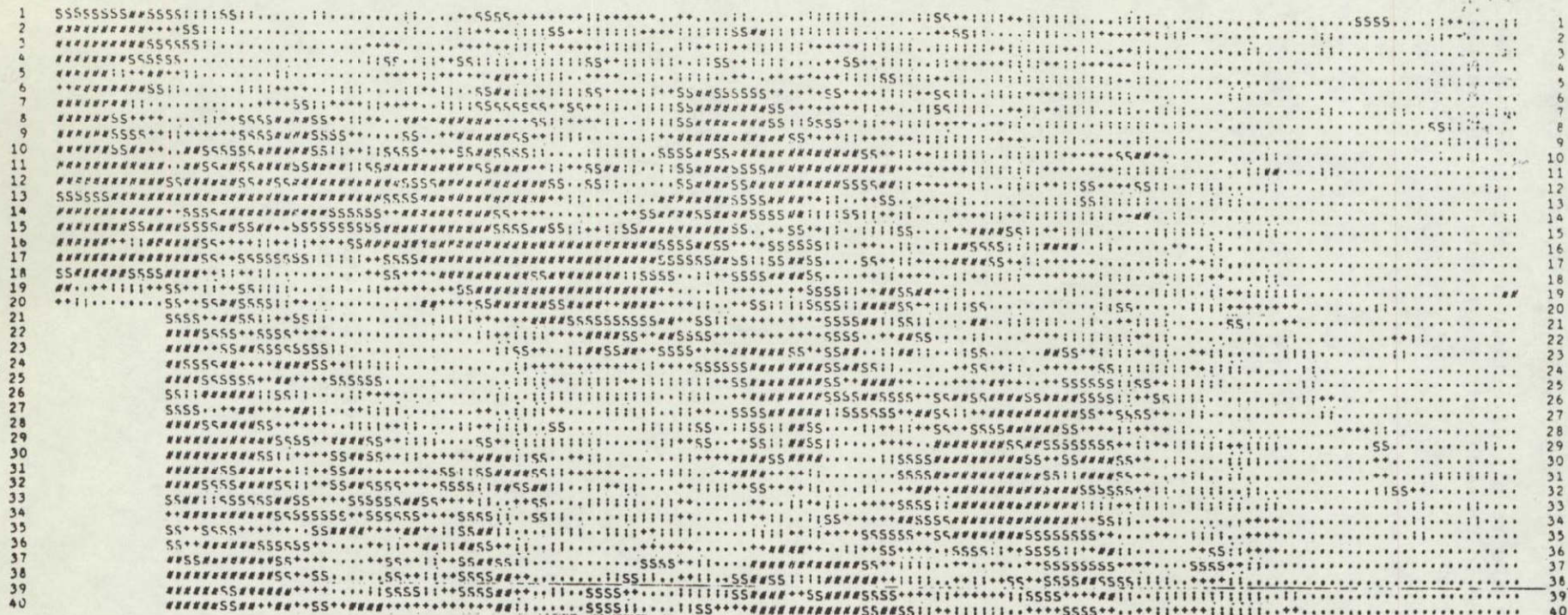


FIG. 3 A OBSERVED VALUE OF VEGETATION COVER  
0- 20% ; 20- 40% + 40- 60% s 60- 80% # 80- 100%

ORIGINAL PAGE IS  
OF POOR QUALITY







ESTIMATED VALUE OF VEGETATION COVERAGE N1542511A

ESTIMATED VALUE OF VEGETATION COVERAGE N1542507A

\*1\*2\*3\*4\*5\*6\*7\*8\*9\*0\*1\*2\*3\*4\*5\*6\*7\*8\*9\*0\*1\*2\*3\*4\*5\*6\*7\*8\*9\*0\*1\*2\*3\*4\*5\*6\*7\*8\*9\*0\*1\*2\*3\*4\*5\*6\*7\*8\*9\*0\*1\*2\*3\*4\*5\*6\*7\*8\*9\*0\*1\*2\*3\*4\*5\*6\*7\*8\*9\*0

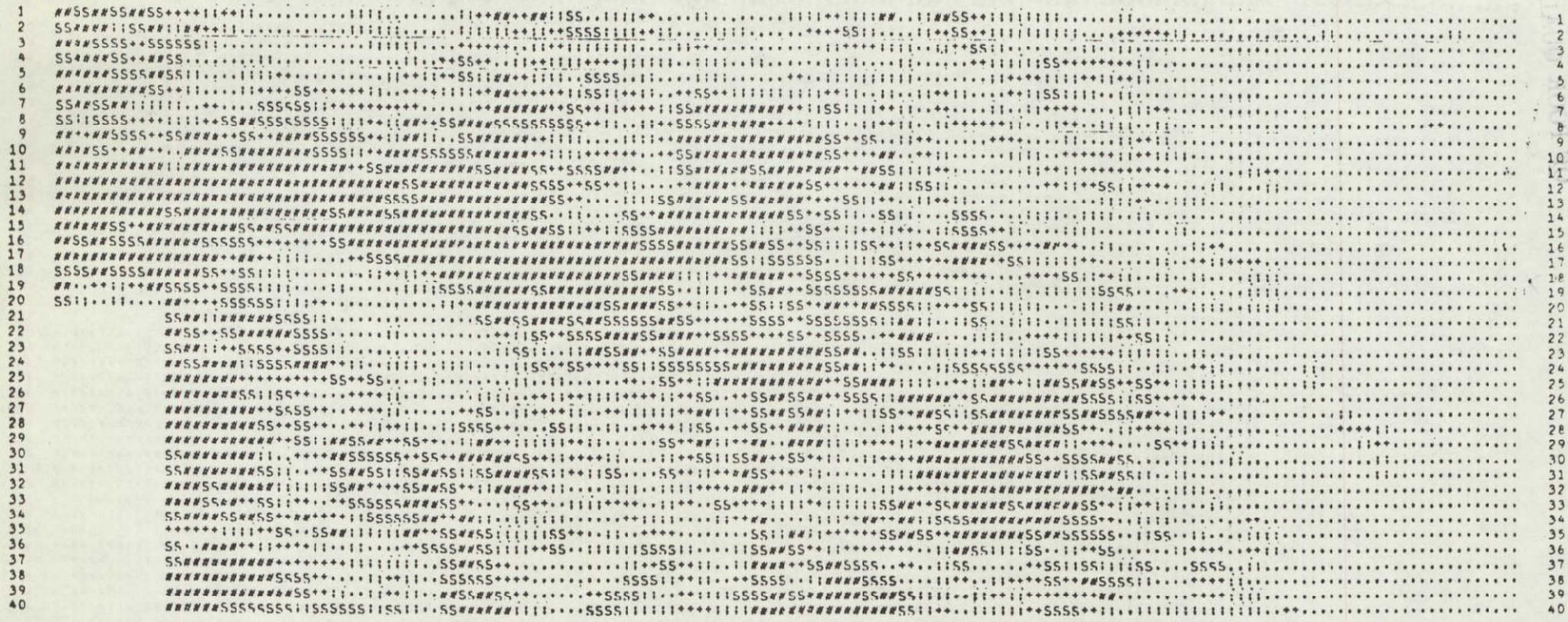


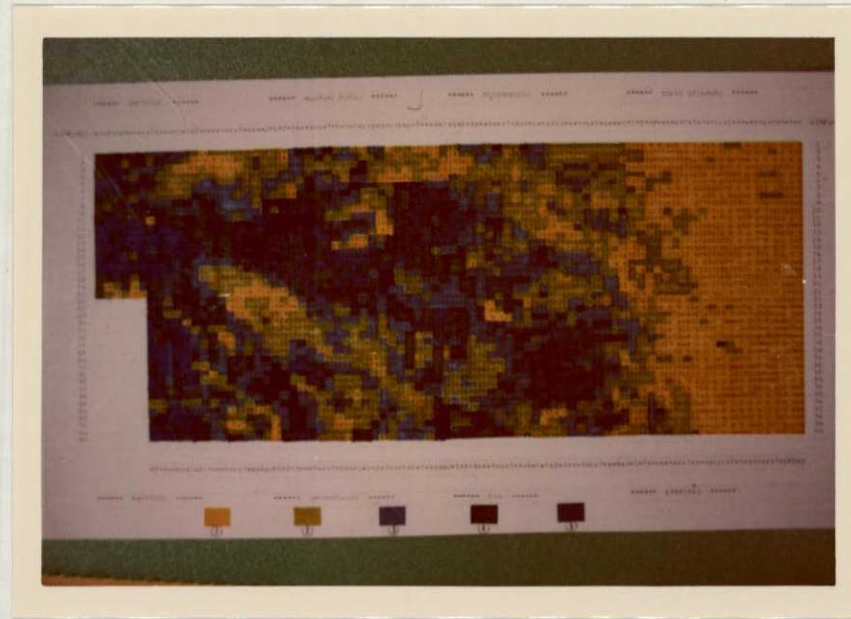
FIG. 3 C VEGETATION COVER ESTIMATED BY PARAMETRIC MODEL

ORIGINAL PAGE IS OF POOR QUALITY

58

ORIGINAL PAGE IS OF POOR QUALITY





- (1) 0~20%
- (2) 21~40%
- (3) 41~60%
- (4) 61~80%
- (5) 81~100%

ORIGINAL PAGE IS  
OF POOR QUALITY

FIG.3 B VEGETATION COVER ESTIMATED BY MULTI-REGRESSION ANALYSIS--COLOR PRINTED

Classification of Shorelines

Dr. Daitaro SHOJI  
Chief Hydrographer

Hydrographic Department, Maritime Safety Agency  
Tsukiji 5-3-1, Chuo-ku, Tokyo, Japan

Abstract

Typical shorelines, reclaimed, Ria and sand are selected as study areas. Digital scene in the CCT ID No.223200473 prepared from MSS is converted to a print map and also to colored images.

In the reclaimed areas in Nagoya and Yokkaichi MSS band 4 shows the progression of the reclamation distinctly. The Ria shoreline of Sima peninsula depicted by MSS shows good correspondence to the real one. Sand beaches along Atsumi peninsula shows good accordance between each shorelines of 4 bands images.

1. Introduction

It is noticed that the LANDSAT data about the oceanographic environment seems to be quite useful for hydrographic service, so the writers examined the method of classification of shorelines about reclaimed lands, Ria shorelines and sand beaches by means of analyzing the black-and-white bulk film and CCT data, using one of the least cloud covered

scene around Ise Bay.

## 2. Techniques

Topographies and water depth adjacent to the shorelines have been surveyed in detail and aerial photographs around the harbour area were taken. A part of the studied area were actually investigated on August 27, 1976.

Band 7 information was used for confirmation of shorelines. Other bands were used for identification of spectral characteristics of land and sea areas adjacent to the shorelines.

The computer, NEAC 2200/500, of Hydrographic Department have been used in order to decode and to analyze the CCT, and required softwares have been prepared by staffs in the office.

A line printer was used for output of analyzed result. Some results were showed on a colour display tube and photographed.

## 3. Accomplishments

### (1) Reclaimed lands

Reclamations in urban seaside areas and near-harbour areas are progressing rapidly to be made factory grounds since 1960's.

In general, characteristics of reclaimed lands were detected spectrally by MSS. The reflectance of surface soils of every four bands has increased depending on the lapse of time after the reclamation, and this tendency is remarkable on band 6 and band 7 data.

It is considered that the progress of a reclamation or a lapse of time is brought about decrease of water content in surface soils, increase of pavements and/or constructions, so it probably makes the increase of surface reflectance. And these tendencies would be observed

especially on band 6 and band 7 data. Reclamations have progressed in order of the construction planning, so that surface radiance of reclaimed lands indicates the degrees of the advancement of reclamation. The newer reclaimed lands show much black pattern on the photograph of black-and-white positive.

Fig.1 shows the colour composite image to be made from CCT of band 4,5 and 7 around Nagoya harbour. The reclaimed lands are shown bluish in colour. On the reclaimed lands in southern and western part of Nagoya harbour, inland areas behind old shorelines (natural shorelines) as displayed greenish in colour were distinguished from reclaimed lands.

Fig.2 shows a colour composite image around Yokkaichi harbour. A colour tone of the reclamation areas, center of this figure, can be divided into four stages, which means a different construction ages. The darker part means the newer reclamation.

Fig.3 shows the differences of the density based on various reclamations in the center of Yokkaichi harbour by CCT data. The X-axis indicates the sum of band 4 and band 5, and Y-axis indicate the difference subtracted band 7 from band 6. CCT values of reclamation can be classified into five groups in the X-Y plane, and the values of the frequency are indicated with Arabic numerals, and for the values over ten the letters A(10,11), B(12,13), C(14,15), D(16,17), E(18,19), F(20,21), G(22,23), H(24,25) and K( $\geq$ 26) are adopted, moreover the numbers of frequency 1 and 2 are omitted to make clear the figure. Among the five clusters in the Fig.3, the lowest density group(below left side) indicates the sea water, and other four groups correspond to the reclaimed lands which were constructed during four consecutive periods of construction. Obviously the monotonous change of the spectral

reflectance of reclaimed lands have a linear relation to the age of their constructions. The older reclamation shows the higher reflectance.

## (2) Ria shorelines

Sima peninsula has a typical Ria shoreline. Fig.4 shows that the sea water was coloured by band 7 data and land areas are composed by band 4 and band 5 data. Shorelines in Fig.4 show good similarity to the real one. It is also possible to discern many objects from the CCT data, for example trees, rocks and houses, without doing a field survey. It is effective that pre-research by MSS data are used for detecting some changes around shoreline.

Near shoreline, band 4 and band 5 radiance from the sea contain some informations about the sand in the sea. We are studying how to make analysis of them.

## (3) Sand beaches

On the sand beach along Atsumi peninsula of the Pacific Ocean side, the shoreline was able to be distinguished by CCT data of every four bands. It might be considered that analyzed MSS data was taken near high tide.

. It is a future problem how to estimate the content of sand volume in the sea water from the radiation of band 4 and/or band 5 data off sand beach areas.

## 4. Significant results

In Japan, lands and near shore areas have been surveyed in detail by several agencies. We are interested that MSS data can be utilized



for the purpose of detecting the indication of minor environmental changes which are displayed as spectral characteristics, for example, of ground reflectance or radiation rather than the method of utility for topographic image.

Significant results in this program are described as follows;

(1) Band 7 data clearly shows the boundary between land and sea areas.

It may be easy to depict the shorelines automatically by CCT data, except for cloud covered areas.

(2) Spectral measurements of the sea surface by MSS data are a new field for hydrographic service, so that LANDSAT data give many ideas for technical development in the future.

If we could get digital values from MSS data, it would be possible to realize the automated processing of so many informations and it was confirmed in this program that LANDSAT data have many merits for our routine works.

## 5. Publications

No.

## 6. Problems

(1) Radiation degrees of low-gain data from the sea surface is less than we can detect, so that radiation differences of useful informations are buried in the noise.

(2) Effective atmosphere model is necessary to determine the path radiance in band 4 and 5 wave regions.

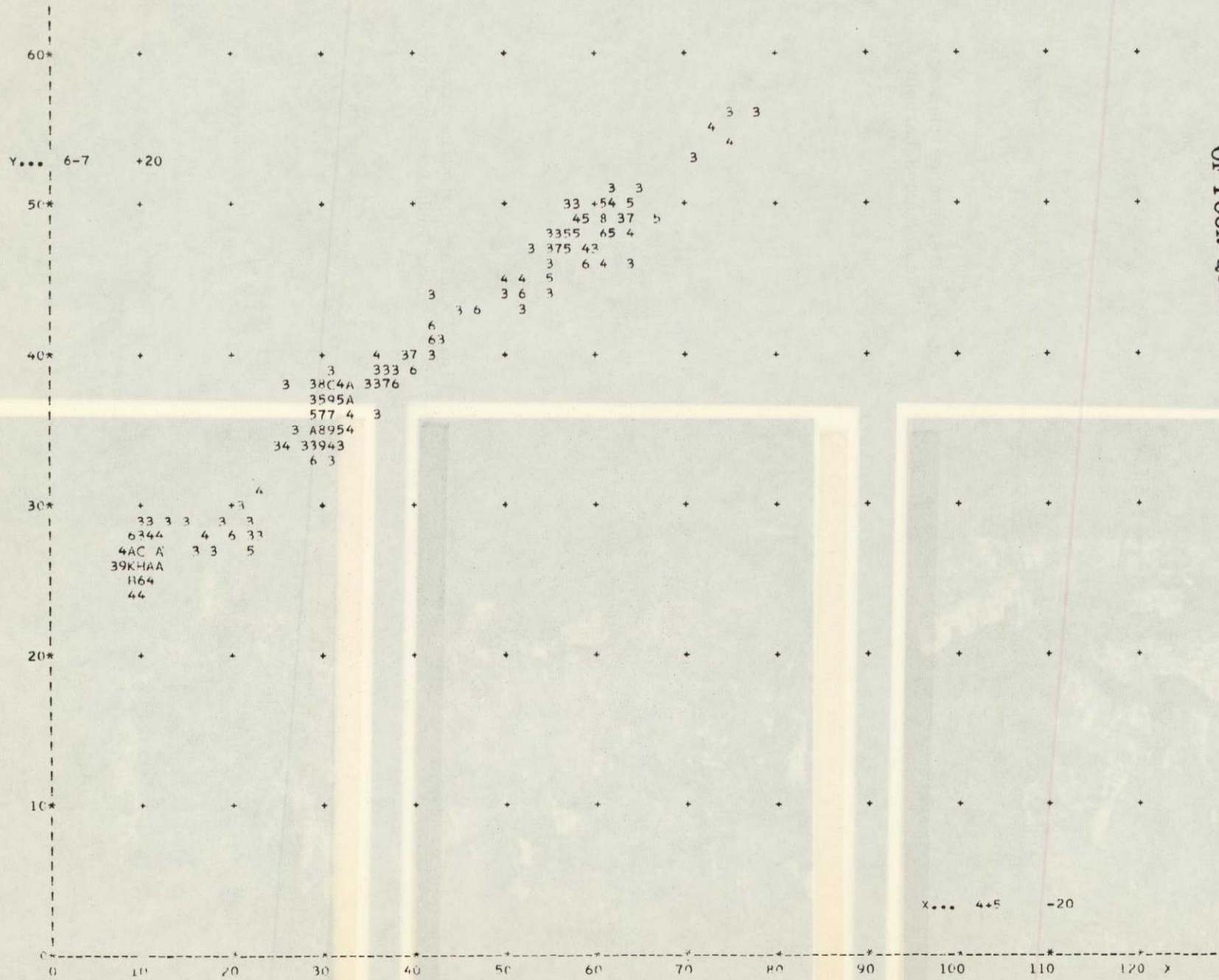
(3) It is necessary to fit the data by ships and/or airplanes in the data by satellites.

#### 7. Data Quality and Delivery

No. . . . .

#### 8. Recommendations

It is desirable to obtain high-gain data for radiation in the sea area even though the geometric resolution becomes worse, for example it is proposed that detectors that have high gain but wide view in band 4 and band 5 be provided as 7th and 8th detector.



ORIGINAL PAGE IS  
 OF POOR QUALITY

Fig.3 Density correlation diagram on the reclamation of Yokkaichi

ORIGINAL PAGE IS  
OF POOR QUALITY



Fig. 1 Color composite image near Nagoya harbour

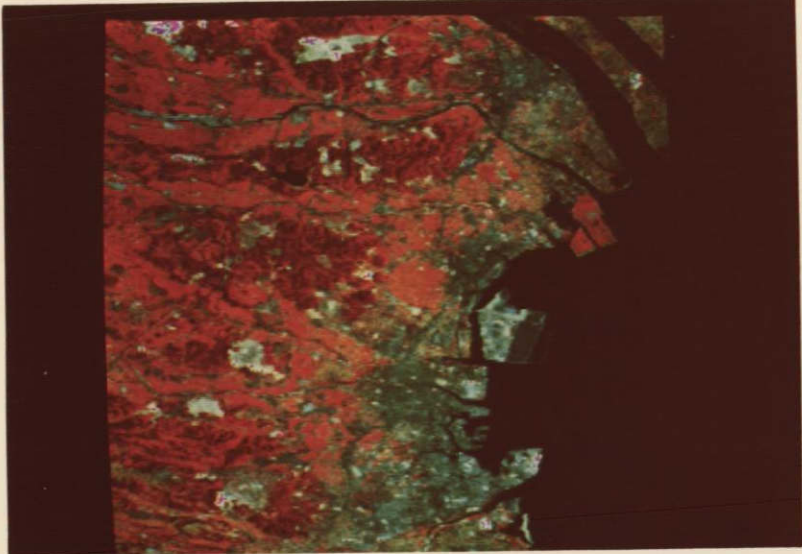


Fig. 2 Color composite image near Yokkaichi harbour



Fig. 4 Color composite image showing Ria shoreline



river mouths. The composite color image was successfully used to depict the state of river water spreading from the mouth.

## 2. Techniques

The monochromatic prints of band 4 were mainly used for interpretation of the water mass distribution. The CCT data were processed with the computer, NEAC 2200/500 of the Hydrographic Department to produce density maps and correlation graphs between different bands. The composite color images of CCT were composed by the Image processor of NEC Research Institute in cooperation with the staff of the Institute.

## 3. Accomplishments

The oceanographic data necessary for the study were collected for the coastal area and the Ise Bay from the Local Fisheries Observation Stations of Wakayama, Aichi and Shizuoka Prefectures, and for the offshore area from the Hydrographic Department, the Meteorological Agency and some of the universities. The station and data of these oceanographic observations are shown in Fig.1. Based on these data the several kinds of distribution chart were prepared to compare them with the patterns in the band 4 prints, that is, the distribution chart for temperature (surface and 100m layer), surface velocity, transparency and surface salinity (Fig.2,3,4,5,6,7 and 8).

From the scenes of "Ise-bay" and "Kumano-nada" prominent waters which seem to have considerably different density from the surrounding waters are seen near the mouths of Tenryu River and of Kumano River, respectively. To analyse these areas more in detail the CCT was used, and investigations were made on the spreading or diffusion of river waters and on the relevancy between the patterns of river water and

the offshore kinematic conditions as well.

The oceanographic condition of the coastal area is often influenced by the variation of path of the Kuroshio, which is a very strong current flowing from the west to the east in the southern offshore area of Japan and in the present study it was necessary to make these offshore kinematic conditions clear. In the preceding few months from the date of scenes the Kuroshio had been changing its path as shown in Fig.9 which is based on the bi-weekly oceanic reports of the Hydrographic Department. In August 1975 the large scale meandering pattern of the Kuroshio was settled in the offshore area enclosing a large cold water mass of 150 miles in diameter, and a part of the Kuroshio water of high temperature was flowing into the area of present investigation along the northern margin of the cold water mass. This influence of the Kuroshio water was obvious from the fact that the temperature of 100 m layer (18 to 19°C) was about 2°C higher than the average temperature of the area (16 to 17°C) with the standard deviation of about 2°C, although it was not clear from the surface temperature distribution because of the uniformly high temperature distribution over the whole area which was usual in that season of the year. No surface current (GEK) data was available in the coastal area, however the offshore current distribution (Fig.4) seemed to support above interpretation.

#### 4. Significant results

##### (1). Identification of water mass and relevancy with offshore conditions

No information of the sea surface was available from the bands 6 and 7, the CCT count of which were all less than 4 and 2 respectively except cloud area, and these bands were used to separate sea from

land and cloud, however it was confirmed that the band 4 and 5 had some information as to the sea surface such as spreading of coastal waters or eddy-like motion of surface water. Interpretation of these information with the available data of oceanographic observation is as follows.

(a). It can be concluded that the front line along the coast from Kumano-nada to Shiono-misaki in the monochromatic prints (Fig. 10 and 11) and in the pseud-color images (Fig.12 and 13) is a boundary between coastal waters and offshore water as the results of comparison with the distribution charts made from the actual oceanographic observation. That is, the front line corresponds to the equi-value lines of 25 m in transparency, 33.6‰ in salinity and 2.5 in water color scale, where the transparency of 25 m and the water color scale of 2 are the characteristic values of very clean water which has very low contents of plankton and nutrient. The oceanographic data used here were obtained at practically same date when the Landsat-2 photographs were taken.

(b). The Landsat prints suggest that the coastal water from Ise bay spreads to Atsumi Peninsula and that the offshore water approaches to 5 miles from the coast from Hamana Lake to Tenryu River, however, comparison with the oceanographic distribution charts does not give so good coincidence as the case (a). This could be attributed to a time lag of about one week between field observation and Landsat scenes and to a change of sea state which might happen during that period. A small portion of slightly different density 10 miles off Atsumi Peninsula in the prints might correspond to the intrusion of offshore water, salinity of which was higher than 34.00‰ (Fig.8).

(2). On the eddy-like pattern off Shiono-misaki

Out of the scenes of "Kumano-nada" only band 4 gives a clear eddy-like pattern off Shiono-misaki, although no evidence to consider the pattern as a real information from sea surface was obtained as far as the CCT count of each band was concerned. There was no oceanographic observation of the area at that period, however it was observed that the flow axis of Kuroshio off Shiono-misaki had moved to far north in early September from its position in late August about 60 miles off Shiono-misaki, and that a oceanic front was formed in the area with Kuroshio. It is highly possible from these situation that the eddy-like pattern had separated from coastal water by the variation of Kuroshio axis. It was also recognised that each one of the six sensors had slightly different sensitivity as was seen from the density maps which were made separately by using the informations of each sensor, although the differences of count were only one or two at the marginal portion of the pattern (Fig.20 and 21).

### (3). Analysis of the Ise Bay water

Almost whole area of Ise Bay was considered to have been covered by rather polluted water from the oceanographic data of the region, which gave salinity values less than 30‰, high water color scale of 6 to 8 and transparency less than 5 m. The CCT counts of band 4 were all less than 13 for the region and also indicate less upward radiation from the sea surface which was not so very clean.

### (4). On the patterns near the mouths of Tenryu River and Kumano River

The sea surface informations could be recognised in the two river mouth region from the prints not only of band 4 but also of bands 5 and 6. The CCT and a color image processor were used to investigate the relevancy among different bands and the spreading and diffusion of the river water into the ocean.

The pseud-color images gave clear representation as to the land



part, the shore-lines, the sandy zones in the river beds (Fig.14), the spreading area of the river water (Fig.15 and 16) and the boundary of the coastal and offshore waters. The oceanographic data gave same direction of the river water spreading.

For the Tenryu River region the density counts were divided into four groups (Fig.17) and the correlation graphs among different bands were prepared for each group (Fig.18 and 19), where the counts which are considered to represent the most clean water throughout whole area are shown by rectangulars. These graphs show that the count ranges 16 to 37 for band 4, 8 to 42 for band 5 and 2 to 19 for band 6. The correlations between band 4 and 5 and between 4 and 6 give relatively linear relation and the surface radiance of band 5 and 6 decrease towards the offshore area more rapidly than that of band 4.

5. Publication

No.

6. Problem

No.

7. Data quality and delivery

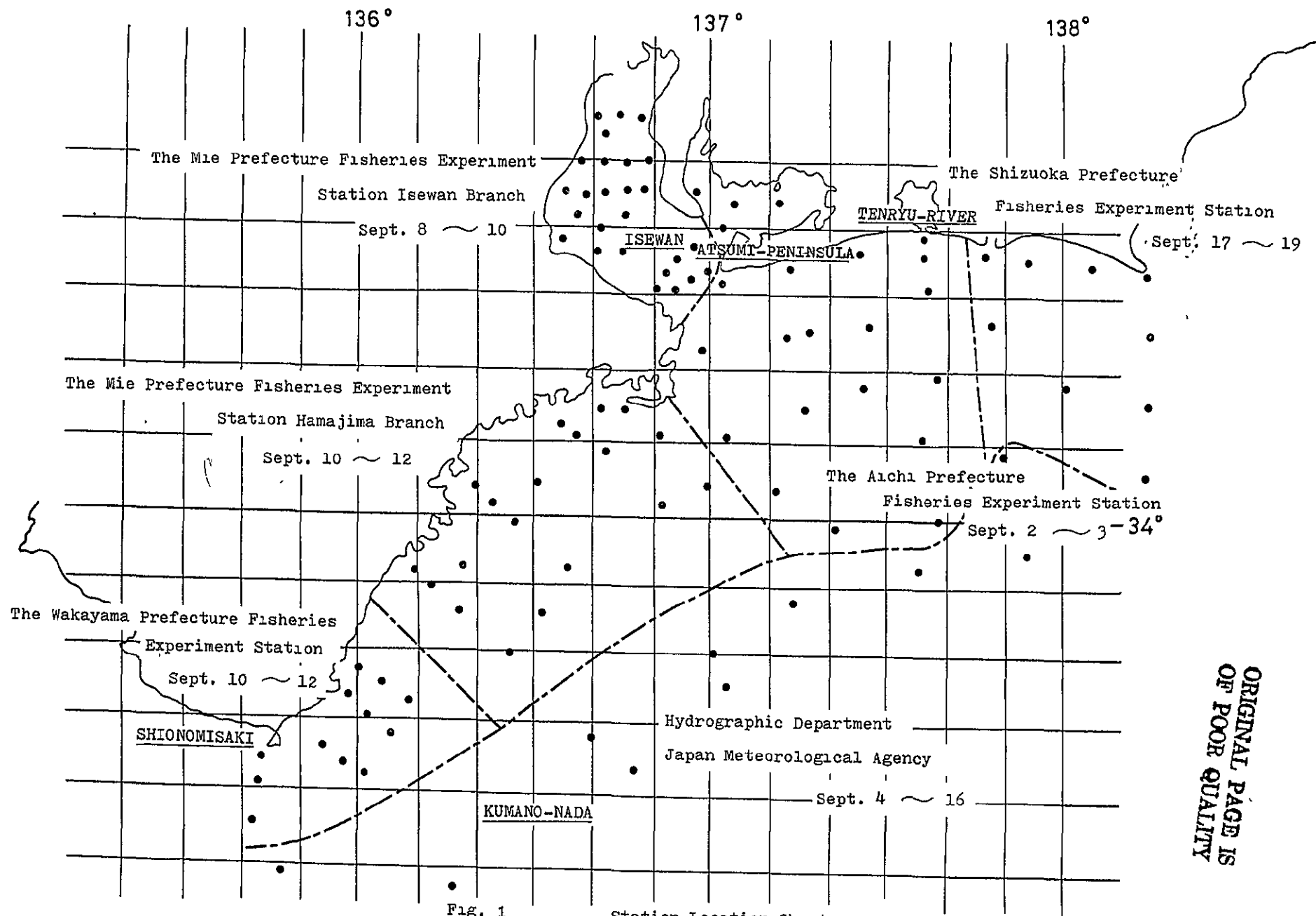
No.

8. Recommendations

No.

## 9. Conclusion

The information of band 4 was effectively used for analysis of the sea condition of a region where the different types of waters are adjacent to each other, especially the waters having different plankton density such as the coastal and offshore waters, however the difference in the CCT count is very small even in a clearly developed boundary and the linear correspondence to the sea truth data was not obtained in wider range. The thermal infra-red information could be combined for a better analysis of this kind.



ORIGINAL PAGE IS  
OF POOR QUALITY

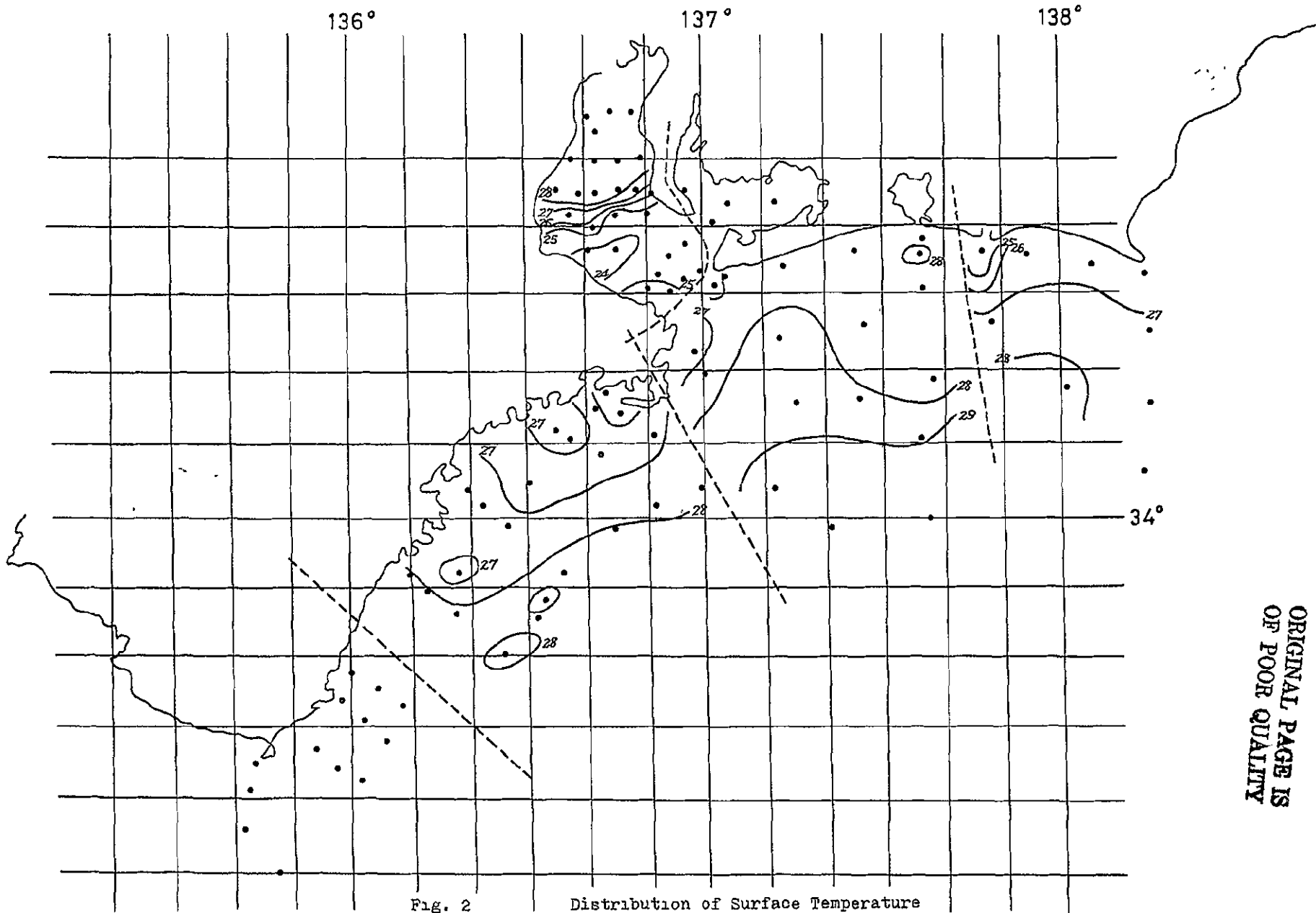


Fig. 2

Distribution of Surface Temperature

ORIGINAL PAGE IS  
OF POOR QUALITY



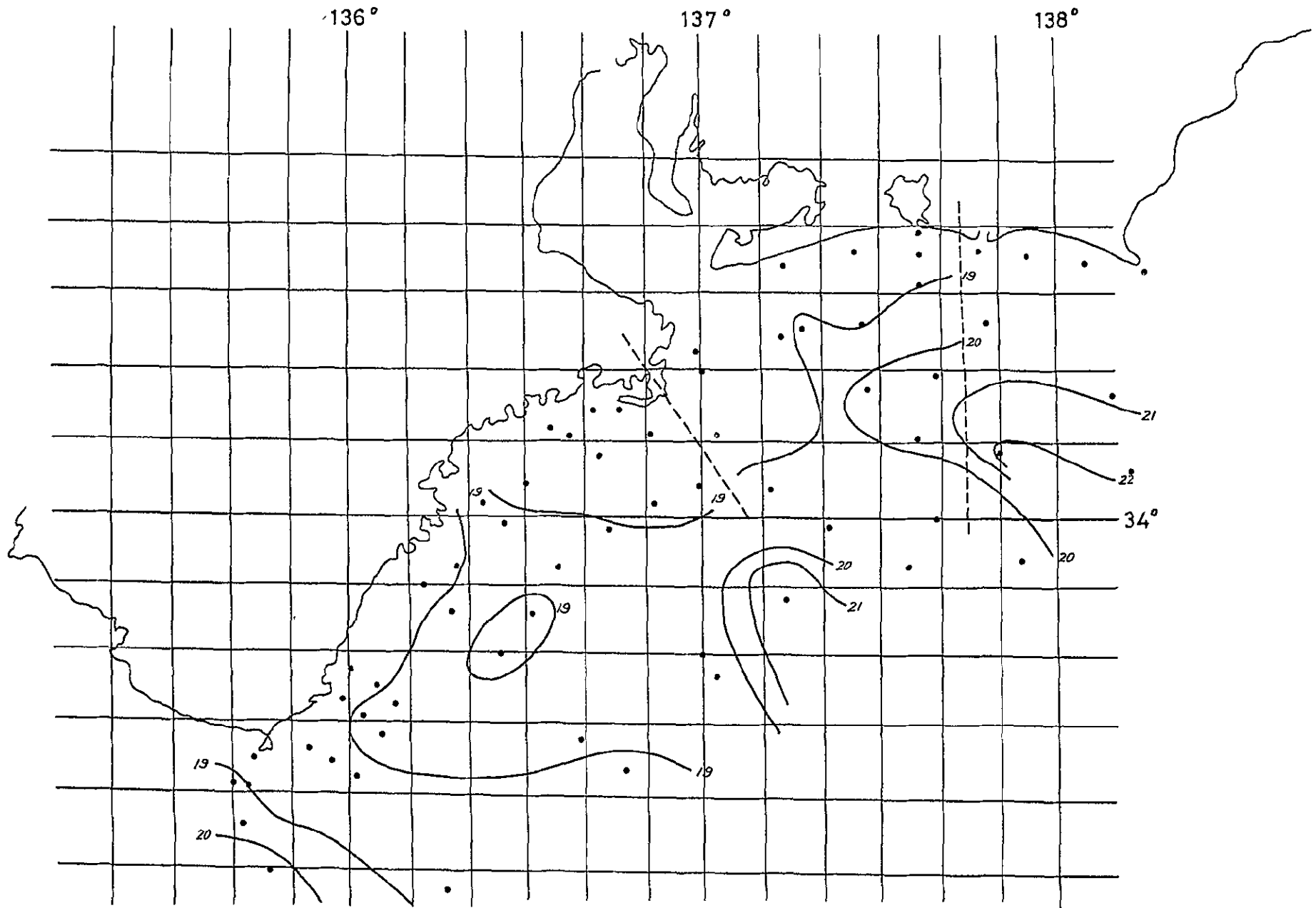


Fig. 3 Distribution of Temperature at the depths of 100m

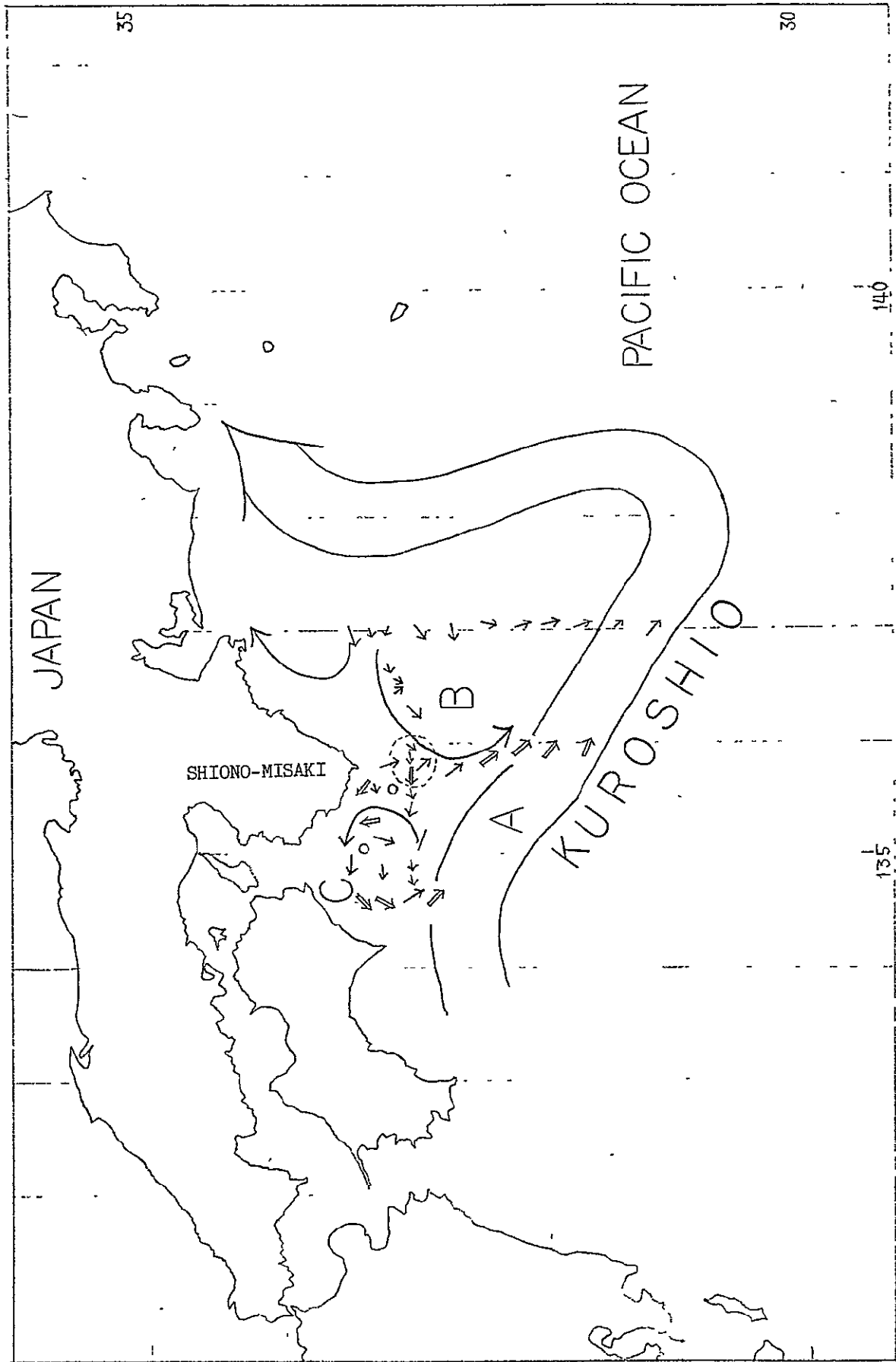
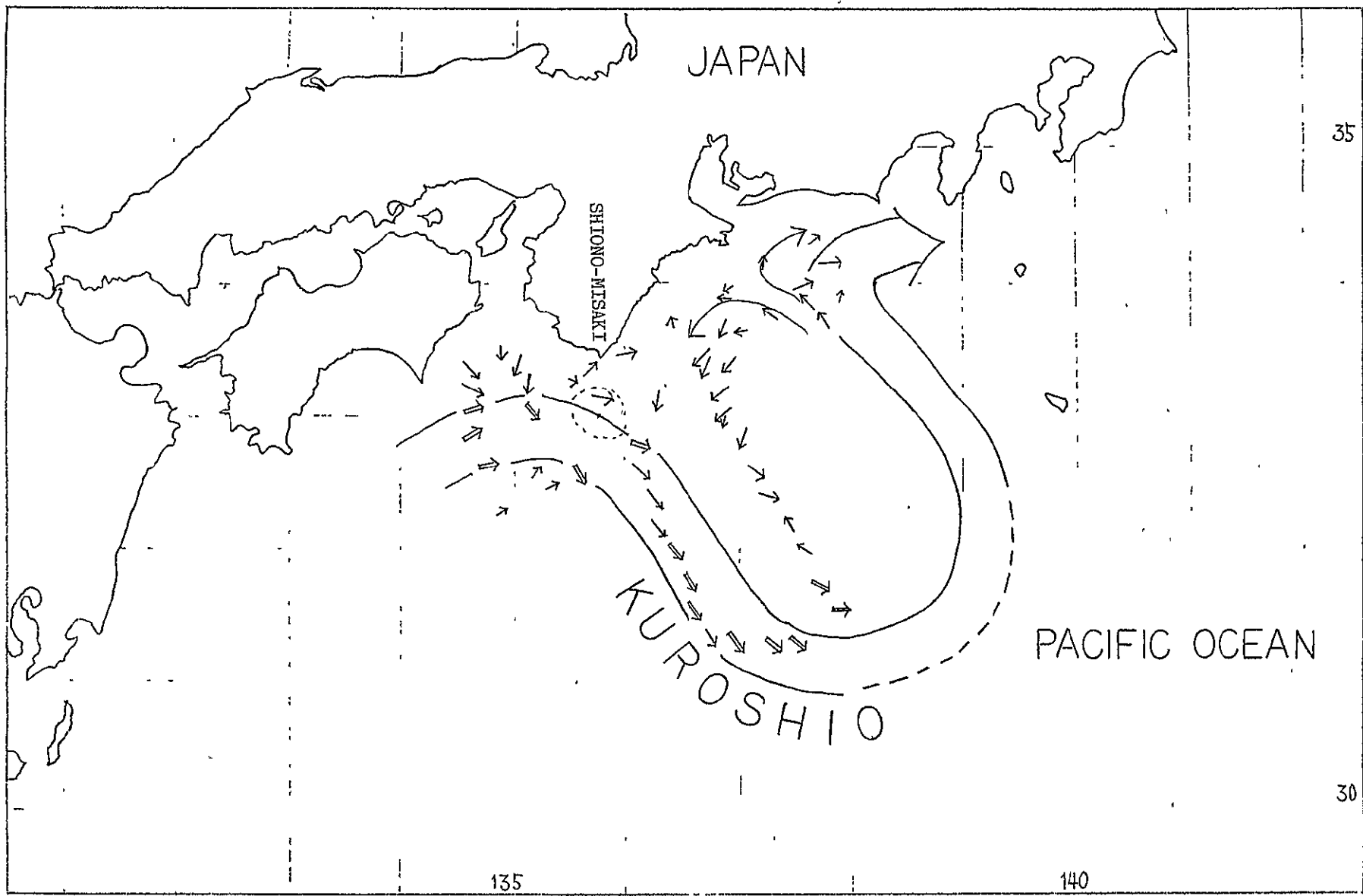


Fig. 4 Surface Current by GEK, Aug.14-Sep.3,1975

35

30



JAPAN

SHIONO-MISAKI

KUROSHIO

PACIFIC OCEAN

135

140

Fig. 5 Surface Current by GEK, Sep.8-16,1975

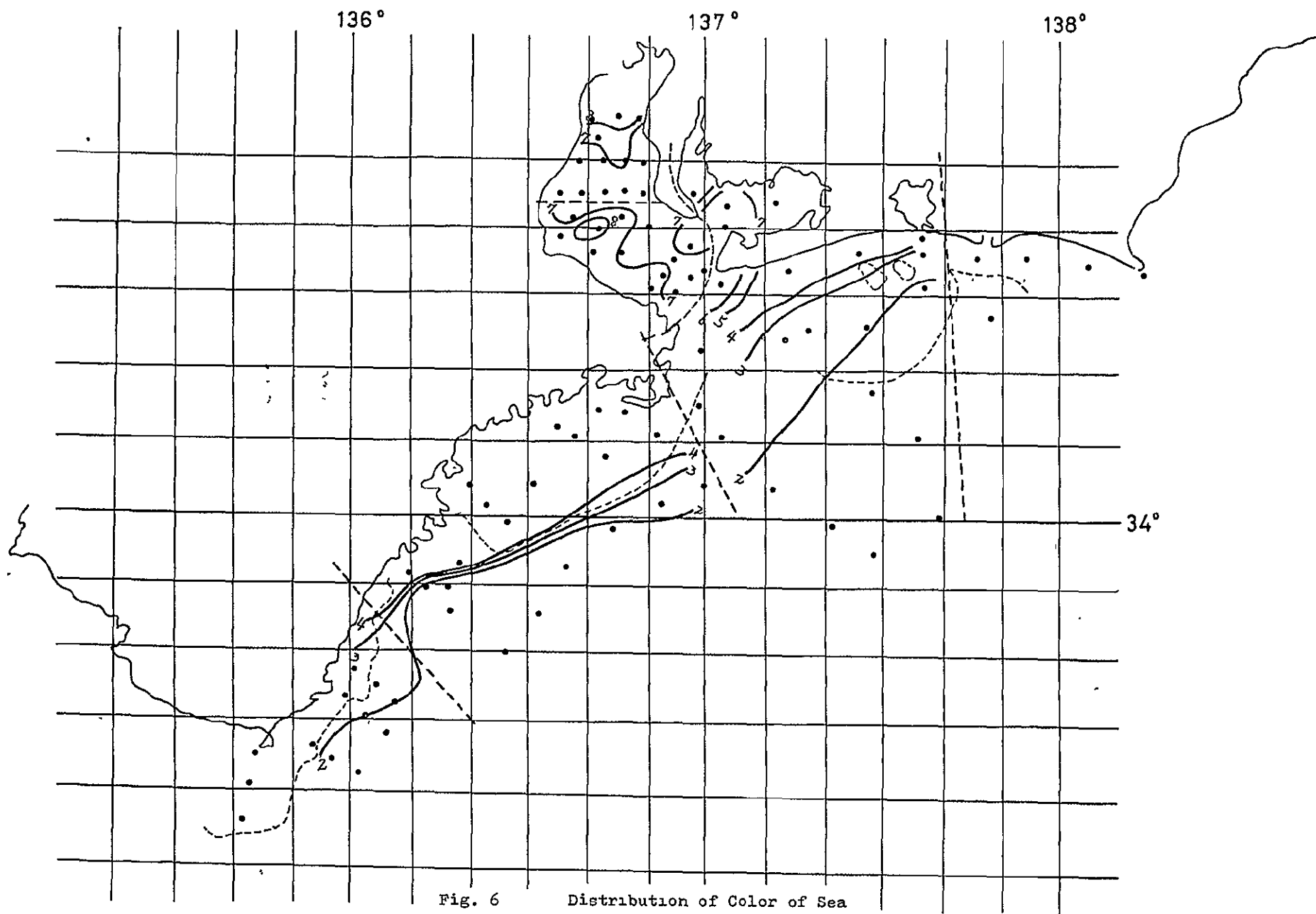
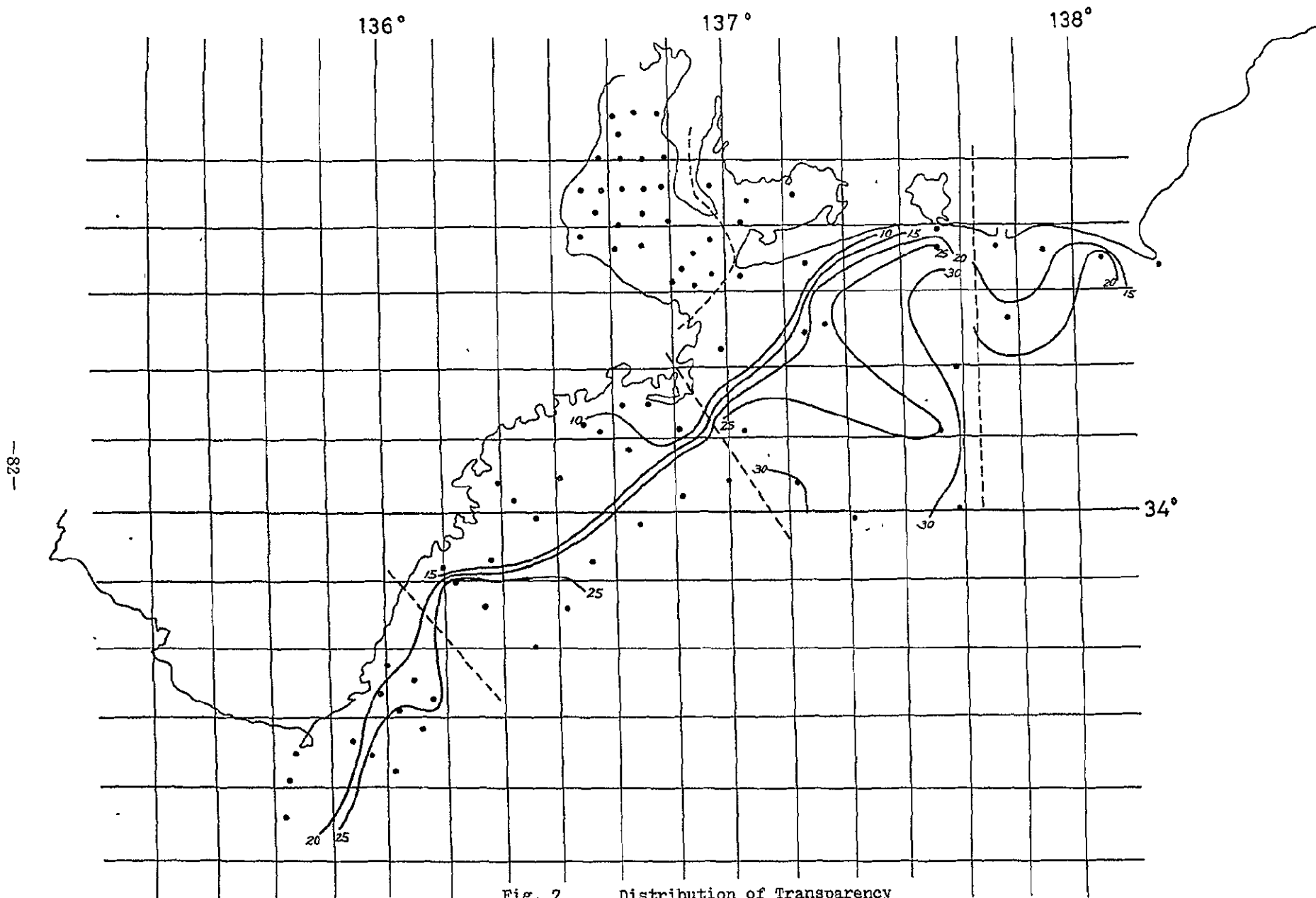


Fig. 6 Distribution of Color of Sea





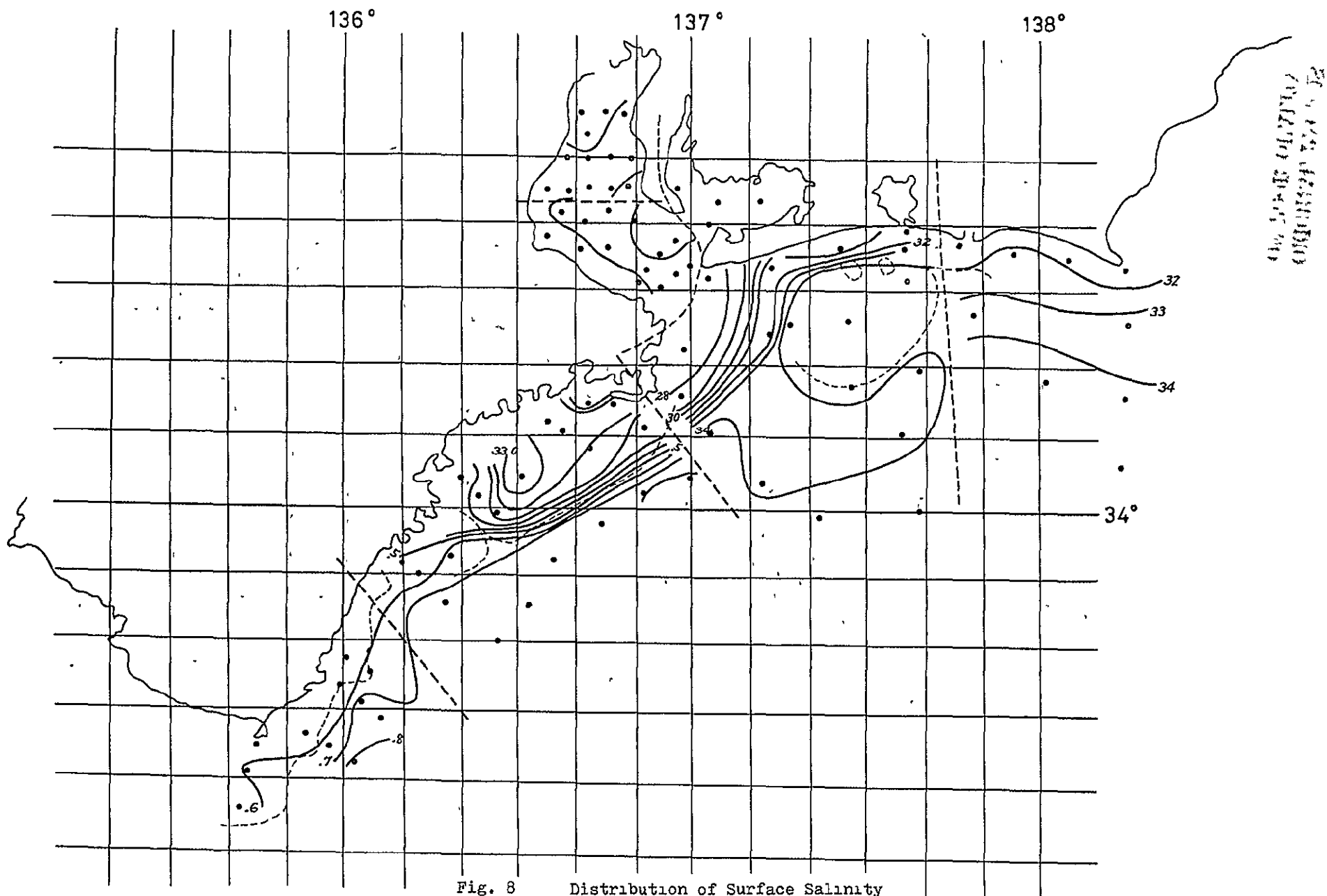


Fig. 8 Distribution of Surface Salinity

海峽部  
表面塩分分布





Fig. 10 Band 4 image enlarged from  
70mm negative film (Isewan)



Fig. 11 Band 4 image enlarged from  
70mm negative film  
(Kumano-nada)

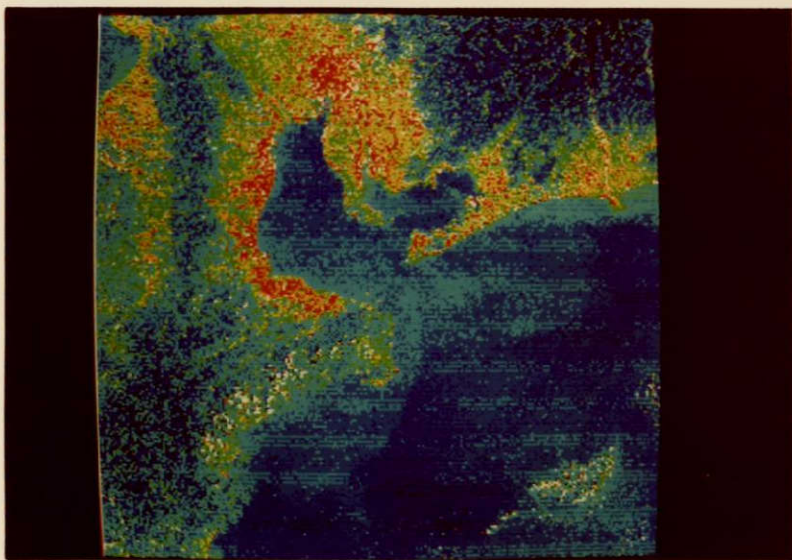


Fig. 12  
Pseudo-colors image of  
band 4 (Isewan)

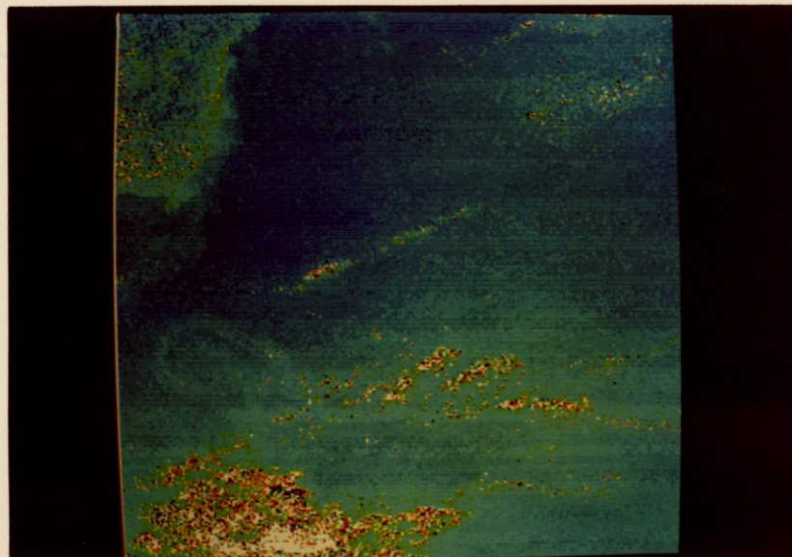


Fig. 13  
Pseudo-colors image of  
MSS band 4 (Kumano-nada)



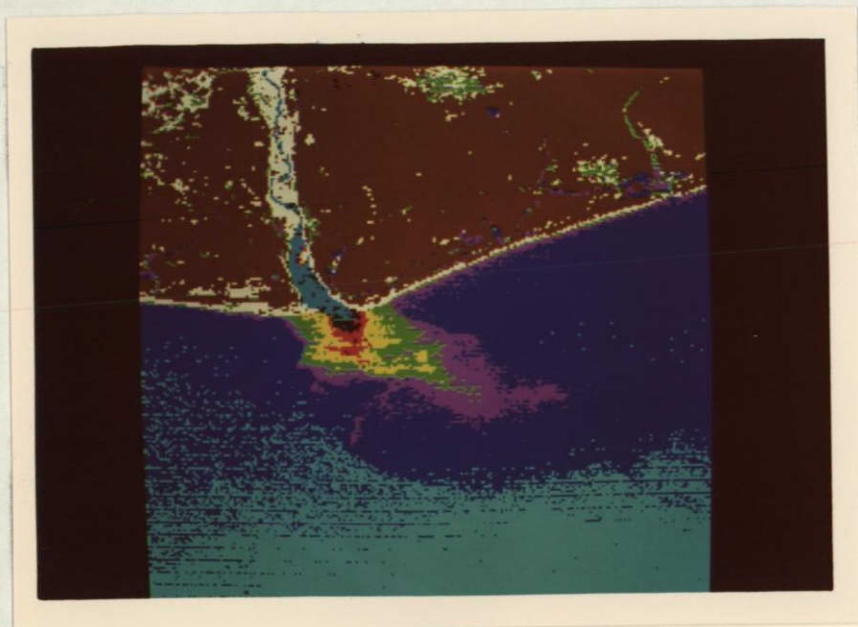


Fig. 14 Composed color image of MSS band 4, 5 and 7 (Tenryu River)

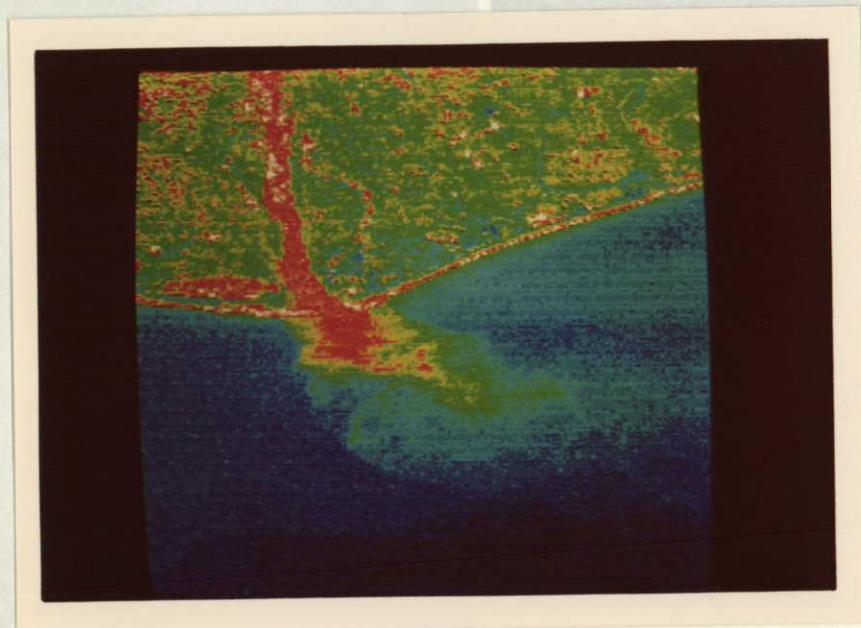


Fig. 15 Pseudo-colors image of MSS band 4

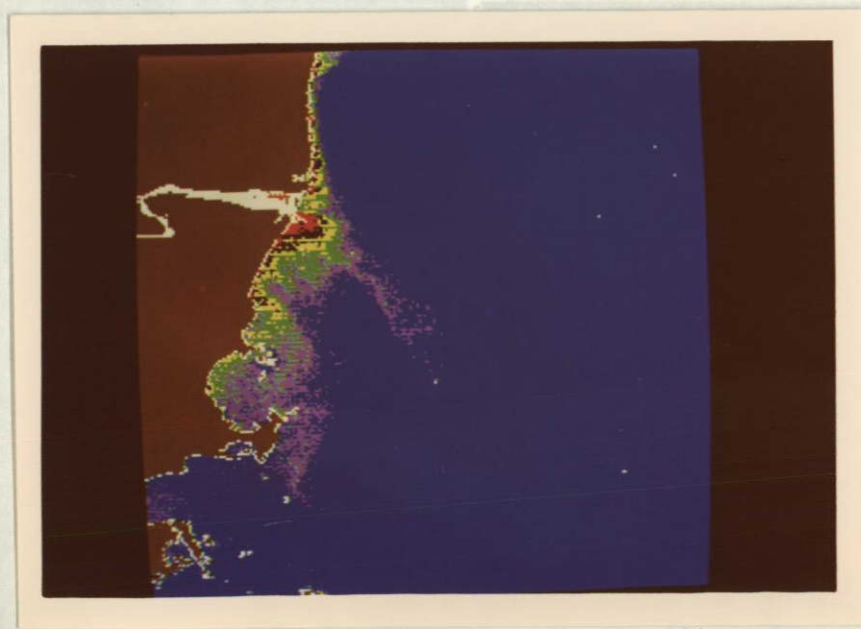


Fig. 16 Composed color image of MSS band 4, 5 and 7 (Kumano River)







ORIGINAL PAGE IS  
OF POOR QUALITY

Band 4

ORIGINAL PAGE IS  
OF POOR QUALITY

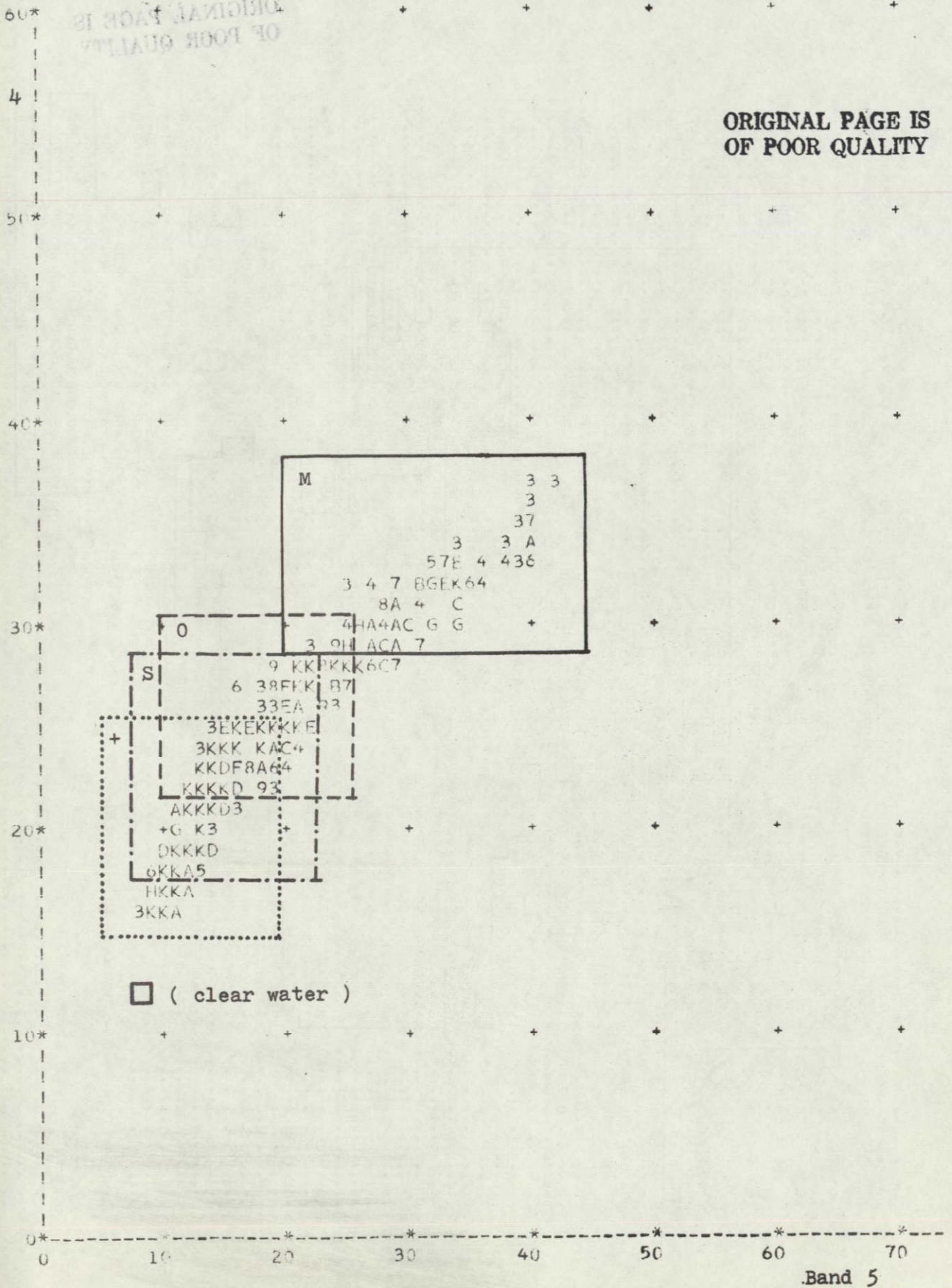


Fig.18 Density correlation between Band 4 and 5 sampled from the Mouth of Tenryu River (fFig. 17 )

ORIGINAL PAGE IS  
OF POOR QUALITY

Band 4

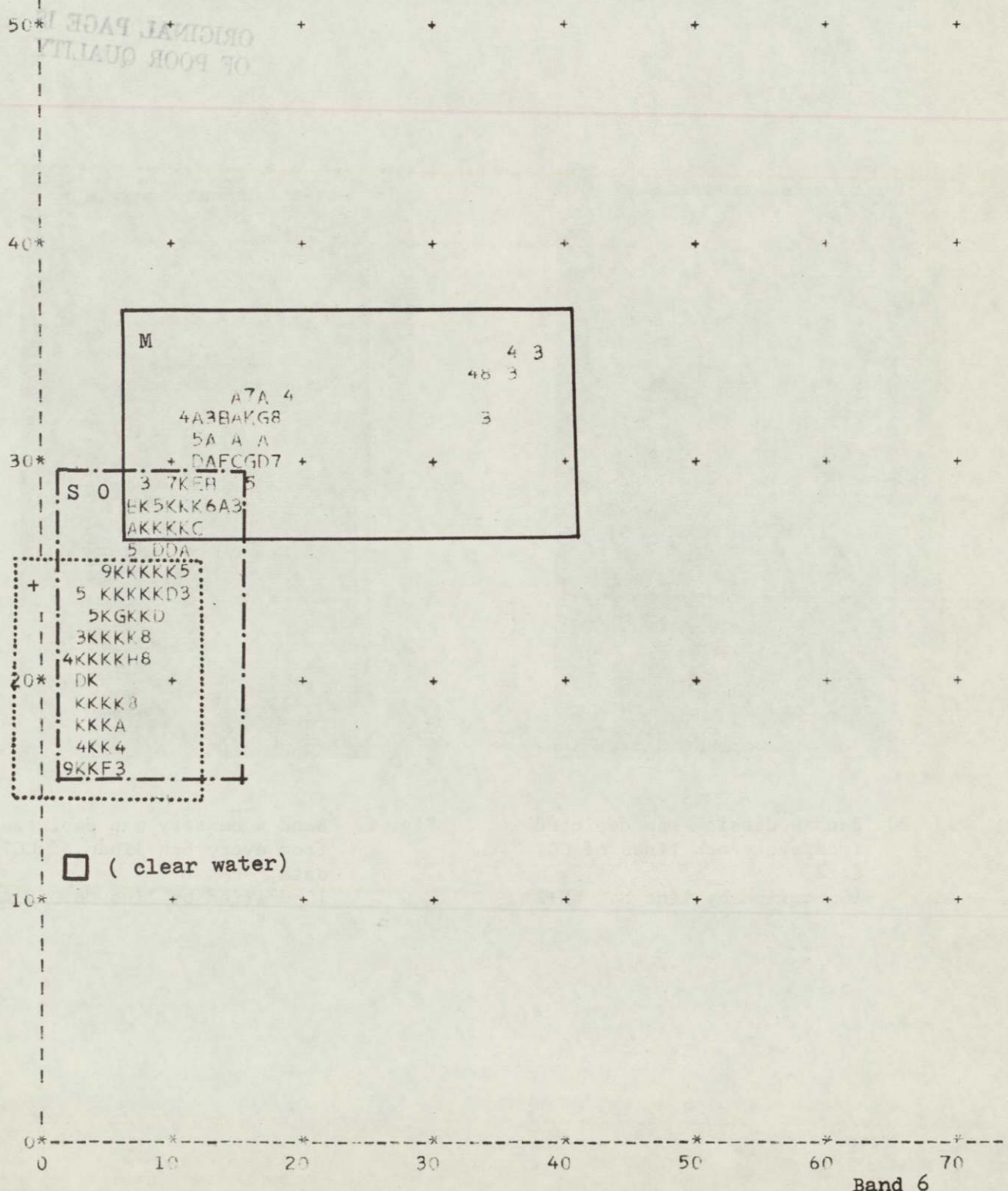


Fig.19 Density correlation between Band 4 and 6 sampled from  
the Mouth of Tenryu River ( Fig. 17 )



ORIGINAL PAGE IS  
OF POOR QUALITY

ORIGINAL PAGE IS  
OF POOR QUALITY

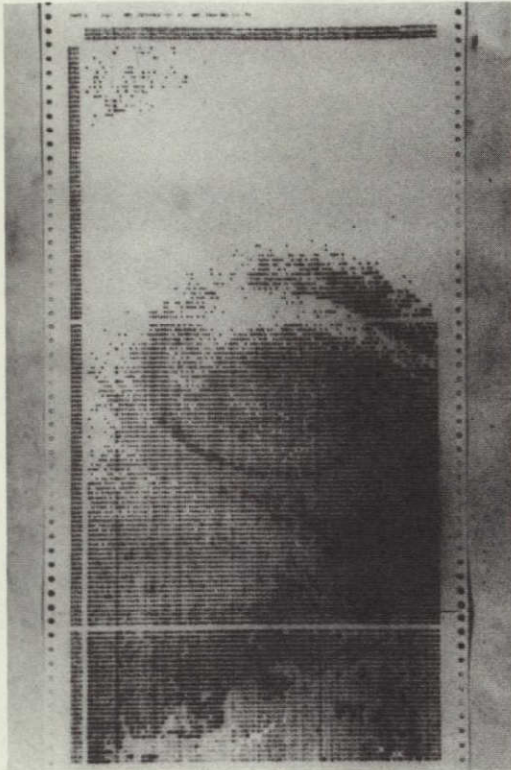


Fig. 20 Band 4 density map depicted  
from every 6th lines of CCT  
data  
(Specified by line No.  $6N+2$ )

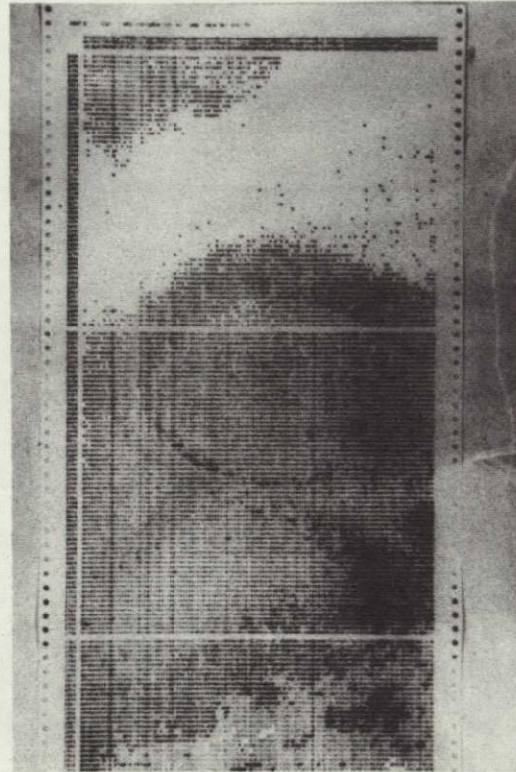


Fig. 21 Band 4 density map depicted  
from every 6th lines of CCT  
data  
(Specified by line No.  $6N+4$ )



# ENVIRONMENTAL CHANGE PATTERN IN CENTRAL JAPAN AS REVEALED BY LANDSAT DATA

Kiyoshi Tsuchiya (National Space Development Agency of Japan, 2-4-1,  
Hamamatsu-cho, Minato-ku, Tokyo, 105, Japan)

Hiroaki Ochiai (Toba National Merchant Marine College, Toba-city  
Mie-ken, 517, Japan)

## ABSTRACT

Based on the MSS data taken in early Autumn by Landsat-1 and 2 of three years time lapse, intensive studies on environmental change pattern in Central Japan including Nagoya City, the 4th largest city of the country is made.

It is found that a patched cirrus reported by weather stations over the land which is hardly recognizable by eyes in the images of MSS affects radiance values significantly in Band 4 while its effect is little in Bands 6 and 7 (Near infrared spectra). The cross correlation coefficient analysis between two images indicates the highest value of 0.96 is obtained for a peninsula with a smooth shoreline followed by a small island with the value of 0.95 while the lowest value is 0.68 for a mountainous area with a river. The analysis of land use in Nagoya area shows there is little change in the metropolitan area while fairly large change took place in the northern periphery of the city where large housing projects are going on.

### 1. Introduction

Due to the fact that the radiance values obtained at the Landsat level is the energy of reflected solar radiation by earth's surface and scattered in the atmosphere, the effect of the atmosphere is doubled. Theoretical studies of atmospheric effects on solar radiation has been made by many investigators, among them are Elterman(1968), Tanaka(1971) and Turner(1974). Rogers(1973) tried to evaluate atmospheric effect on the observed value of Landsat data, while Tsuchiya(1973, 1976) and Tsuchiya, Nakamura, Iwata and Ochiai(1975) discussed the effect of thin cirrus on the radiance value of Landsat MSS data.

Among a few good images taken over Japan during Landsat-2-Follow-On Project is the one covering central Japan including Nagoya City taken on Sep. 11 1975.



From the view point of season this image can be said that it was taken 20 days before the Landsat-1 image which was taken on Oct. 5 1972 in spite of the fact that there is three years time lapse. Making use of these two images data an attempt is made to find out environmental change in Nagoya area.

The first subject discussed is the comparison of radiance values of four selected areas in reference with the meteorological conditions. The numerical analysis on the environmental change through computation of cross correlation coefficient between the two images described before is the second subject. The third subject is the change of land use in Nagoya city and its suburbs.

## 2. The image of central Japan taken by Landsat-1 and 2

In Fig. 1 (a - d) are shown the images of central Japan including Nagoya city, the fourth largest city of Japan with 2 million population. The images were taken by Landsat 1 and 2 on Oct. 5 1972 and Sep. 11 1975 respectively. Throughout the study the former is called the old while the latter is called the new for short. Comparing the new and old images a large difference in the appearance is recognized over the ocean where clouds are visible in the old image while not in the new. As far as a part of the image over the land, no significant difference is recognized.

## 3. Atmospheric condition

In an attempt to see the actual atmospheric condition, weather map analysis is made and shown in Fig. 2. The area corresponding to the Landsat image is indicated by broken line. In the figure the weather, clouds and winds are plotted in standard WMO code. Numerals in the figure are visibility in the unit of km.

On Oct. 5 1972 most of the stations reported patched thin cirrus and smog was observed at Nagoya. General cloud distribution was such that the clouds were thicker towards east, west and south. On Sep. 11 1975 no cloud was observed at the weather stations within the image boundary. The distribution of visibility on both days is similar except eastern part where that of Oct. 5 1972 showed a poor visibility. The poor visibility of Nagoya is due to smog which is caused by dusts and smoke from the factories and heavy traffics. It is interesting to see that the visibility at Nagoya is same on both days. In order to see the vertical atmospheric condition, radio sounding at Hamamatsu (as to location see Fig. 2. (b)) are plotted and shown in Fig. 3.



ORIGINAL PAGE IS  
OF POOR QUALITY

ORIGINAL PAGE IS  
OF POOR QUALITY

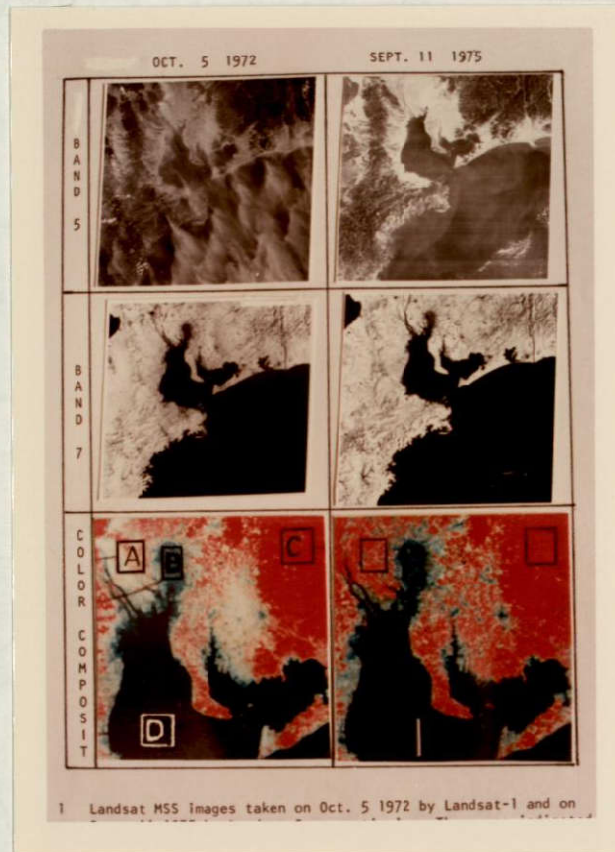


Fig. 1 Landsat MSS images taken on Oct. 5, 1972 by Landsat-1 and on Sept. 11, 1975 by Landsat-2 respectively. The areas indicated by letters A, B, C and D are the areas over which digital analysis is made in section 4.

C-2



ORIGINAL PAGE IS  
OF POOR QUALITY

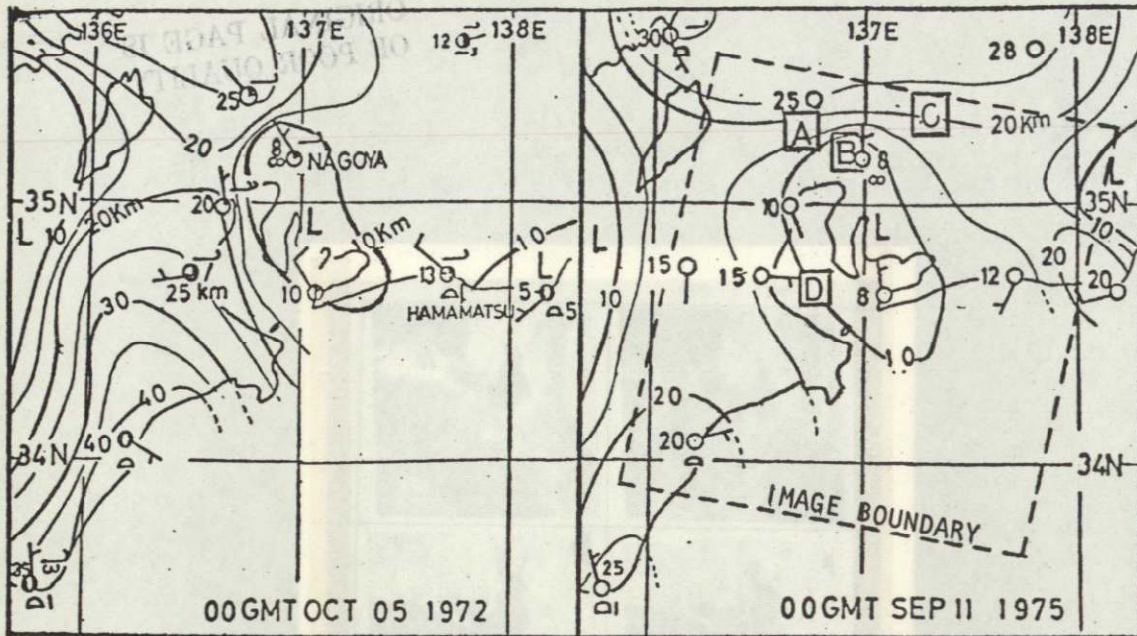


Fig. 2 Weather map at 00 GMT on Oct. 5 1972 and Sep. 11 1975. Numerals are visibility in kms and solid line is iso-visibility line.

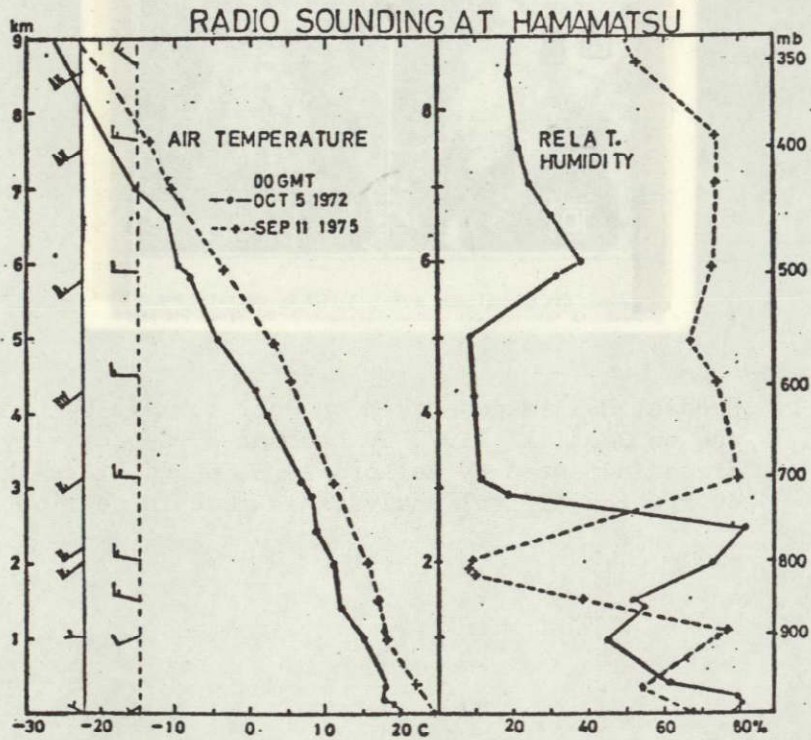


Fig. 3 Radio sounding at Hamamatsu at 00 GMT on Oct. 5 1972 and Sep. 11 1975 respectively showing vertical distribution of air temperature and relative humidity. Winds are also shown in standard WMO Code.



The vertical distribution of air temperature on both days is similar except a very slight inversion in the lower layer close to the ground level observed on Oct. 5 1972, however there is a fairly large difference in the distribution of relative humidity which is shown in the right hand side of the figure. The phase of vertical distribution is somehow opposite. There is an extremely dry layer at 800-mb level on September 11 1975 while on Oct. 5 1975 above 700-mb level it is very dry except at 500-mb. On Sep. 11 1975 a fairly thick wet layer exists between 400 and 700-mb levels.

If aerosols in the upper layer is assumed same, the main factors contributing to solar radiation reaching the ground is smog and water vapor. Since water vapor is a unique function of air temperature, it is considered that total amount of water vapor or precipitable water in the air column on both days is not much different in spite of the difference in vertical distribution pattern of relative humidity.

#### 4. Radiance values of four selected areas

Making use of the CCT's supplied from NASA the mean values and standard deviations of digital numbers corresponding to radiance over four selected areas, i. e. a farming area, Nagoya City, a mountain area with thick ever green trees and sea surface of Ise Bay are computed and shown in Table 1. The locations of the areas are shown in Fig. 1 and 2.

Table 1 Mean and standard deviation of digital number of four selected areas. A: Farming area, B: Nagoya City, C: Mountain area with thick evergreen trees, D: Sea surface.

		00 GMT OCT 5 1972				0048 GMT SEP 11 1975			
		B4	B5	B6	B7	B4	B5	B6	B7
A	M	39.3	32.0	43.5	21.5	22.8	22.9	47.1	21.7
	S.D.	7.0	3.2	4.7	3.0	3.1	4.8	6.9	4.5
B	M	37.8	31.7	29.1	12.1	27.7	30.5	31.1	10.9
	S.D.	6.3	3.0	2.9	1.6	2.8	4.5	5.4	2.6
C	M	23.1	14.5	33.3	19.5	12.5	10.7	38.1	19.8
	S.D.	8.3	3.2	6.7	4.5	2.0	2.9	8.4	5.0
D	M	25.7	15.5	11.3	3.4	13.3	9.5	4.0	0.3
	S.D.	1.4	1.3	1.4	0.8	0.8	0.8	0.9	0.0



Over the land areas, there is a certain similarity, i. e. the digital numbers of Bands-4 and 5 of Oct. 5 1975 are systematically larger than those of Sep. 11 1975 even if the incoming solar radiation is a little smaller. On the other hand at Band 6 the value of the latter is larger and at Band 7 the value is nearly equal. Apparently the effect of thin cirrus and atmospheric condition are well reflected in the values of Bands-4 and 5 while the contribution of them is not so large in Bands-6 and 7 or it can be concluded that the effect is negligible.

The global albedo defined as the ratio of outgoing and incoming solar radiation at the outside of the atmosphere is computed and shown in Table 2. In the conversion of digital number into radiance, the values in Landsat User's Handbook(1972) is used.

Table 2 Global albedo for the four selected areas (%)

	OCT. 5 1972				SEPT. 11 1975			
	B4	B5	B6	B7	B4	B5	B6	B7
A	45.4	36.0	49.0	49.1	24.3	23.9	49.0	45.5
B	43.6	35.8	32.9	27.6	29.5	31.6	32.2	22.9
C	26.8	16.4	37.5	44.5	13.4	11.1	39.5	41.6
D	12.0	17.5	12.6	7.7	14.2	9.8	4.1	0.0

In average over the land the value of Band 4 of the old is larger than that of the new by 16 % while the difference becomes -0.6 % and 3.7 % in Bands- 6 and 7 respectively. The larger value of the old in Bands- 6 and 7 can be attributed to the effect of vegetation since the leaves of vegetation are more green with larger reflectance in near-infrared spectra.

##### 5. Numerical analysis of environmental change during the three years

In order to find out the degree of environmental change, a cross correlation analysis is made using the values of Band 7 data. Since the radiance value has the least atmospheric effect as is indicated in the previous analysis. In the computation of cross correlation coefficient, the following procedures are taken. First, reference areas are selected from the old image the location of which is indicated in Fig. 4.



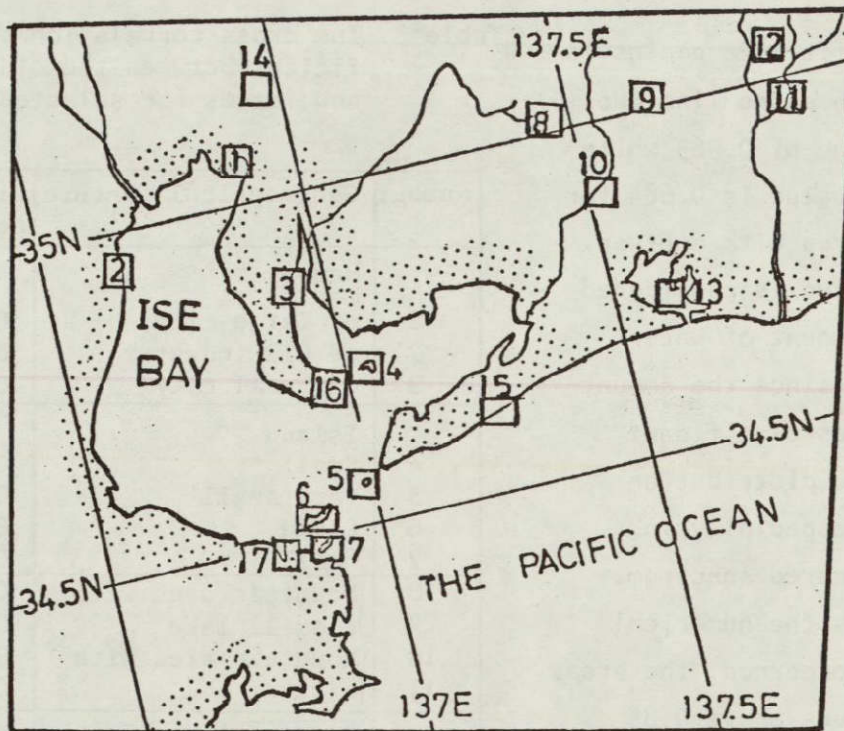


Fig. 4 A map showing the the locations where reference templates were taken.

From each reference area a template composed of 64x64 picture elements (pixels) is made. Then cross correlation coefficients are computed between the template and the corresponding areas in the new image. In order to avoid mis-registration, the computation is made by Eq. (1).

$$C(m,n) = \frac{\sum_{i=1}^M \sum_{j=1}^M [X(i+m, j+n) - \bar{X}(m,n)][Y(i,j) - \bar{Y}]}{\sqrt{\sum_{i=1}^M \sum_{j=1}^M [X(i+m, j+n) - \bar{X}(m,n)]^2} \sqrt{\sum_{i=1}^M \sum_{j=1}^M [Y(i,j) - \bar{Y}]^2}} \quad (1)$$

where,  $X$  and  $Y$  denote radiance values of each pixel in the new and the old images respectively and  $M$  is fixed as 64. The size of the areas in the new image is fixed to be 4 times as large as a template with the template approximately in the center. Then computation is made by changing  $l$  and  $m$  then the largest value of cross correlation coefficients is selected. The result of computation is indicated in Table 3.



The best fit is a peninsula with a smooth shore line (No 15) with the value of 0.963 while the poorest value is 0.684 for a mountain area with a river. This poor value is considered due to the amount of water in the river since the amount of water gives significant effect on the distribution of radiance especially in the near-infrared spectrum.

As far as the numerical values are concerned, the areas with the values above 0.85 may be defined as the area with little environmental change. It should be also added that the area named as a city (No 14) is picked up from eastern part of Nagoya city where land use change took place during the three years.

Table 3 The cross correlation coefficient between the old and the new images for selected areas

Number	Geographical feature	Cr. Cor. Coeff.
	Harbor	
1	of Large city	0.840
2	of Oil industry	0.888
3	of Small city	0.887
	Island	
4	Small	0.928
5	Very small	0.928
6	Large	0.935
7	Small	0.946
8	Mountain area with a small lake	0.789
9		0.811
10		0.801
11	Mountain area with a river	0.684
12	Summit with trees	0.809
13	Lake with a bridge	0.935
14	Large city	0.762
	Peninsula	
15	with smooth shore line	0.963
16	Same as above	0.955
17	with Complicated shore line	0.938

## 6. Land-use analysis in Nagoya City

Further land use classification is made for Nagoya area. The area analyzed is approximately  $20 \times 20 \text{ km}^2$ . Classification is made into 6 categories, i. e. forest, agricultural, open, urban, suburban, water, new urban areas and others. The result of analysis is indicated in Fig.5 in which original 16 pixels are combined into one pixel therefore pixel in the figure corresponds to the area of  $316 \times 316 \text{ m}^2$ . In the figure a large area of blue color in the center is urban area and denotes the metropolitan area of Nagoya City. Comparing two images it can easily be



recognized that very little change took place in metropolitan area while changes took place in the periphery of the city.

To show more clearly the land use change, based on the two classified images, a land use change analysis is made and shown in Fig. 6 which shows large change in the areas to the north of metropolitan area. Ground surveys indicate that a number of large scale housing projects were going on at the observation time. It is also seen a fairly large variation of land use in the south-eastern area, however, here individual size is not so large.

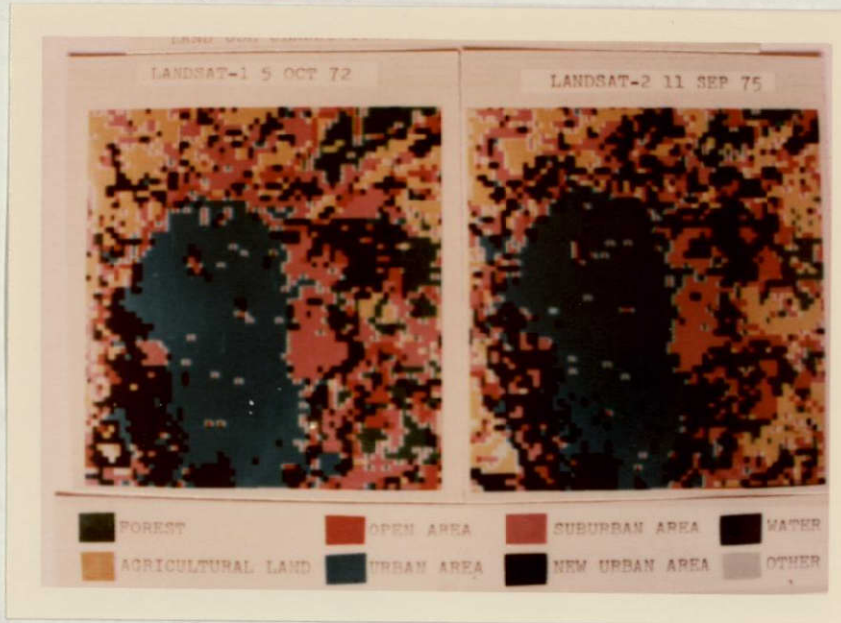


Fig. 5 Land use classification of Nagoya City and its suburbs. Left hand: Oct. 5 1972, Right hand: Sep. 11 1975

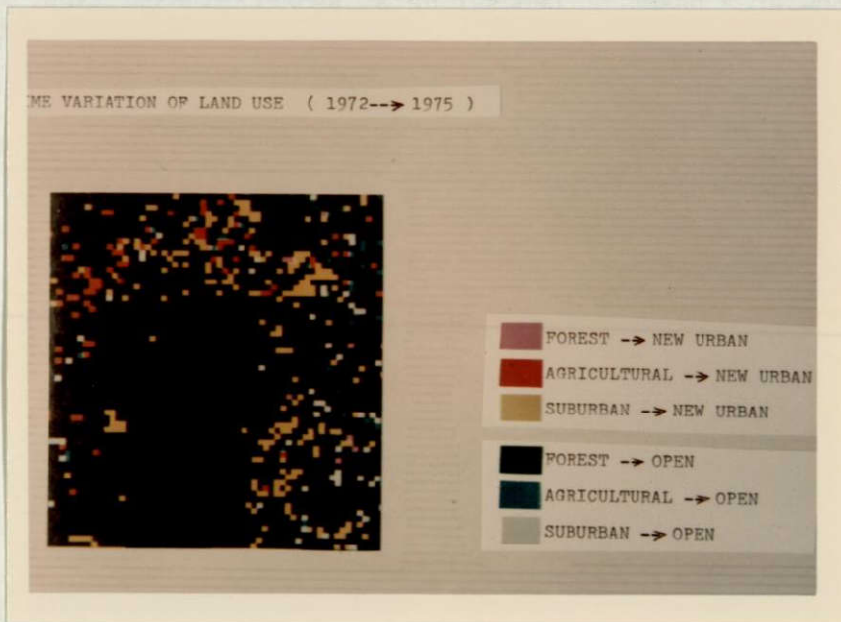


Fig. 6 Land use change in Nagoya City and its suburbs during 3 years between Oct. 5 1972 and Sep. 11 1975.

ORIGINAL PAGE IS  
OF POOR QUALITY



## 7. Concluding Remark

The foregoing analyses lead to the following conclusion. In the digital analysis of Landsat data, care must be taken for thin cirrus which often is hard to recognize visually. At the same time MSS data can be effectively used for the study of atmospheric radiation. Cross correlation analysis indicates the highest value obtained in central Japan is 0.963 for the area where little change occurred in land use. This suggests that a certain care must be taken in applying GCP matching method in precision processing of landsat raw data. Landsat MSS data are extremely useful for making land use map for a large area.

### References

- Elterman, L., 1968: Visible and IR attenuation for altitude of 50 km. AFCRL-68-0153.
- Rogers, R. H., K. Peacock and N. J. Shah, 1973: A technique for correcting ERTS data for solar and atmospheric effects. NASA, SP-351, 1787-1804.
- Tanaka, M, 1971: Radiative transfer in turbid atmosphere II. Angular distribution of intensity of solar radiation diffusely reflected and transmitted by turbid atmosphere. J. Meteor. Soc. Japan, 49, 339-342.
- Tsuchiya, K. and T. Kamiko, 1973: Application of ERTS data to the detection of thin cirrus and clear air turbulence. NASA-SP-327, 673-680.
- \_\_\_\_\_, 1976: Study of mesoscale phenomena, winter monsoon clouds and snow area based on Landsat data. NASA-CR-14635, 33pp.
- \_\_\_\_\_, H. Nakamura, T. Iwata and H. Ochiai, 1975: Characteristics of multi-spectral images obtained from space around Japan. Pro. 11th Int. Symp. on Space Tech. and Sci. 903-908.

ORIGINAL PAGE IS  
OF POOR QUALITY

## PURPOSE OF INVESTIGATION

The Seto-Inland Sea in Japan, nearly enclosed by the western part of the Honshu, the northern Kyushu and the Shikoku (Fig.1) is one of the most beautiful seas in the world having numerous tiny islands of green pine trees. However, the sea has been seriously polluted with the rapid development of industries in those fifteen years. The water pollution in the sea is not only reducing value of its beautiful scenery, but also destroying fishery environments and gradually becoming harmful for human living.

In the present investigation, it is aimed for assisting in the monitoring of water pollution in the sea to have a general pattern of turbid water. In the sea, most part of which is the artificially polluted water, using multispectral imageries by the LANDSAT-1 and -2.

## USED DATA

Each sea regions in the Seto-Inland Sea were taken in multispectral imageries by the LANDSAT-1 and -2 on the dates in Table-1. The LANDSAT multispectral imageries taken on the dates underlined in Table-1 were used in the present investigation because of its low cloudiness.

Table-1

---

OSAKA-BAY and KII-STRAITS :

on 24 Oct., 1972, 3 Jan., 1973 by the LANDSAT-1

---

HARIMA-NADA, BISAN-SETO and HIUCHI-NADA :

on 12 Nov., 1972, 23 Jan., 1973, 4 Jul., 1973 by the LANDSAT-1,  
and 30 Dec., 1975 by the LANDSAT-2

---

AKI-NADA, IYO-NADA and THE EASTERN SUO-NADA :

on 15 Aug., 1972, 8 Oct., 1972, 6 Jan., 1973 and 5 Jul., 1973  
all by the LANDSAT-1

---

THE WESTERN SUO-NADA :

on 21 Oct., 1975 by the LANDSAT-2

---

THE SOUTHERN SUO-NADA, that is the sea north of THE BUNGO STRAITS :

on 15 Aug., 1972 by the LANDSAT-1

---

#### ANALYTICAL TECHNIQUE

The light incident upon the multispectral scanner on board LANDSAT consists of two parts. One is useful light for oceanographic investigations scattered from fine particles suspended in the turbid water, such as river-discharged sediments, artificial pollution materials and plankton, and reflected at the bottom when the sea is sufficiently shallow (hereafter under-water informations). Another is harmful light for interpreting under-water informations diffusely reflected from cloud covers, smog layers, sea fogs, and from inclined surfaces of numerous wavelets when the optical



condition is fit (hereafter atmospheric informations). Therefore, any imageries or pictures in the visible region of the sea taken from the space are of complex pattern due to the image combination of under-water informations and of atmospheric informations. Thus, it is necessary in any oceanographic investigation using LANDSAT data to extract patterns of under-water informations separately from the ones of atmospheric informations.

Among these light components, the useful lights from under-water informations are more attenuated in longer wavelength regions, strongly in the near-infrared region, before transmitted through the water layer. Whereas the harmful lights from atmospheric informations are nearly not attenuated by water layer in all wavelength regions because they traverse only in the atmosphere. According to such a difference of the attenuation character, gray patterns in the sea in imageries of the band of MSS-4 (0.5-0.6 $\mu$  in wavelength) or of MSS-5 (0.6-0.7 $\mu$ ) represent under-water informations together with atmospheric informations, and the ones of MSS-7 (near-infrared, 0.8-1.1 $\mu$ ) do only atmospheric informations. Thence, oceanographic informations can be extracted by the image masking technique, that is, by the image subtraction of the pattern in the MSS-7 from the one in the MSS-4 or the MSS-5 by appropriate photographic or digital processes.

In the present investigation, photographic image-masking processes were made for the MSS-4, MSS-5 and MSS-7 imageries of the Osaka Bay and the northern Kii Straits on 24 Oct., 1972, of Harima-Nada, Bisan-Seto and Hiuchi-Nada on 12 Nov., 1972, 23 Jan., 1973 and 4 July 1973, of the Aki-Nada, Iyo-Nada and the eastern Suo-Nada on 15 Aug., 1972, and of the western Suo-Nada on 21 Oct., 1975. A digital process for the image-masking was applied to MSS-4 and the MSS-7 CCT data of the Hiuchi-Nada on 12 Nov., 1972, 23 Jan., 1973 and 30 Dec., 1975.

## PATTERNS OF TURBID WATER EXTRACTED

- 1) Osaka Bay and the northern Kii Straits, by LANDSAT-1, on 24 Oct., 1972. (Fig.2)

By applying the photographic image-masking technique to the multispectral scanner imageries taken on 24 Oct., 1972, patterns of turbid water were made (Fig.2), where land areas and cloud covers, maybe including smog layers, are shown white in color and under-water informations, areas of turbid water in this case, are represented as patterns of darker or the darkest gray color. The darkest gray patterns came from the couple of MSS-5 (orange band) and MSS-7 (near infrared band) imageries, which show dense turbid waters in the upper-most layer, maybe within 2 or 3 meters or so (G.A.Maul, 1975) because of rather large value of the attenuation coefficient in the orange band. The darker gray patterns were made by the image-masking process using the couple of MSS-4 (green band) and MSS-7 imageries, which represent turbid waters in a layer up to the depth a little bit deeper than the one in the couple of MSS-5 and MSS-7 because the attenuation coefficient in the green band is smaller than the one in the orange band. Then, the remained areas of lighter gray color mean fairly clear water extracted by a density-slicing process.

A large volume of turbid water discharged from the Yoshino River in Shikoku which was caused by a heavy rain falling on Oct. 22 extends in the nearly western-half part of the northern Kii Straits reaching the southeast corner of the Harima-Nada and flowing southward along the east coast of Shikoku.

As the northeast corner of the Osaka Bay near Osaka City and Kobe City was unfortunately covered by clouds and a likely smog layer, the heavily polluted water there produced in the largely populated and highly industrial

zone was not revealed in the imagery. However, the largeness in volume of the turbid water can be inferred from the pattern of turbid water broadly distributing in the central part of the bay and extending to the northeast corner of the Harima-Nada passing through the Akashi Channel north of the northern tip of the Awaji Island.

There appears in Fig.2 an interesting eddy-like pattern of turbid water north of the Kitan Channel, the south mouth of the Osaka Bay. It is clear that this eddy was developed by the northward flowing the tidal current which stage was at one and a half hours after the time of the maximum westward flowing in the Akashi Channel. Through the southwestern part of this eddy-like turbid water is seen in Fig.2 as if it connected to the turbid water from the Yoshino River in the sea southeast off the Awaji Is., it is likely assumed as to a part of turbid water produced in the Osaka Bay not to a part of the turbid water from the Yoshino River by a classification analysis with a 2-dimensional feature space of MSS-4 and MSS-5 brightness levels.

- 2) Harima-Nada, Bisan-Seto, by LANDSAT-1, on 12 Nov., 1972 (Fig.3) and on 23 Jan., 1973 (Fig.4)

Patterns of turbid water in the central part of the Seto-Inland Sea, that is, the Harima-Nada, Bisan-Seto, and Hiuchi-Nada on 12 Nov., 1972 and on 23 Jan., 1973 are shown in image-masking imageries in Fig.3 and Fig.4, respectively. It is noted in both figures that patterns of turbid water are generally similar on 12 Nov., 1972 and 23 Jan., 1973 except of the pattern of turbid water extending southward in the eastern region of the Harima-Nada on 12 Nov., 1972. The pattern of turbid water from the Yoshino River on 12 Nov., 1972 (Fig.3) is also very similar to the one on 24 Oct., 1972 (Fig.2).

- 3) Hiuchi-Nada, by LANDSAT-1 on 12 Nov., 1972 (Fig.5), on 23 Jan., 1973 (Fig.6), and by LANDSAT-2 on 30 Dec., 1975 (Fig.7)

Fig.5, Fig.6 and Fig.7 are distribution charts of turbid water on 12 Nov., 1972, 23 Jan., 1973 and 30 Dec., 1975, respectively, made by digital image-masking process where the apparent turbidity is separated in three relative ranks due to brightness level in digital maps. Though each patterns of these three days are different each other in some degrees, there appears a general pattern that nearly the southwestern-half of the Hiuchi-Nada is commonly more turbid whereas the eastern part of the sea is always less turbid. This suggests together with the former cases of Fig.3 and Fig.4 that each image-masking imagery approximately represents a general pattern of turbid water in each corresponding sea region.

- 4) Aki-Nada and Iyo-Nada, by LANDSAT-1, on Aug., 1972

There are rather few LANDSAT data for the region of the Aki-Nada north-west off Matsuyama City in Shikoku. Furthermore, the transparency in the atmosphere was insufficiently good for interpreting any under-water information in the only image-masking imagery made from the LANDSAT-1's multispectral imageries on 15 Aug., 1972. Thus, any information about turbid water was not succeeded to be extracted in the Aki-Nada and Iyo-Nada.

- 5) The Western Suo-Nada, by LANDSAT-2, on 21 Oct., 1975 (fig.8)

The image-masking imagery in Fig.8 was from LANDSAT-2's MSS-4 and MSS-7 imageries on 21 Oct., 1975 which shows patterns of turbid water in and near the Shimonoseki Channel nearly at the time of the turn of tides from the westward flow to the eastward flow in the channel. Fairly large masses of turbid water are seen in the sea region near Ube City and Onoda City, both of which are famous for the industry of cement production, then the fairly large part of the turbid water there is assumed as to



artificially polluted water. The patterns of the turbid water in Fig.8 shows that the turbid water from the Ube City is flowing eastward whereas the one from the Onoda City is seen to be nearly at the slack. This difference is caused by the difference in the tidal time that the turn of tides in the central region of the Suo-Nada occurs faster than that one in the Shimonoseki Channel.

#### GENERAL PATTERN OF TURBID WATER

Each distribution pattern of turbid water changes with the time in accordance with daily tides with seasonal variation of tides and furthermore, with occasional rainfall. However, two cases of successfully repeated LANDSAT observations for each same sea regions as in Fig.3 , Fig.4 and Fig.5, Fig.6 and Fig.7 suggest that a general pattern of the turbid water can be extracted for each region. Basing upon this fact was made a chart of general pattern of turbid water in the Seto-Inland Sea by making the pattern in Fig.2 represented the general pattern of turbid water in the sea region in 'A' in Fig.9, the pattern in Fig.3 the general pattern in 'B', and the pattern in Fig.8 the general pattern in 'C'. Unfortunately any general pattern of turbid water could not be extracted in the Aki-Nada south off Hiroshima City where the water is fairly polluted, and the Iyo-Nada where the water is generally clearer than the other regions in the Seto-Inland Sea. For comparison, two charts of the Chemical Oxygen Demand (COD) are presented in Fig.10 and Fig.11. Patterns of turbid water in Fig.9 and of COD in Fig.10 and Fig.11 are nearly corresponding each other in most sea regions which shows that LANDSAT's multispectral data are useful in monitoring the state of water pollution even though successfully available LANDSAT data are rather occasional.

## Reference

MAUL, G. A., and H. R. GORDON; On the use of the Earth Resources  
Technology Sattelite (LANDSAT-1) in optical oceanography.  
Remote Sensing of Environment 4, 95-128 (1975)

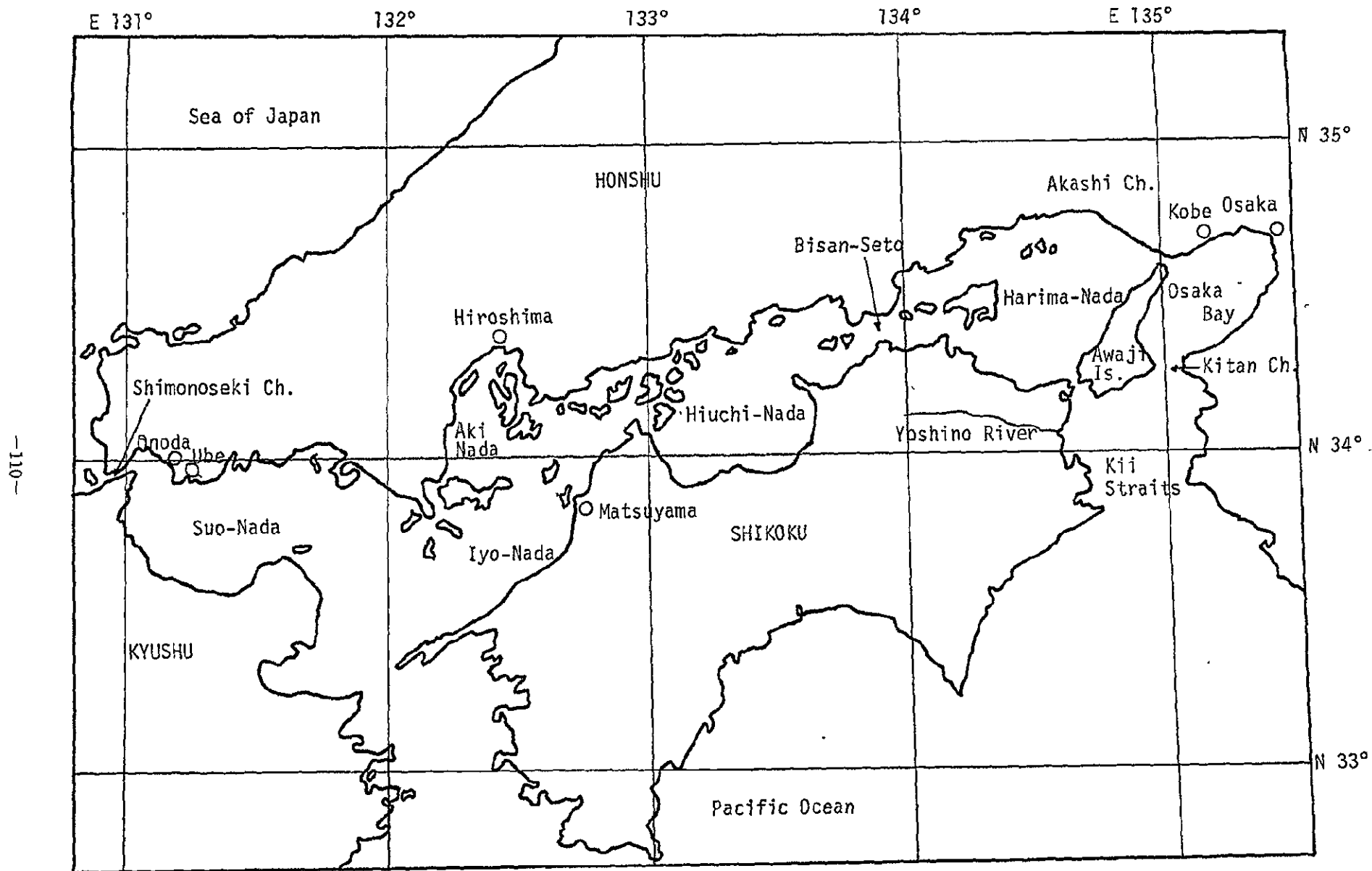


Fig. 1 Map of the Seto-Inland Sea

ORIGINAL PAGE IS  
OF POOR QUALITY

ORIGINAL PAGE IS  
OF POOR QUALITY



Fig. 2 Patterns of turbid water in the Osaka Bay, the Kii Straits and the eastern part of the Harima-Nada sea extracted from LANDSAT-1's MSS imageries taken on Oct. 24, 1972.



Fig. 3 Patterns of turbid water in the Harima-Nada sea and the Hiuchi-Nada sea extracted from LANDSAT-1's MSS imageries taken on Nov. 12, 1972.



ORIGINAL PAGE IS  
OF POOR QUALITY

ORIGINAL PAGE IS  
OF POOR QUALITY

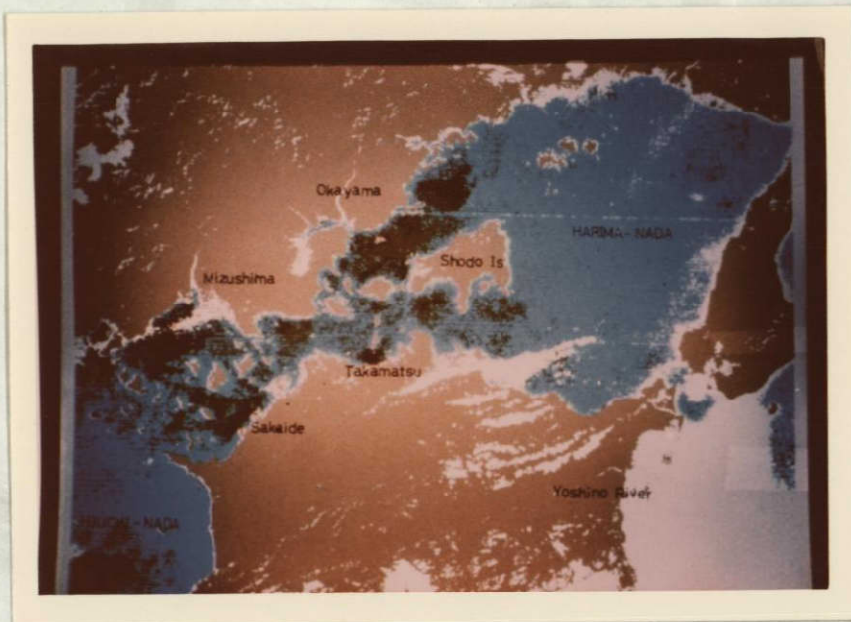


Fig. 4 Patterns of turbid water in the Harima-Nada sea and the Hiuchi-Nada sea extracted from LANDSAT-1's MSS imageries taken on Jan. 23, 1973.



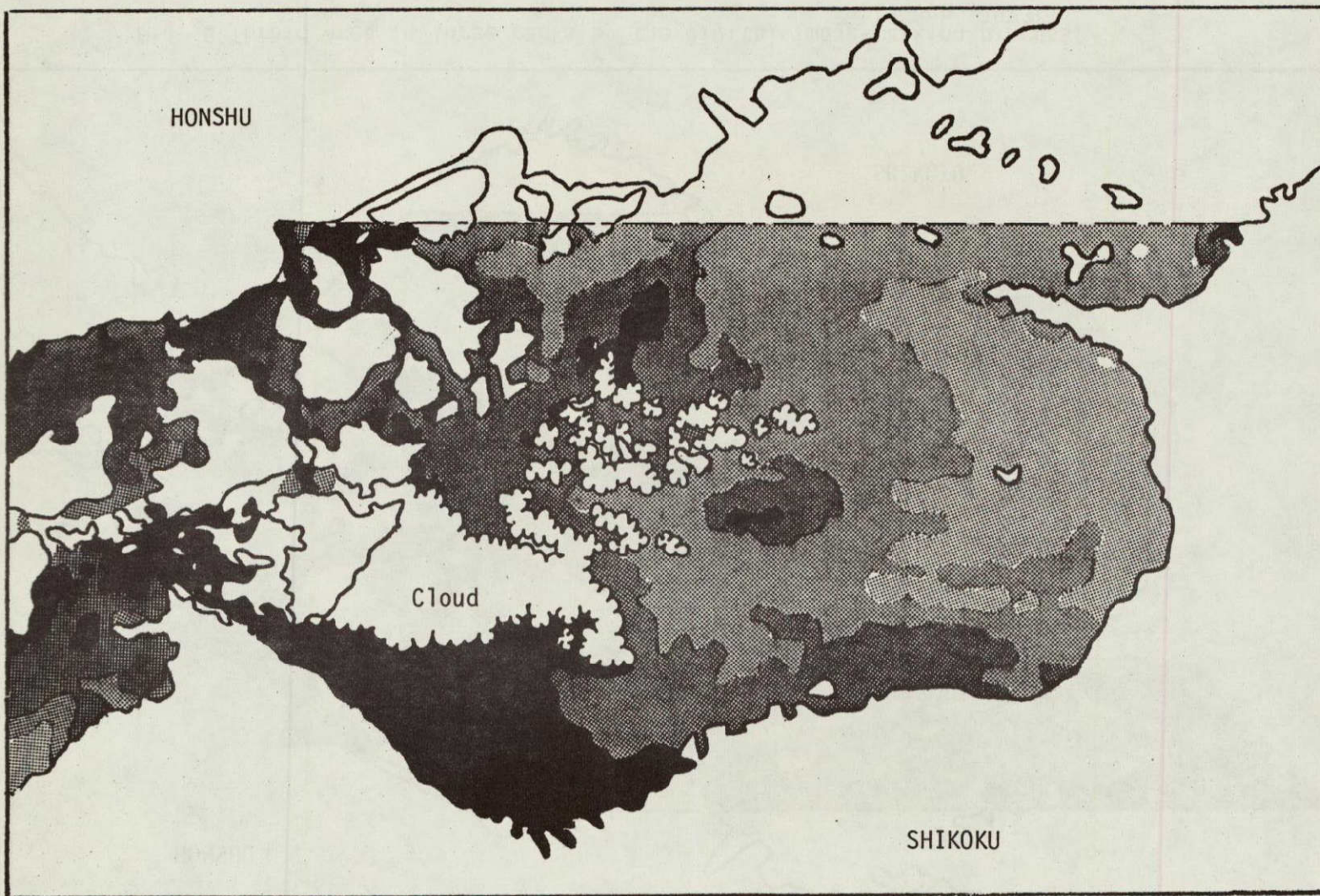


Fig. 5 Turbid area in three ranks by the digital image-masking process  
12 Nov. 1972

ORIGINAL PAGE IS  
OF POOR QUALITY



05 500Z GRVTL  
081010Z 1703 1

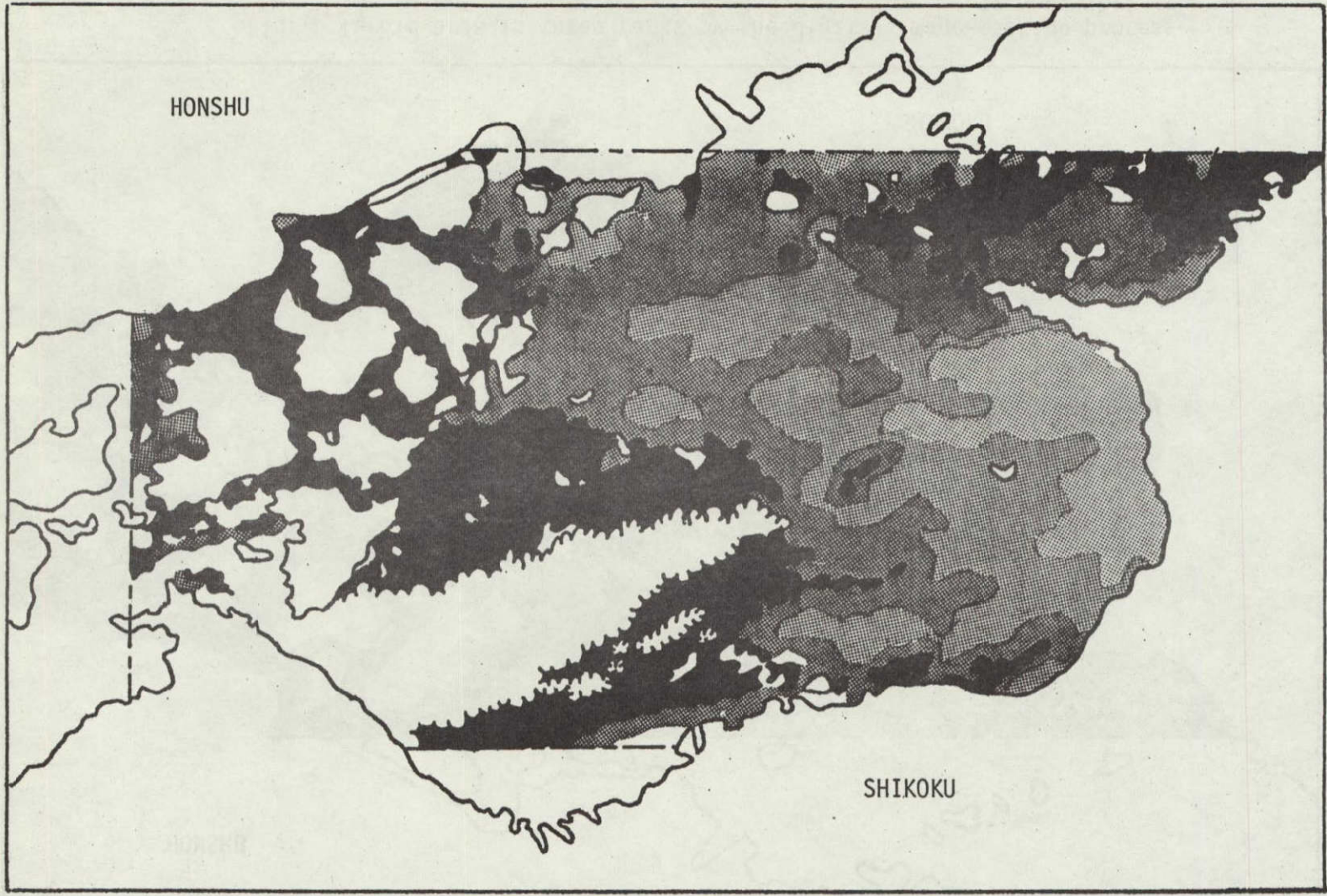


Fig. 6 Turbid area in three ranks by the digital image-masking process  
23 Jan. 1973





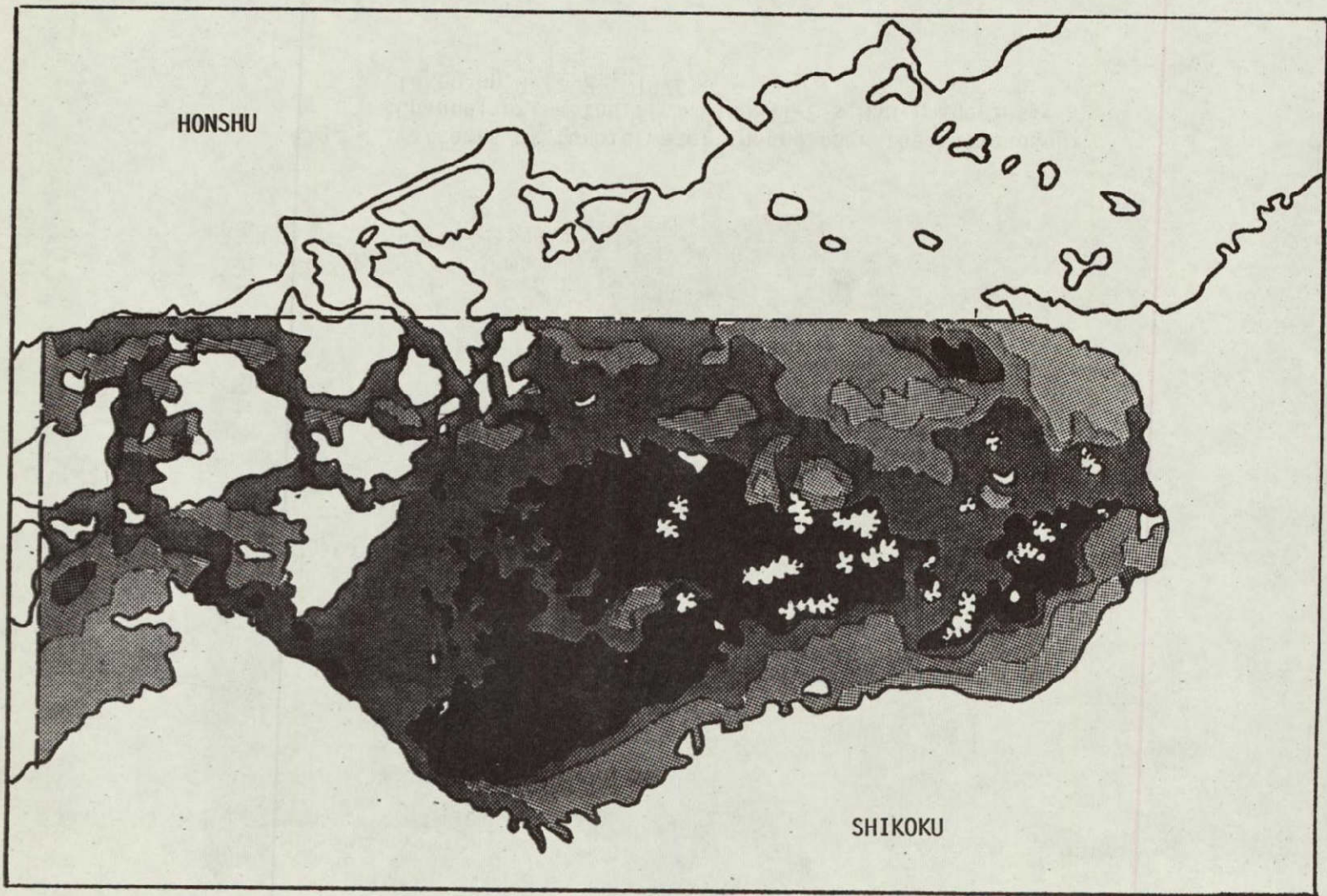


Fig. 7 Turbid area in three ranks by the digital image-masking process  
30 Dec. 1975

ORIGINAL PAGE IS  
OF POOR QUALITY

ORIGINAL PAGE IS  
OF POOR QUALITY



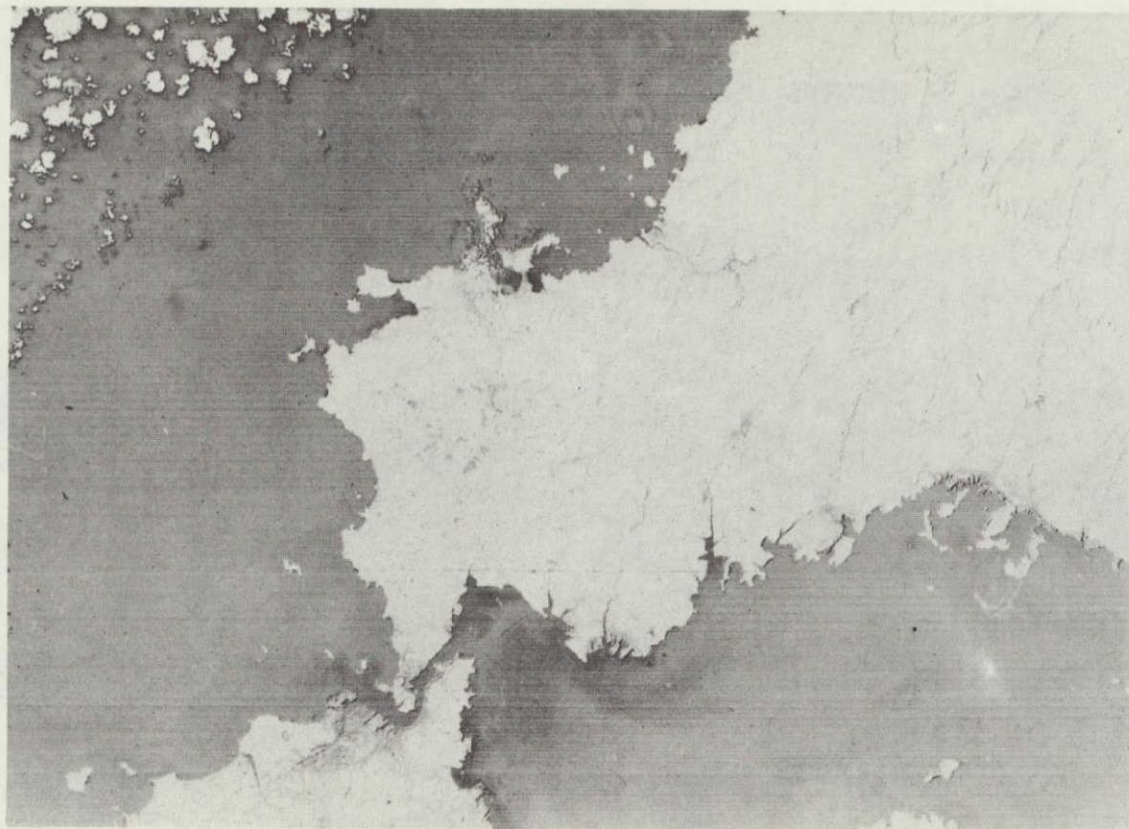


Fig. 8 Patterns of turbid water in and near the Shimonoseki Channel extracted from LANDSAT-2's MSS imageries taken on Oct. 21, 1975

ORIGINAL PAGE IS  
OF POOR QUALITY

ORIGINAL PAGE IS  
OF POOR QUALITY

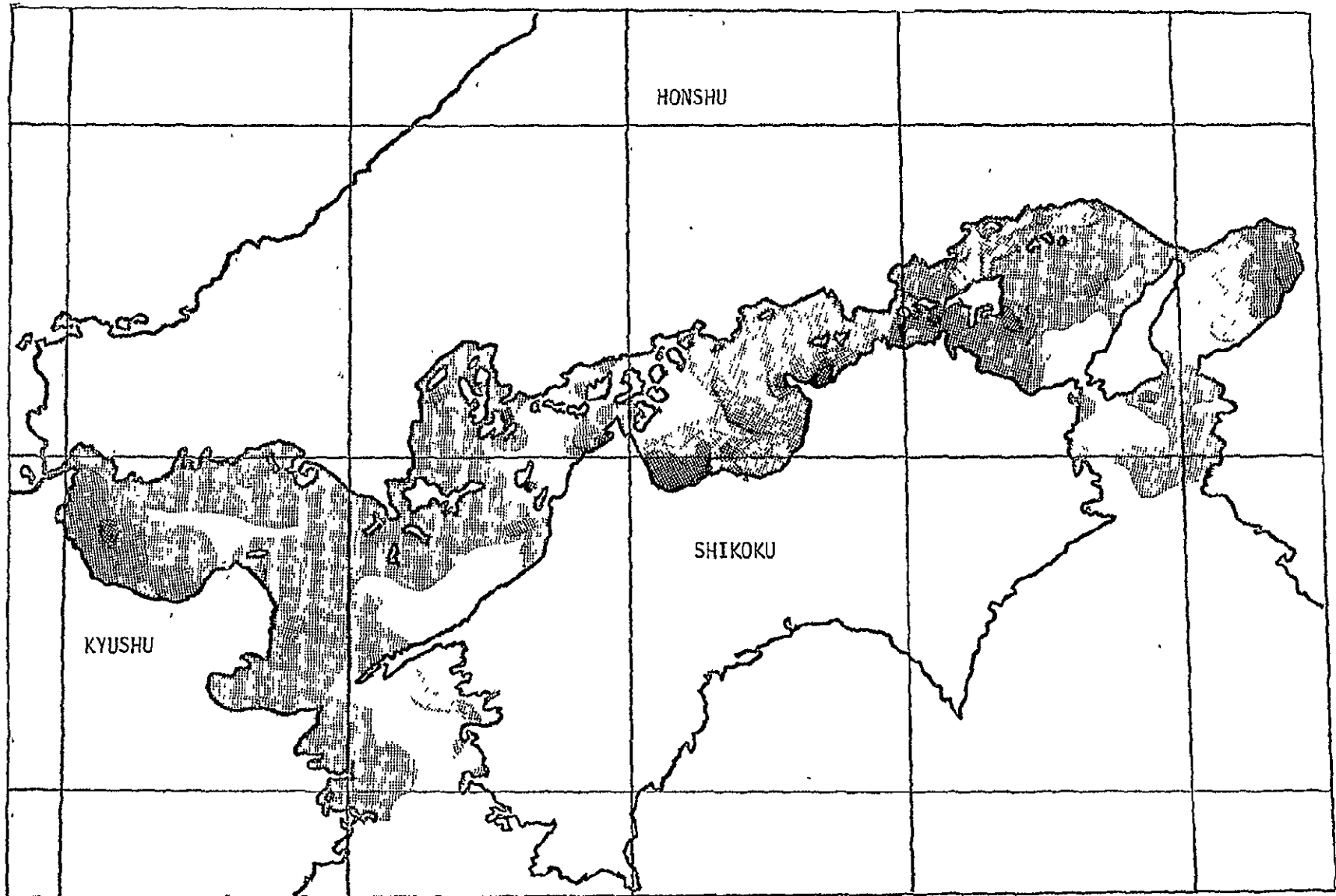


Fig. 10 Horizontal distribution of surface COD  
17 Oct. 1972

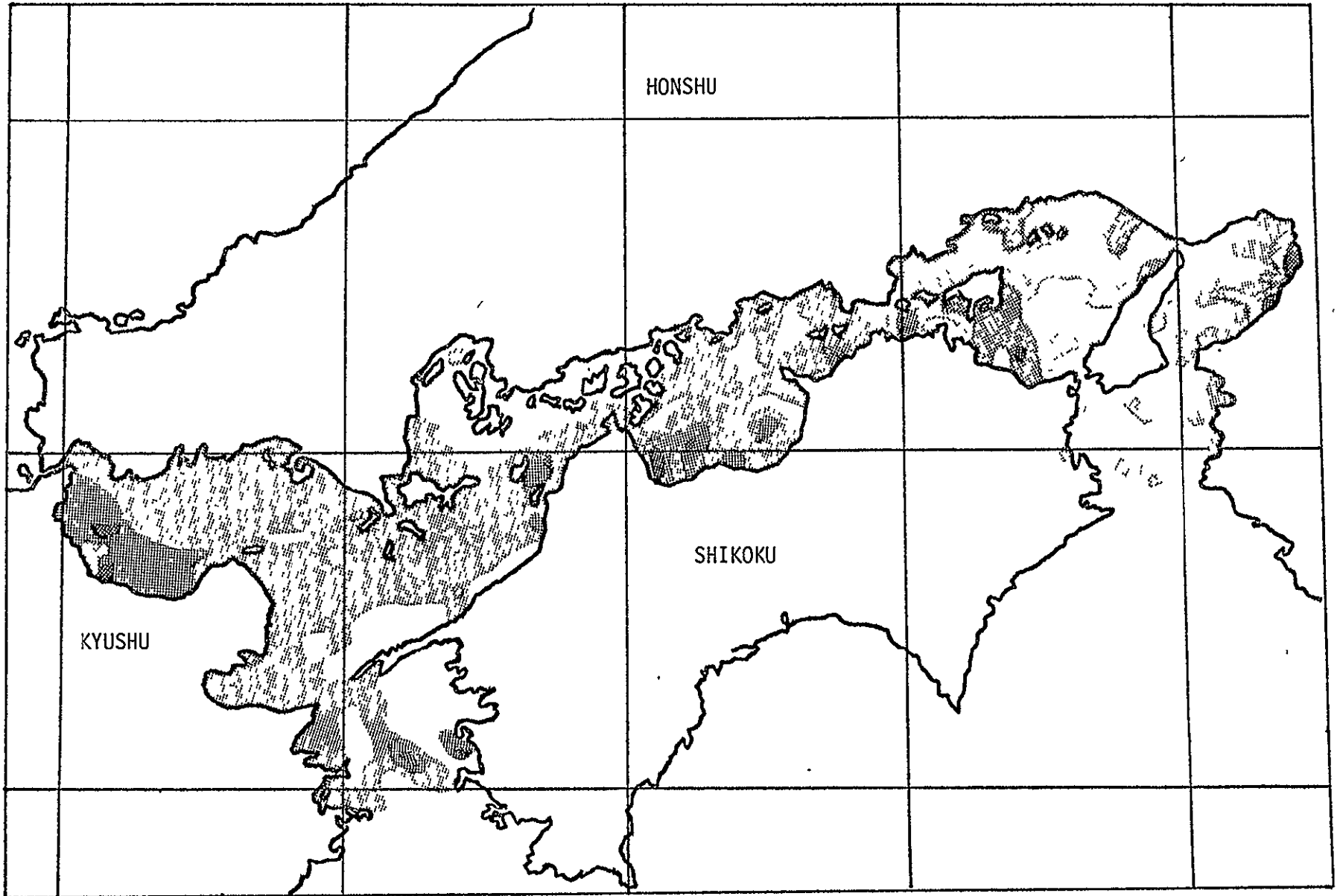


Fig. 11 Horizontal distribution of surface COD  
10 Jan. 1973



ORIGINAL PAGE IS  
OF POOR QUALITY

Significant Application of LANDSAT-2 MSS Data  
to Marine Environment

PRECEDING PAGE BLANK NOT FILMED

Hiroaki OCHIAI

Toba Merchant Marine College, Toba-shi, Mie-ken, Japan

Abstract

Remotely sensed data obtained from LANDSAT-2 was confirmed that it was very useful for the monitoring of marine environment through the year around coastal area of Japan. Indeed more than one hundred scenes which contained various oceanic phenomena were already produced from MSS data and analysed during the LANDSAT-2 investigation term agreed with NASA.

In this report, the author described the significant application of LANDSAT-2 MSS data acquired over Japan in nearly three years and revealed several coastal features including red tide, river effluent, coastal process and etc. with the supporting data obtained by air-borne remote sensing using multispectral scanner.

Sea surface data observed by ship as routine work and special experiment were also used for data analysis as sea truth. In data analysis aspect, the author tried both analog processing and digital processing standing on application field.

1 Introduction

The objective of this LANDSAT-2 study is mainly inquiring for the marine environment around Japan and monitoring of it. So, the author set up the test sites in Ise Bsy, Kumanonada and Seto Inland Sea where various coastal features were experienced in recent year.

In this report, the author pointed out few topics which depend on the special experiment using aircraft and ship. One of the topics is the detection of the most effective wavelength for the monitoring of red tide in Ise Bay and Seto Inland Sea. And one more topic is the detection of characteristic of water mass from spectral distribution by digital analysis.

120  
PRECEDING PAGE BLANK NOT FILMED



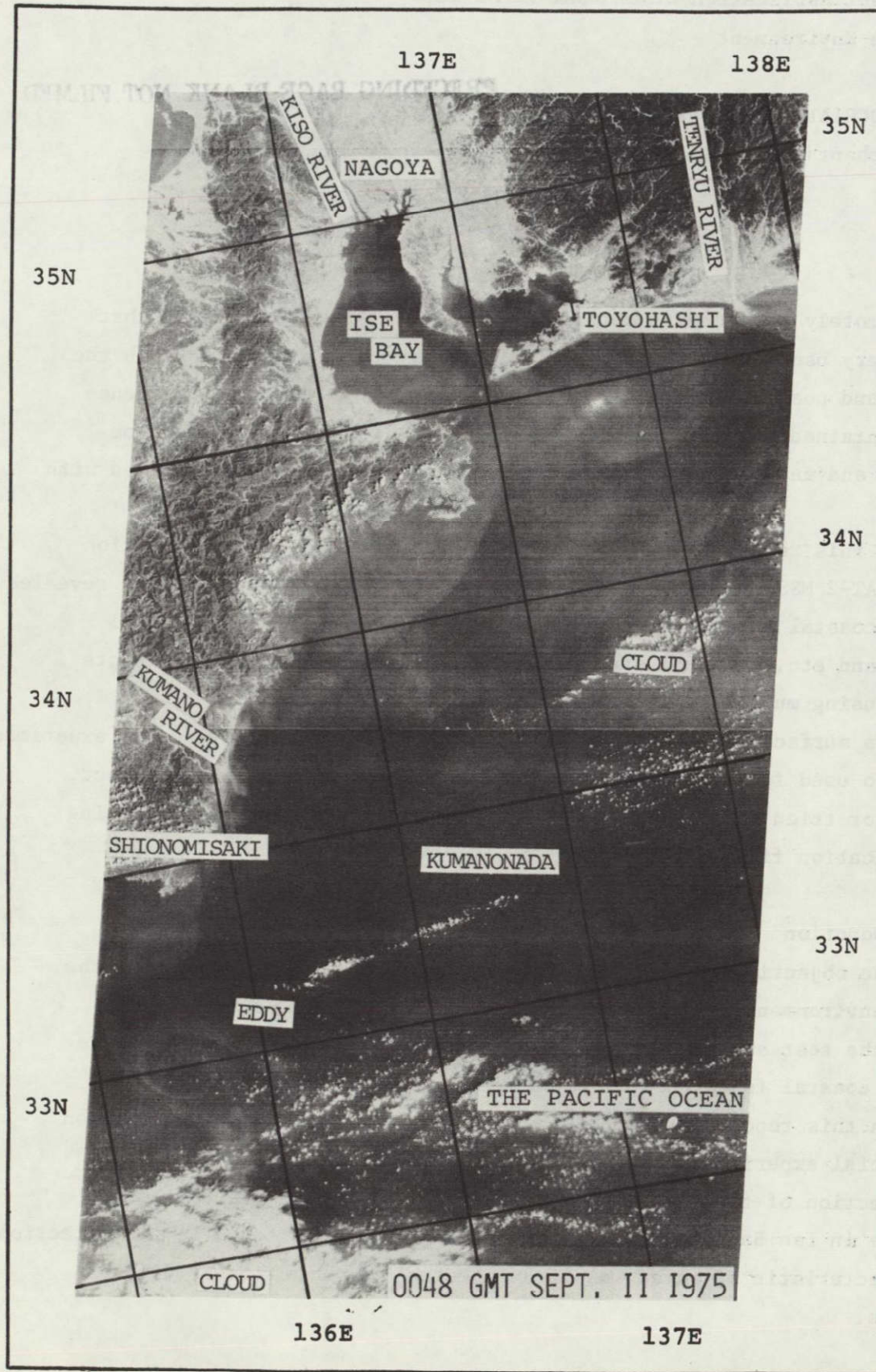


Figure 1 LANDSAT-2 MSS-4 imagery mosaic.  
Sept. 11, 1975



## 2 Techniques

### 2-1 Aircraft and Instrument

Before the launching of LANDSAT-2, the author started the pre-observation for collecting the fundamental sea surface data around Japan especially in Ise Bay and Seto Inland Sea. In these area, air-borne remote sensing were performed several times using three types of aircraft. Cessna-402 was used for ordinary observation and YS-11 turbo jet plane was used for special flight as long hour flight. And helicopter was used for low altitude observation around the boundary of water mass in the mouth of Ise Bay.

For the purpose of collecting the supporting data, three types of the air-borne multispectral scanner were used. They were Daedalus-1250, JSCAN-AT-5M and JSCAN-AM-12M. Among the above mentioned three types of the multispectral scanner, JSCAN-AT-5M and JSCAN-AT-12M were ones developed by the author's study group in Japan.

After the successful launching of LANDSAT-2, the author tried several special experiments synchronized with the passing of LANDSAT-2 over the selected test sites in Ise Bay and Seto Inland Sea.

On September 11, 1975, a synchronized observation between aircraft and LANDSAT-2 succeeded around Ise Bay and very good informations were carried out from both of LANDSAT and air-borne multispectral scanner data.

### 2-2 Sea truth data

Sea truth data were collected by observation ships. In Ise Bay, two types of ship were used for observation. One of them was hydroboat equipped with data collecting system consisting of various sensors and she was used for daily observation between Toba and Gamagori Port acrossing Ise Bay four times a day. So, sea surface data as temperature profile or salinity profile were detected easily on a data recorder as a pattern.

Each one time a month, marine observation ships which belong to the Fisheries Experiment Aichi and Mie Prefecture were used for special observation. In this case, environmental data were collected widely at more than forty stationary points every time.



In Seto Inland Sea, data obtained by passenger ships which engage in daily service were used for analysis as sea truth. And "Red tide report" by fishing boat to The Branch Office of Fishing Agency in Kobe was also used for analysis as sea truth.

### 3 Accomplishment

#### 3-1 Ise Bay experiment

Ise Bay which is locating in southern coast of central Japan is connecting with Kumanonada of Pacific Ocean through the narrow water ways Irago and Momotori Channel. It has the total area of water of  $2.06 \times 10^6 \text{ km}^2$ .

As shown in Figure 1, Ise Bay is divided into two parts by Chita Peninsula located near the mouth of Mikawa Bay. And small western half of it is called Chita Bay and another half is called Mikawa Bay.

Along the coast line of Ise Bay, several heavy industrial zones were located especially in northern part of it as Nagoya and Yokkaichi. Recently, almost whole area of Ise Bay including small bays were rapidly polluted with the increasing of industrial effluent from the industrial zone and social discharge through the river which flows into bays in the surrounded area.

#### (A) Red tide

Recently, we are experiencing so many times red tide through all seasons of the year and the total number of appearance of red tide in Ise Bay was exceeded one hundred in 1975. On January 29, we experienced a severe red tide close to the mouth of Kiso River which we have never experienced in winter season in past.

As shown in Table 1, more than forty five cases of notable red tide were reported in 1975 and some of them were not only very severe, but the scale was also reportable.

Especially, red tide appeared on May 7-8 in Mikawa Bay, May 26-27 in Ise Bay, August 26-September 4 in Ise Bay and September 8-10 in Mikawa Bay were very notable cases. Because, on these days a large amount of fish and shell were diseased in almost whole part of the area where red tide



Table 1 Report of Red Tide Sighted in  
Ise Bay and Mikawa Bay (only notable case)

Date	Area	Color	Date	Area	Color
1975					
Jan. 29	Mouth of Kiso River	Brown	June 16	Western coast of central Ise Bay	Brown
30					
March 26	Southwest part of Ise Bay	Yellow	June 19	Gamagori Port	Brown
April 7	Along the western coast of central Ise Bay	Light brown	20	Eastern part of Mikawa Bay	Light brown
			June 25		
April 9	Eastern part of Mikawa Bay	Brown	30	Toyohashi Port	Brown
11			July 6	Mouth of Toyo River	Green
April 16	Northwest part of Ise Bay	Yellow	July 9	Western coast of central Ise Bay	Brown
17			11		
May 1	Eastern part of Mikawa Bay	Pink	July 15	Eastern part of Mikawa Bay	Pink
May 7	Eastern part of Mikawa Bay	Light brown	16	Along the western coast of	Brown
			8	Kinuura Port	
May 21	Kinuura Port	Light brown	17	Chita Peninsula	
			Aug. 11	Yokkaichi Port	Brown
May 23	Western coast of central Ise Bay	Pink	Aug. 20	Central part of Ise Bay	Pink
			Aug. 26	Southwest part of Ise Bay	Light brown
May 26	Western coast of northern Ise Bay	Brown	Aug. 27	Yokkaichi Port	Dark green
			Aug. 28	Gamagori Port	Black
May 26	Nagoya Port	Brown	30	Matsuzaka Port	Brown
			May 26	Sept. 1	Southwest coast of Ise Bay
May 27	Eastern part of Mikawa Bay	Brown	Sept. 2	Kinuura Port	Brown
			May 27	Sept. 2	Southwest coast of Ise Bay
May 28	Northern coast of eastern Mikawa Bay	Brown	4		
			June 3	Sept. 8	Northern part of Ise Bay
June 4	Western coast of central Ise Bay	Brown	10	Eastern part of Mikawa Bay	Green
			June 4	10	Almost area of Mikawa Bay
June 6	Eastern coast of Ise Bay	Pink	Oct. 1	Almost area of Mikawa Bay	Brown
			June 6	3	Kinuura Port
June 10	Western coast of Ise Bay	Brown	Oct. 8	Eastern part of Mikawa Bay	Brown
			June 10	10	



ORIGINAL PAGE IS  
OF POOR QUALITY



Figure 2 Enlarged MSS-4 imagery shown  
in Figure 1.



Figure 3 Aerial color photograph around  
red tide area in Mikawa Bay.  
Sept. 11, 1975

ORIGINAL PAGE IS  
OF POOR QUALITY



was reported. Red tide consisting of animal nature plankton appears as a red color pattern usually. But brown and black colored ones were also experienced recently. On July 6 and early September of 1975, we experienced the green color pattern in Mikawa Bay and it is called "Nigashio" or "Green water" in this district.

From early April to late December in 1975, LANDSAT-2 passed over Ise Bay fifteen times. But due to the weather, only few scenes were obtained in this term if we could have better weather condition on the LANDSAT-2 passing day, we would be pleased to have another useful information concerning red tide around Ise Bay.

As noted before, LANDSAT-2 revealed a very efficient information around Ise Bay and Kumanonada on September 11, 1975. In MSS-4 imagery we could find out a typical pattern in Mikawa Bay and this pattern was estimated as red tide by comparing this with air-borne remote sensing data. In eastern Mikawa Bay, very notable red tide was not identified in Mikawa Bay, as shown in Figure 3, we could recognize it in the aerial color photograph obtained by the author. Red tide pattern was detected in eastern Mikawa Bay around Toyohashi Port and this pattern was just the same color of brown as reported on September 10, the day before in this area.

In thermal imagery obtained by air-borne multispectral scanner, red tide pattern was detected distinctly in the area pointed out Figure 2 and Figure 3.

Depending on the author's experience, the most effective wavelength for the monitoring of red tide consisting of Noctiluca was confirmed as thermal channel of air-borne multispectral scanner. Red tide consisting of Prorocentrum was also recognized remarkably in the thermal channel too.

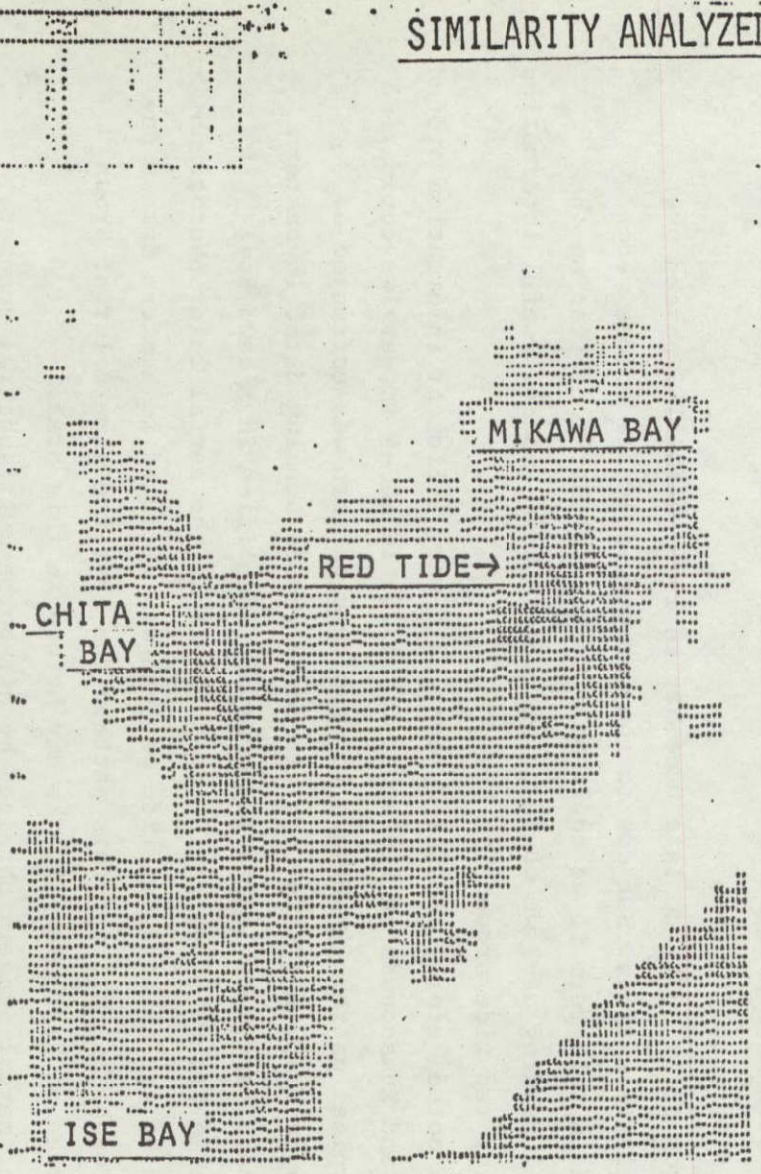
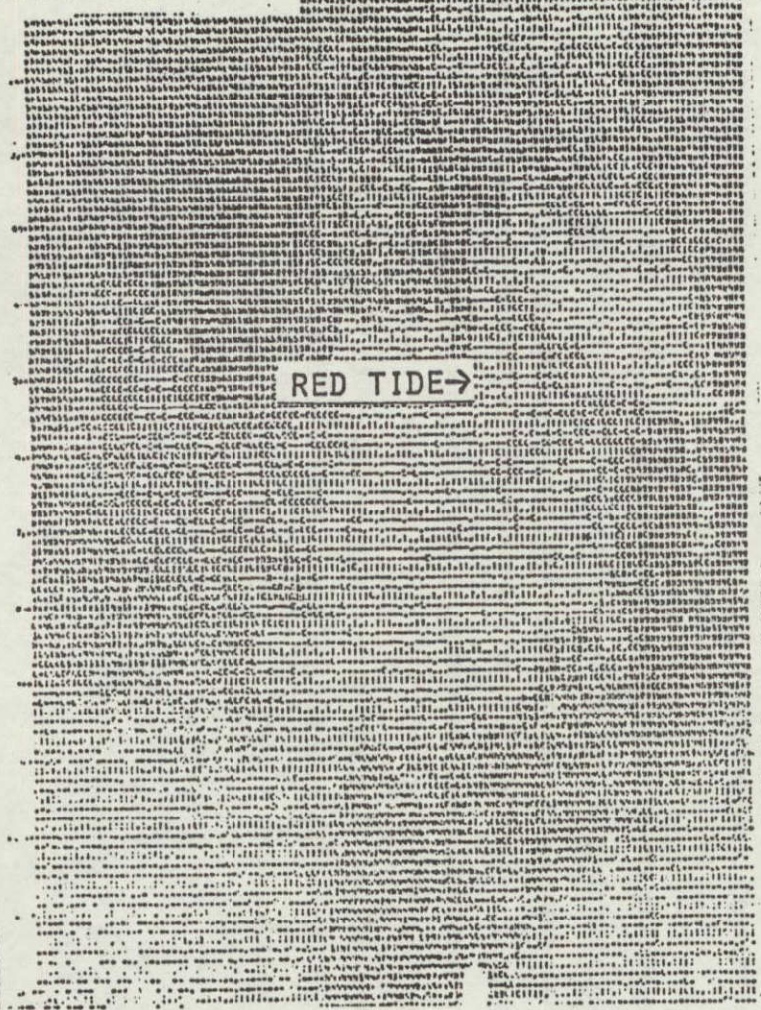
On present stage, we can not carry out the thermal pattern from MSS data obtained by LANDSAT-2. So, the most effective wavelength for the monitoring of red tide was considered as MSS-4 in the analog processing. In another three channel we could not find out the pattern estimated as red tide in this case.



Band	Wavelength (nm)	Resolution (m)	Gain
1	0.45	100	1.0
2	0.65	100	1.0
3	0.85	100	1.0
4	1.25	100	1.0
5	1.65	100	1.0
6	2.15	100	1.0
7	2.35	100	1.0
8	2.55	100	1.0
9	2.75	100	1.0
10	2.95	100	1.0
11	3.15	100	1.0
12	3.35	100	1.0
13	3.55	100	1.0
14	3.75	100	1.0
15	3.95	100	1.0
16	4.15	100	1.0
17	4.35	100	1.0
18	4.55	100	1.0
19	4.75	100	1.0
20	4.95	100	1.0
21	5.15	100	1.0
22	5.35	100	1.0
23	5.55	100	1.0
24	5.75	100	1.0
25	5.95	100	1.0
26	6.15	100	1.0
27	6.35	100	1.0
28	6.55	100	1.0
29	6.75	100	1.0
30	6.95	100	1.0
31	7.15	100	1.0
32	7.35	100	1.0
33	7.55	100	1.0
34	7.75	100	1.0
35	7.95	100	1.0
36	8.15	100	1.0
37	8.35	100	1.0
38	8.55	100	1.0
39	8.75	100	1.0
40	8.95	100	1.0
41	9.15	100	1.0
42	9.35	100	1.0
43	9.55	100	1.0
44	9.75	100	1.0
45	9.95	100	1.0
46	10.15	100	1.0
47	10.35	100	1.0
48	10.55	100	1.0
49	10.75	100	1.0
50	10.95	100	1.0
51	11.15	100	1.0
52	11.35	100	1.0
53	11.55	100	1.0
54	11.75	100	1.0
55	11.95	100	1.0
56	12.15	100	1.0
57	12.35	100	1.0
58	12.55	100	1.0
59	12.75	100	1.0
60	12.95	100	1.0
61	13.15	100	1.0
62	13.35	100	1.0
63	13.55	100	1.0
64	13.75	100	1.0
65	13.95	100	1.0
66	14.15	100	1.0
67	14.35	100	1.0
68	14.55	100	1.0
69	14.75	100	1.0
70	14.95	100	1.0
71	15.15	100	1.0
72	15.35	100	1.0
73	15.55	100	1.0
74	15.75	100	1.0
75	15.95	100	1.0
76	16.15	100	1.0
77	16.35	100	1.0
78	16.55	100	1.0
79	16.75	100	1.0
80	16.95	100	1.0
81	17.15	100	1.0
82	17.35	100	1.0
83	17.55	100	1.0
84	17.75	100	1.0
85	17.95	100	1.0
86	18.15	100	1.0
87	18.35	100	1.0
88	18.55	100	1.0
89	18.75	100	1.0
90	18.95	100	1.0
91	19.15	100	1.0
92	19.35	100	1.0
93	19.55	100	1.0
94	19.75	100	1.0
95	19.95	100	1.0
96	20.15	100	1.0
97	20.35	100	1.0
98	20.55	100	1.0
99	20.75	100	1.0
100	20.95	100	1.0

MSS-4

SIMILARITY ANALYZED



ORIGINAL PAGE IS  
OF POOR QUALITY

Figure 4 Print maps of LANDSAT-2 MSS data shown in Figure 1 and Figure 2.



In digital analysis, the author tried enhancement of the data to produce a digital pattern of red tide distinctly in the first step, and as shown in Figure 4, the two print maps were printed out. Compared with the two print maps, the red tide pattern shown in Figure 2 and Figure 3 was produced more clearly in similarity analysis. Although red tide pattern was detected in enhanced MSS-4 print map, it was not so distinct in the eastern area of Mikawa Bay. But in the similarity analyzed print map, we could recognize red tide pattern very clearly.

(B) River effluent

In Figure 4, another patterns were recognized in Chita Bay and Ise Bay. And these patterns were estimated as the influence of river effluent from surrounding bay. In Chita Bay, the river water polluted by suspended substance from Yahagi River influences its environment very much. By the report of Environmental Department of Aichi Prefecture, the normal account of suspended substance at the mouth of Yahagi River was 45 in 1975. But after the heavy raining, it exceeded extremely higher than 100. So, white-colored river water from Yahagi River influences near area of the mouth of Ise Bay.

In Ise Bay, a large amount of river water from Kiso River and Nagara River influences sea water severely, especially when after heavy raining anti-clockwise flow was recognized in the past observation data. The normal account of suspended substance at the mouth of Kiso River was 39, although maximum account record shows 130 in 1975. We could recognize that Yahagi River was more polluted than Kiso River by the suspended substance. Figure 5 is the typical expanding pattern of river effluent from Yahagi River which obtained by air-borne remote sensing after raining.

In the similarity analysis, the analysed data was displayed on the color display system and classified by the color code as shown in Figure 6. Namely, when the standard point was set at red tide area in Mikawa Bay, the similarity analysed image would be display as right image and if standard point was set at the area polluted by the suspended substance at the mouth of Yahagi River, color coded pattern would be



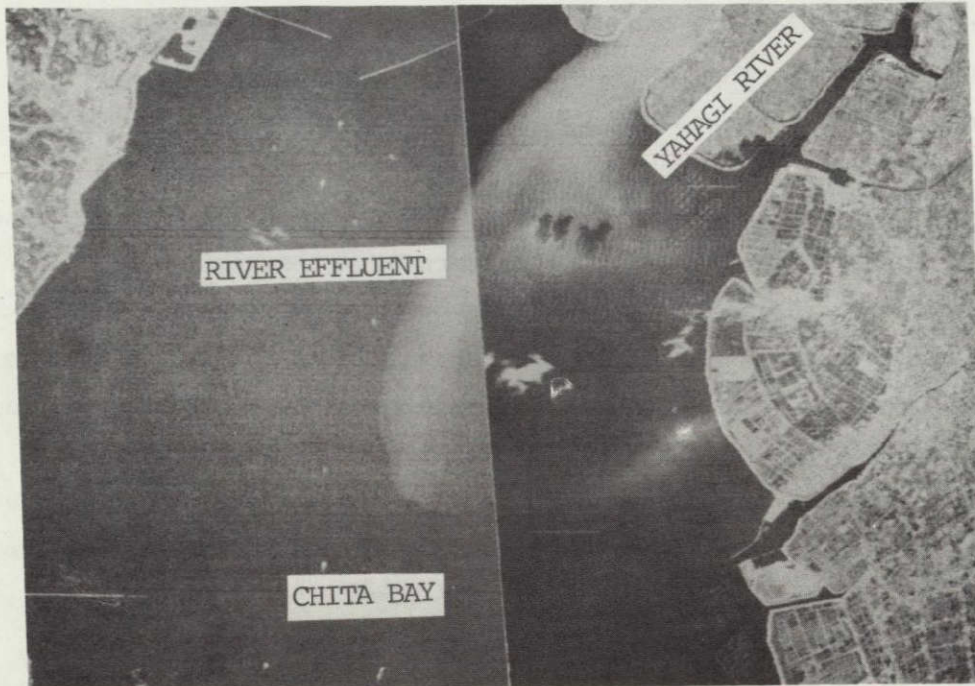


Figure 5 River effluent from Yahagi River in Chita Bay obtained by JSCAN-AT-12M multispectral scanner.



(B)

(A)

Figure 6 Similarity analysis for red tide in Mikawa Bay and river effluent from Yahagi River indicated in Figure 1 and Figure 2.  
(A) Similarity to red tide.  
(B) Similarity to mouth of Yahagi River.



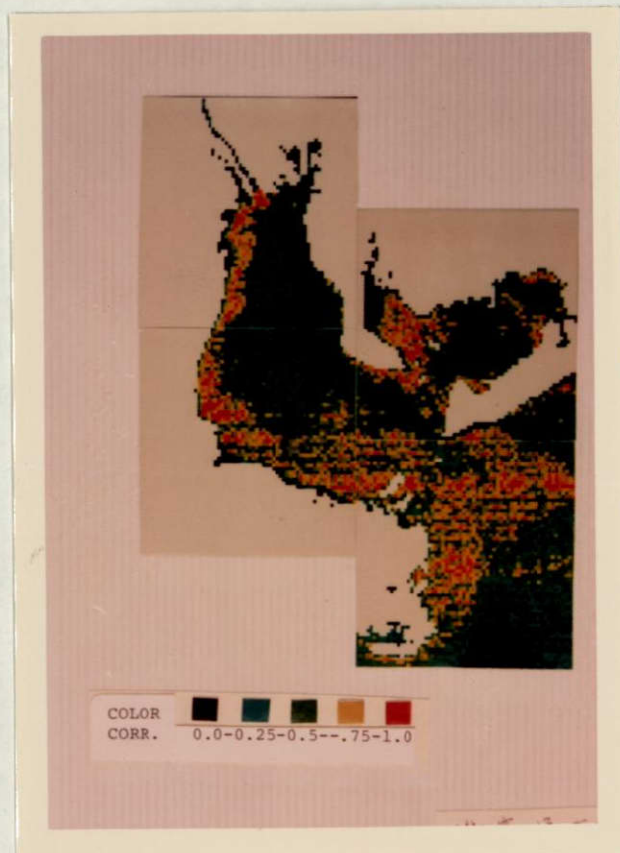


Figure 7 Similarity analysis for river effluent from Kiso River indicated in Figure 1.

ORIGINAL PAGE IS  
OF POOR QUALITY

display as left pattern. In these imageries the most similarity area to the standard point were shown in red color. The color correlation was 1.0 in this stage. Between blue color and red color, the color correlation was set up five stages and the account of correlation was divided into the interval of 0.25. By the same technique, the author analyzed the MSS data and the standard point of similarity was set up at the mouth of Kiso River. And as shown in Figure 7, the typical correlation pattern was produced around whole area of Ise Bay and anti-clockwise flow of seawater in Ise Bay was recognized from the pattern. The river water from Kiso River and Nagara River flows along the west coast of Ise Bay towards south. In this case, the characteristic of the sea water at the mouth of Ise Bay was estimated just the same as the river water from Kiso River in reflectance. So, it was considered that a large amount of river water from the northern and western part of Ise Bay where Kushida River and Miya River flows into the bay especially after heavy raining was transformed by current which flows along the western coast of Ise Bay towards the mouth of Ise Bay and also damed up by the oceanic water from Kumanonada. The boundary of the polluted water from Ise Bay was estimated as 15 km from the mouth of the bay.

### 3-2 Kumanonada experiment

#### (A) River effluent

The river effluent from Kumano River was noted as highly polluted by the suspended substance and it was caused by the construction of a dam for hydro-power generating along the upper river side. By the author's previous report (1), river effluent from Kumano River was recognized that it was influenced more than 90 km from the mouth and it extended to the southern part of Kumanonada near Kuroshio Current. In Figure 1. river effluent from Kumano River was well detected in MSS-4 imagery and it seemed to be connected with the big eddy located at about 180 km from Shionomisaki in the southeast direction. So, it was the most significant pattern we experienced through the LANDSAT-1 and LANDSAT-2 investigation.



ORIGINAL PAGE IS  
OF POOR QUALITY

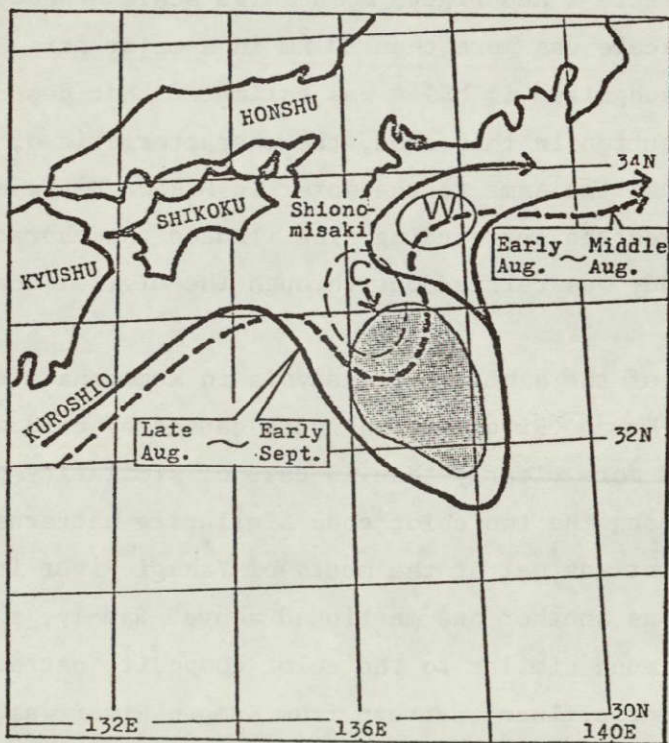
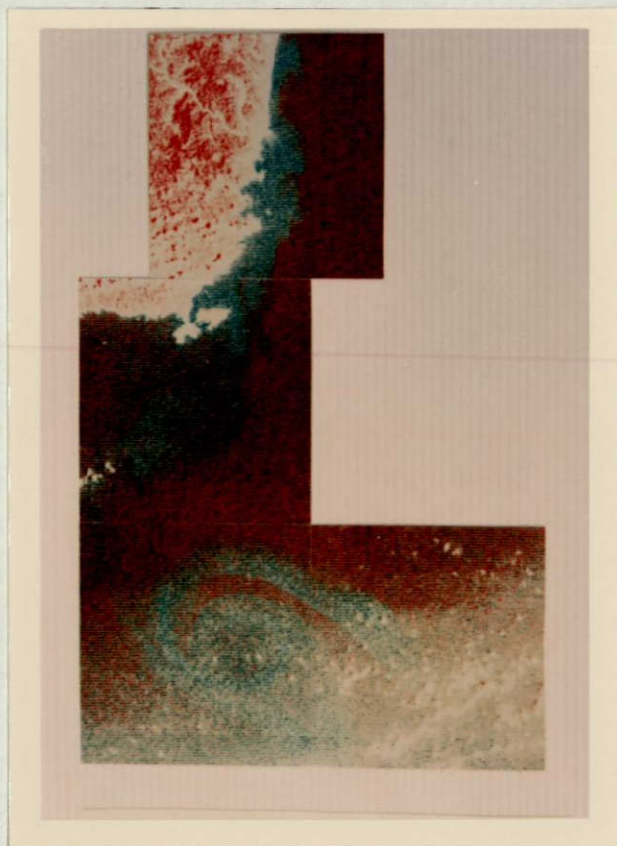


Figure 8 Color composite image by digital analysis for eddy indicated in Figure 1 and location of cold water mass in Kumanonada 1975.



In this experiment, the author tried enhancement of the data and displayed as the composite false color imagery consisting of MSS-4 in cyan color and MSS-6 in red color using digital processing.

Being compared this with the imagery processed by analog method shown as figure 1, the pattern of river water from Kumano River and the eddy by the cold water mass probably caused by a upwelling were recognized more clearly.

(B) Cold water mass

In early June of 1975, a large scale of cold water mass suddenly appeared off the southern coast of Kyushu and the cause of this cold water mass was considered as the effect of the upwelling. At the beginning of August, the cold water mass shifted its position to the southeast area of 90 km off Shionomisaki. Then the cold water mass changed its shifting course to the southeast direction and the center position of it in early September was 180 km off southeast of Shionomisaki.

The area of the cold water mass expanded as two times as compared with it in August. The water temperature at the depth of 100 m was 16°C and at the depth of 200 m was 12°C. These were 5°C or 6°C colder than at the same level in Kuroshio Current.

As shown in Figure 1 and Figure 8, a large scale of eddy was recognized distinctly and its scale was more than 30 km in a major axis. The reason why this eddy was recognized in MSS-4 was estimated that depending on the spectral distribution in this area, the characteristic of the water mass was identified as just the same to the water in Mikawa Bay where red tide was prevailing towards the surrounding area. Indeed the characteristic of the water forming the eddy was carried out through the digital analysis as shown in Figure 9.

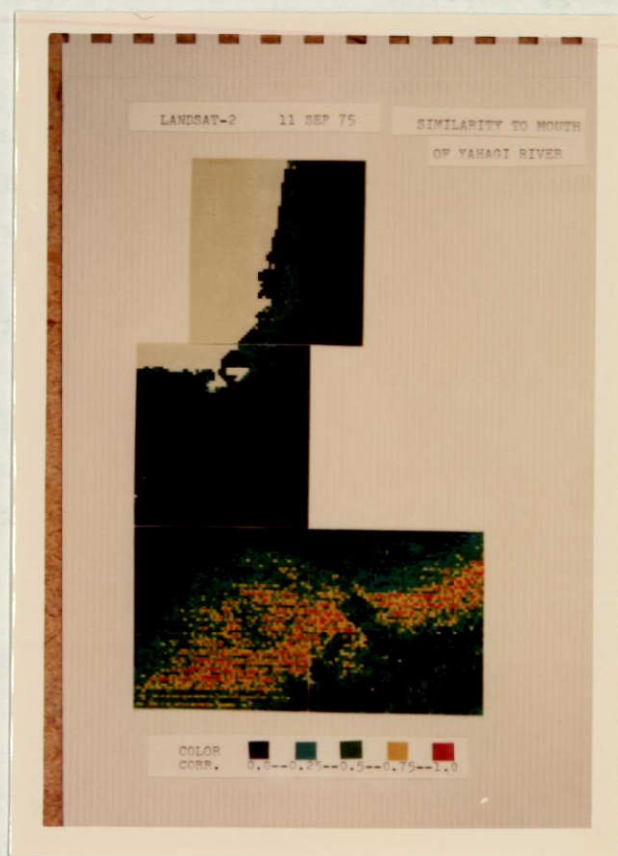
By the effect of the similarity analysis in Kumanonada experiment, river effluent from Kumano River and the eddy caused by cold water mass were well recognized more clearly than in case of similarity point set up in Mikawa Bay. Among the two color code similarity patterns, the one whose similarity point was set at the mouth of Yahagi River in Chita Bay was not so distinct as another one mentioned above. Namely, the pattern around the eddy was much similar to the color composite pattern shown in Figure 8. And river effluent pattern from Kumano River was also very similar to the color composite imagery in the same analysis.



ORIGINAL PAGE IS  
OF POOR QUALITY



(A)



(B)

Figure 9 Similarity analysis for river water from Kumano River and eddy indicated in Figure 1 and Figure 8.  
(A) Similarity to red tide in Mikawa Bay.  
(B) Similarity to mouth of Yahagi River in Chita Bay.



From this point of view, it was recognized that the river effluent from Kumano River which seemed highly polluted by suspended substance in the analog processed imagery was actually not so polluted by suspended substance as estimated by another before. It was confirmed that the characteristic of the water expanded from the mouth of Kumano River was much similar to the one of the water in Mikawa Bay than of the water around the mouth of Yahagi River.

(C) Coastal current

Influenced by the abnormal flow of Kuroshio Current, the coastal current along the southern coast of Tokai District has changed considerably its flow pattern in 1975. As shown in Figure 8 meandered Kuroshio Current closed to the coast line nearer than normal case when cold water mass appeared in Kumanonada.

In Figure 1, we could recognized the expanding pattern of river effluent from Tenryu River which extended to the southeast direction. Along the coast line of Enshunada, when Kuroshio Current was not meandered at off Kumanonada, coastal current flows westwards as the countercurrent of Kuroshio Current. In case of the data obtained by LANDSAT-1, almost typical flow pattern of river effluent from Tenryu River was extending to westwards only.

But in this case, the expanding pattern of river effluent from Tenryu River showed nearly opposite character and the author estimated the reason why the coastal current changed its flow direction as follows. Due to the large scale meandering of Kuroshio Current, a warm core was formed off the mouth of Ise Bay and under its influence, Kuroshio Current was boosted up to the shore line abnormally and coastal current which existed as countercurrent disappeared. The flow of coastal water of Enshunada changed its direction towards east by strength of Kuroshio Current.

3-3 Seto Inland Sea experiment

Seto Inland Sea which has a total water area of 22,000 km<sup>2</sup> is located in west part of Japan and is the biggest inlet in Japan. Due to the increasing of industrial effluents from coastal zone such as the districts of Kinki, Chugoku, Shikoku and Kyushu where newly developed 'kombinat' as Sakai, Takasago, Mizushima, Ube, Sakaide, Niihama and Ooita are existing, the sea water in Seto Inland Sea was rapidly polluted and its environmental condition became seriously bad.

(A) Red tide

The report announced by the Branch Office of Fishery Agency in Kobe





Figure 10 LANDSAT-2 MSS-4 imagery. Dec. 30, 1975

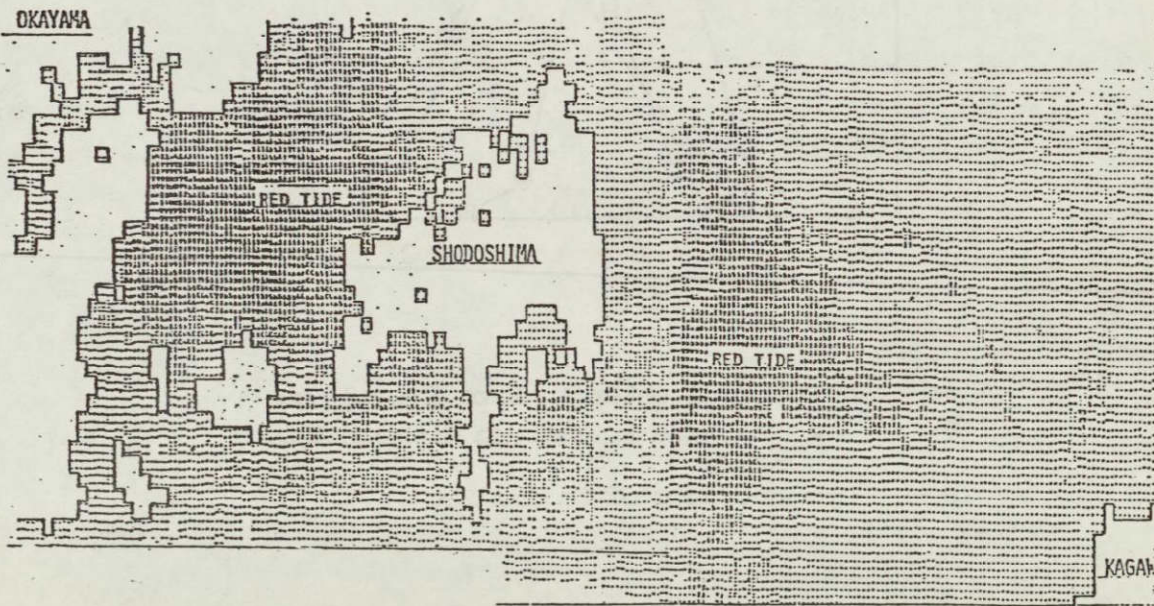


Figure 11 Print out of similarity analysis of red tide  
shown in Figure 10.



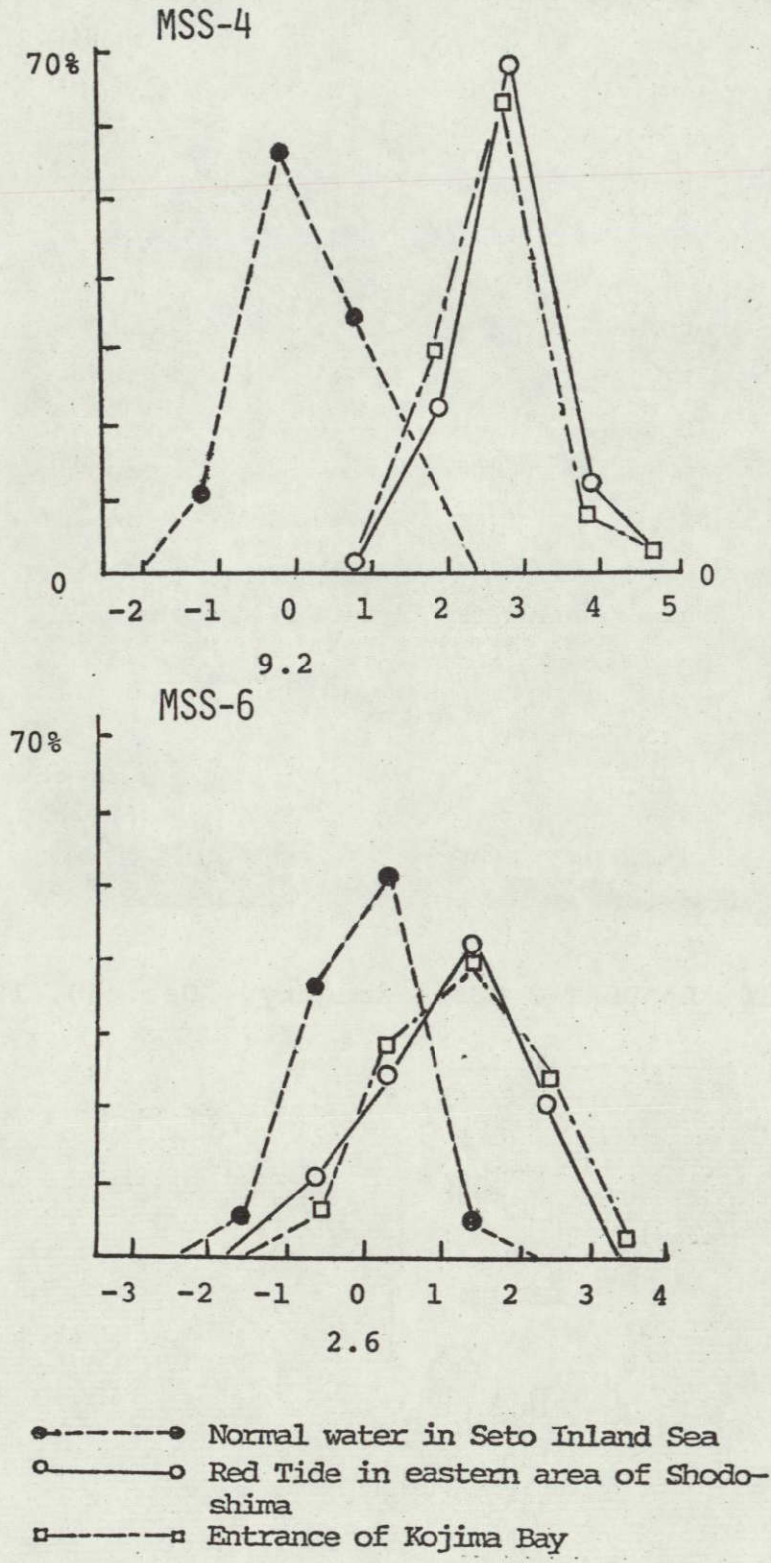


Figure 12 Spectral distribution of MSS data around Seto Inland Sea.



is telling us that the total number of observation of red tide exceeded three hundred in 1975. The frequency of the red tide appearance in Seto Inland Sea increased very rapidly. In 1950, just a quarter century ago, the total number of appearance of it was only few cases for a year and the observed area was restricted in Osaka Bay and Harimanada only, and the occurrence was limited in warm season. But recently, red tide appeared through the year and area of red tide appearance was expanding to almost whole area of Seto Inland Sea.

In this experiment, MSS data acquired on December 30, 1975 was used for analysis of both process by analog and digital. From late December of 1975 to early January of 1976, severe red tide consisting of *Skelltonema* were reported by a fishing boat around Harimanada. In Figure 10, several patterns indicated by black arrows were estimated as red tide patterns and a considerable big pattern was detected in MSS-4 imagery around off eastern coast of Shodoshima. During the investigation, the author tried air-borne remote sensing for the purpose of monitoring of red tide using multispectral scanner around Harimanada and Osaka Bay.

Although the mechanism of red tide was not yet solved clearly, the most effective wavelength for its observation was recognized as thermal channel for these area through the observation by air-borne MSS.

In digital analysis, the characteristics of water mass around Harimanada were carried out and the similarity analysis was also performed to the area around the Shodoshima as shown in Figure 11. The characteristic of water mass was identified in the data distribution patterns. Among the three channels, MSS-4 was recognized as the most effective wavelength for the monitoring of red tide in the data distribution. The standard reflectance counted for unpolluted normal water in Seto Inland Sea in MSS-4 was 9.2 in this case and its deviation was each  $\pm 2$ . But the center of the data distribution of polluted water at the mouth of Kojima Bay and the eastern area of off-Shodoshima were situated around 12 counts and these pattern were similar to the data distribution at the red tide area in Mikawa Bay as indicated in Figure 6. And the deviation of the count



was  $\frac{+}{-} 2$  and this value was just the same as un-polluted water. From this point of view, the data distribution at the red tide area shown in Figure 12 was recognized as a typical distribution pattern and this was very prominent use of digital processing especially similarity analysis.

### 3-4 Hokkaido experiment

#### (A) Sedimentation

Along the southern coast of Hokkaido between Tomakomai and Urakawa, typical expanding pattern of sediment was detected in MSS-4 imagery as shown in Figure 13. As indicated in the author's report (2) MSS-4 imagery is very useful to detect the distribution of sediment, especially the one of suspended sediment from the river. In Figure 13, expanding pattern from the mouth of Saru River was extending to the southwest direction more than 15 km long. Saru River was noted as polluted water with suspended substance and its density is more concentrative compared with the river of surrounding area. As the river water contains so much of the suspended substance in the normal condition, this river was named Saru River. Saru means flowing sand in Japanese.

Along the northeast coast of Hokkaido between Monbetsu and Abashiri as shown in Figure 14, the distribution pattern of sediment was recognized in MSS-4 imagery as the index of shore current in this area. At the outside of Lake Saroma, a round-type pattern indicated by black arrow was detected and this was estimated as sediment bulges into the sea through sandy shoals which form the outside bank of Lake Saroma.

### 4 Conclusion

The objective of this study was analyzed the marine environment in the coastal area by the use of MSS data obtained by LANDSAT-2.

During the LANDSAT-2 overpasses, air-borne remote sensing and sea truth data have been collected for comparing and confirming the coastal phenomena around Japan. The major conclusion that have been described in this report are as follows:



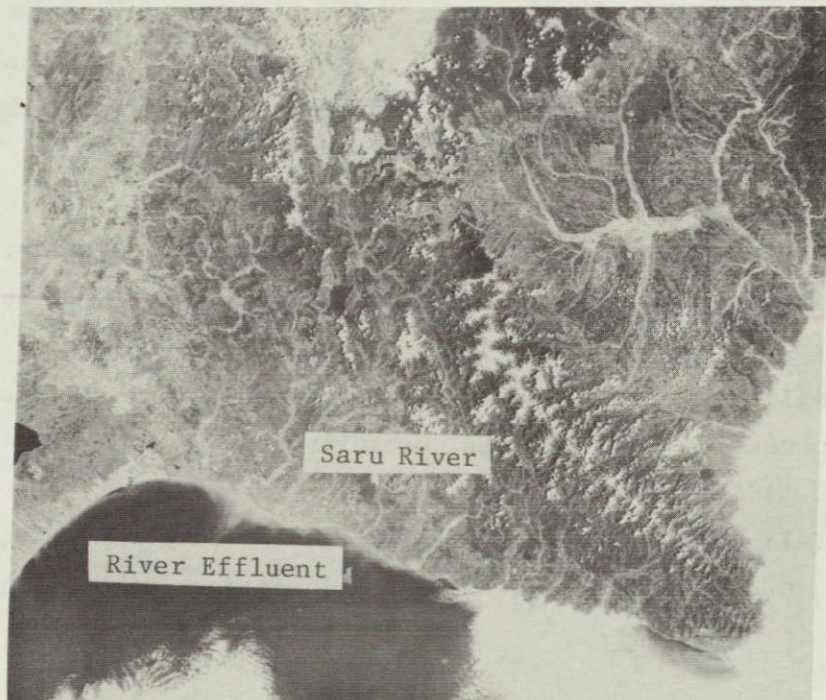


Figure 13 Distribution pattern of sedimentation  
June 11, 1975

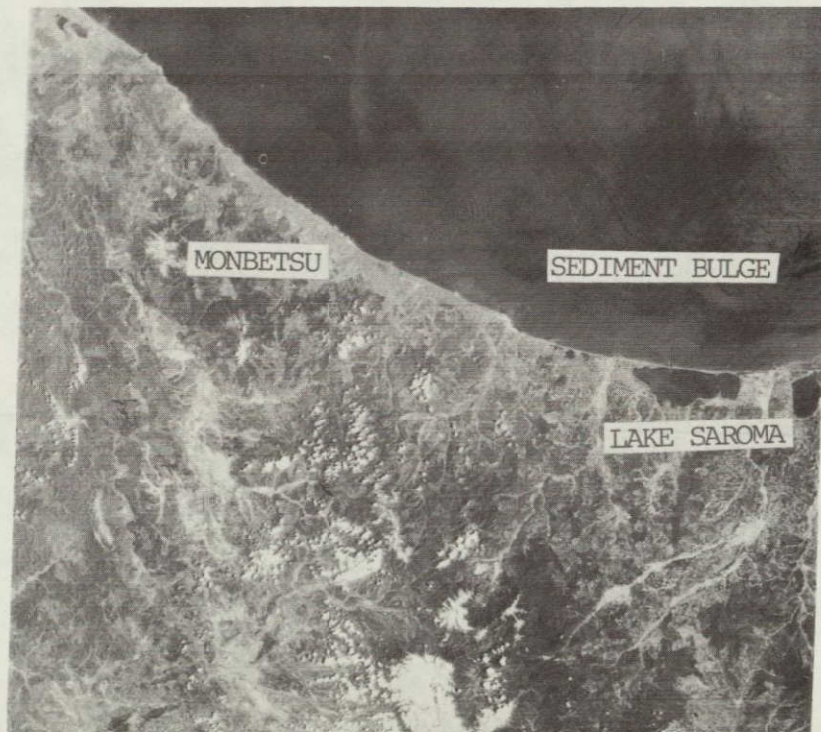


Figure 14 Sediment bulge detected in MSS-4 imagery  
June 11, 1975



- ORIGINAL PAGE IS  
OF GOOD QUALITY  
AND FAITHFULLY REPRODUCED
- (1) The most effective wavelength for the monitoring of red tide was recognized as MSS-4.
  - (2) In digital processing, the similarity was very effective to catch the information for coastal phenomena as red tide and suspended substance.

Reference:

- (1) Hiroaki OCHIAI: Multispectral Observation of Marine Environment with ERTS-1, Umitosora or Sea and Sky, Vol. 50, No. 1(1974) Associate of Marine Meteorogy.
- (2) Hiroaki OCHIAI: Multi-disciplinary Application of LANDSAT-2 Data to Marine Environment in Central Japan, Quaterly report of LANDSAT-2 investigation to NASA(1976)
- (3) Hiroaki OCHIAI: Application of LANDSAT-2 Data to Environmental Studies in Coastal Zone, Quaterly report of LANDSAT-2 Investigation to NASA(1977)



# Application of Landsat MSS Data to the Study of Oceanographical Environment

Kiyoshi Tsuchiya (National Space Development Agency of Japan, 2-4-1,  
Hamamatsu-cho, Minato-ku, Tokyo, 105, Japan)

Hiroaki Ochiai (Toba National Merchant Marine College, Toba-city, Mie-  
ken, 517, Japan)

Kaname Takeda (Science and Technology Agency, 2-2-1, Kasumigaseki,  
Chiyoda-ku, Tokyo, 100, Japan)

## ABSTRACT

Based on Landsat MSS data of three years time lapse, the change of sea surface condition in Seto Inland Sea and coastal region is studied. It is found that red tide popularly called after its apparent color expanded. It is also found that red tide which used to concentrate in the bay or inland sea extends into an open sea. A small ocean vortex similar to mesoscale atmospheric vortex is revealed by the Band 4 image of Landsat MSS data.

A simple manual photographic method, "Equi Density Slicing Method" is applied to a single band image of MSS which indicates this method, is effective to detect sea surface pollution.

### 1. Introduction

Recently the coastal region is suffering from red tide popularly called after its apparent color. Red tide is caused by unusually abundant generation of plankton which is caused by nutrification of water. When red tide appears, fish is killed resulting in damage to coastal fishing industry.

Maruyasu and Ochiai (1976) pointed out that Bands 4 and 6 data of Landsat MSS are useful for the detection of red tide. Although visual analysis can distinguish polluted sea surface from clean area it is hard to distinguish red tide from other pollutants such as oil slick. An attempt is made to apply numerical analysis for the detection of red tide. In addition a simple photographical method which is useful for the study of sea surface pollution detection will be stated.



## 2. Occurrence of red tide in Seto Inland Sea

The name of red tide has become very popular recently, however this phenomenon is not recent finding. In Table 1 is shown annual frequency of red tide in Seto Inland Sea which the authors have collected from all available sources at present. Seto Inland Sea, located between western mainland of Japan and Shikoku has been noted for its beautiful scenery and clean water. This Inland Sea is also very important place for coastal fishing industry ( as to the location see Fig. 1).

Table 1 Annual occurrence of red tide in Seto Inland Sea

Year	Number of appearance case	Number of damaged case
1967	48	8
1968	61	12
1969	67	18
1970	79	35
1971	136	39
1972	164	23
1973	210	18
1974	298	17
1975	300	29
1976	326	18

It can be seen that the number of observation increased from 48 in 1967 to 326 in 1976 or 7 times as many as that in 1967. In spite of rapid increase of occurrence, the increase of damaged cases is not so large as the total occurrence case.

In order to see an effect of season on the occurrence, monthly frequency of recent two years is plotted and shown in Fig. 2, which clearly indicates seasonal effect on its occurrence. High frequency of occurrence is limited in the warm season between April and September.

## 3. Landsat MSS images showing the sea surface pollution

In Fig. 2 is shown Landsat MSS images of Seto Inland Sea taken



ORIGINAL PAGE IS  
OF POOR QUALITY

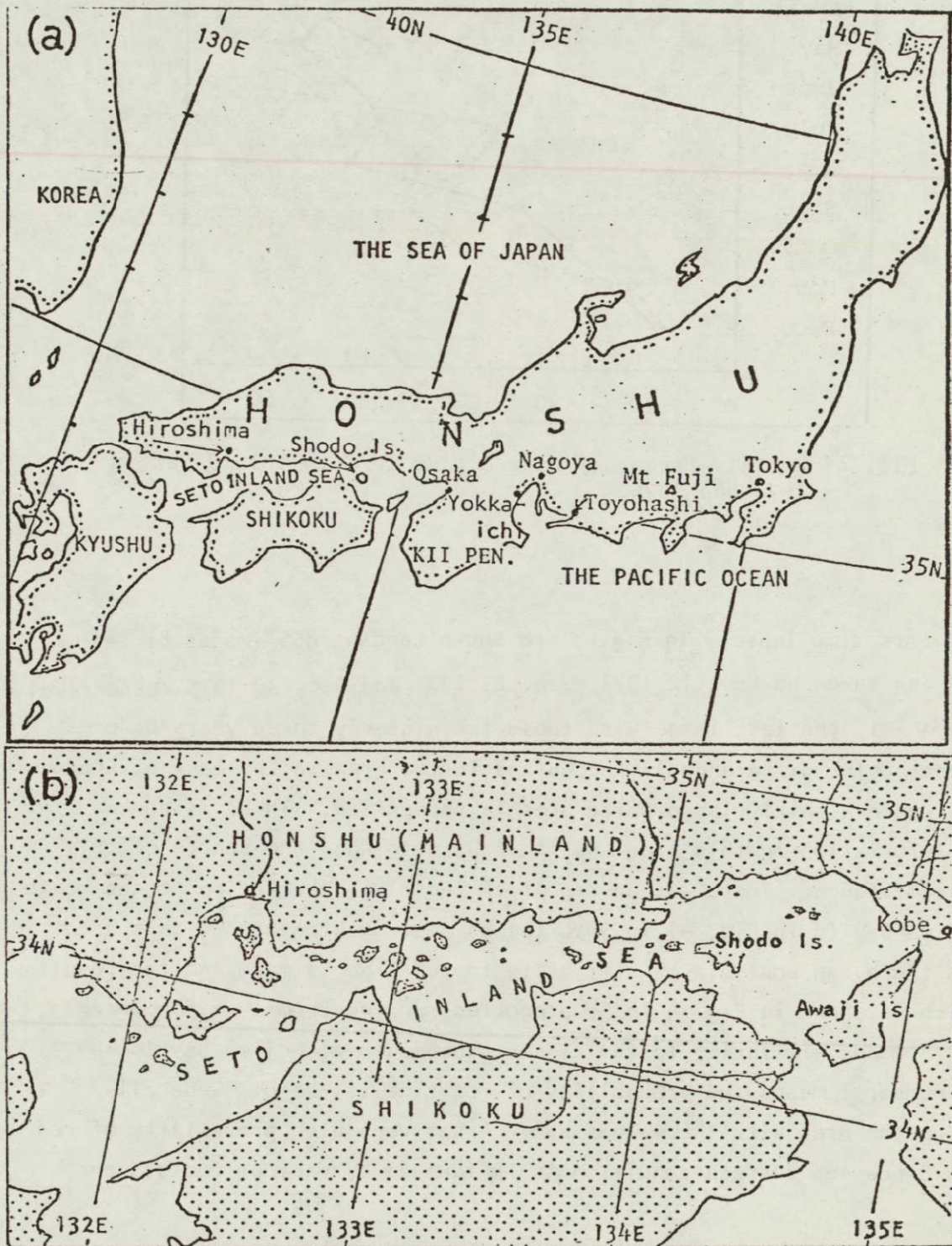


Fig. 1 (a) Map of Japan showing approximate position of cities.  
(b) Map of Seto Inland Sea.



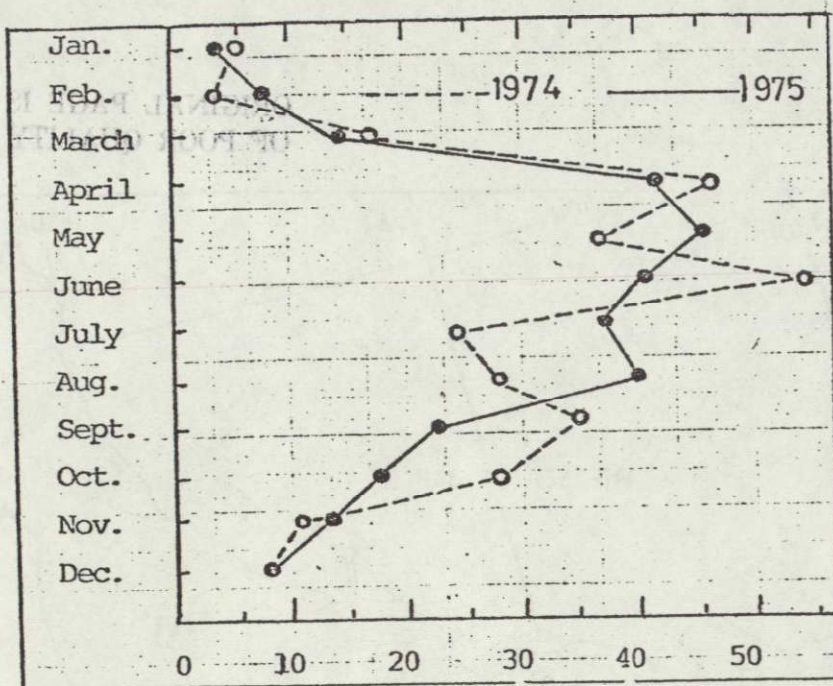


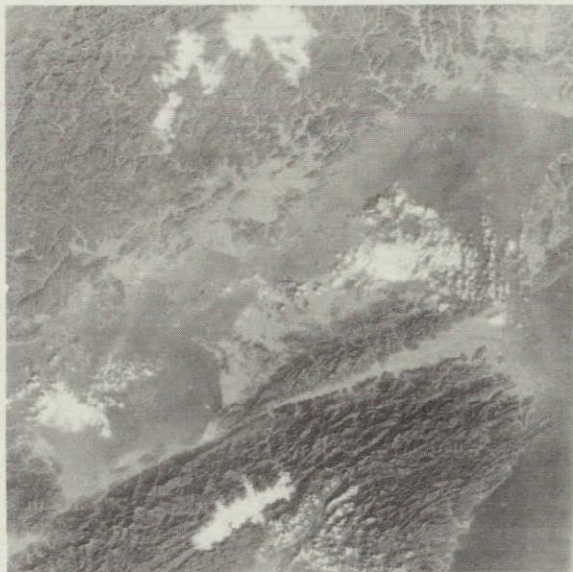
Fig. 2 Monthly frequency of red tide in Seto Inland Sea in 1974 and 1975.

three years time lapse. In Fig. 3 are shown Landsat MSS images of Seto Inland Sea taken on Nov. 12 1972, Jan. 23 1973 and Dec. 30 1975 respectively.

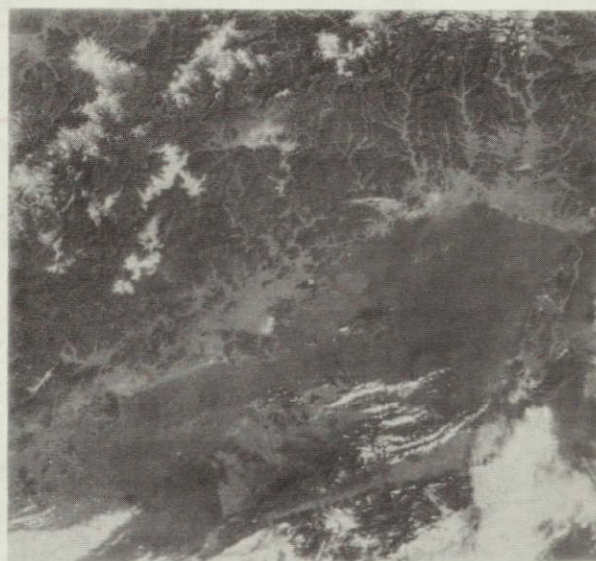
Comparing the last image with those taken nearly three years before, one spectacular difference is recognized in the area to the east of Shodo Island where a fairly large white area is recognized. There is no sea truth information in this area and it is hard to know the source of this high reflectance. There was an report of red tide observation at the mouth of Kojima Bay (A in Fig. 4) in Seto Inland Sea. Making use of this area as sea truth, an analysis of similarity to red tide is made and the result of which is shown in Fig. 4 in 5 categories ranging from 1 to 5. The number 5 means similarity to red tide at the mouth of Kojima Bay is 100 %, while number 1 means the probability of red tide is zero. Generally speaking the area with the values above 4 has very high probability of red tide. Since sea surface condition is influenced by various factors and



(a) NOV. 12 1972



(b) JAN. 23 1973



(c) DEC. 30 1975



ORIGINAL PAGE IS  
OF POOR QUALITY

Fig. 3 Landsat MSS images. (a) Nov. 12 1972, (b) Jan. 23 1973, (c) Dec. 30 1975. All the images and Band-4.

ORIGINAL PAGE IS  
OF POOR QUALITY



the speed of variation is rather fast, it does not mean that red tide exists always in the same place, however the result of the analysis indicates that the surface of Seto Inland Sea to the east of Shodo Island has changed during the past three years.

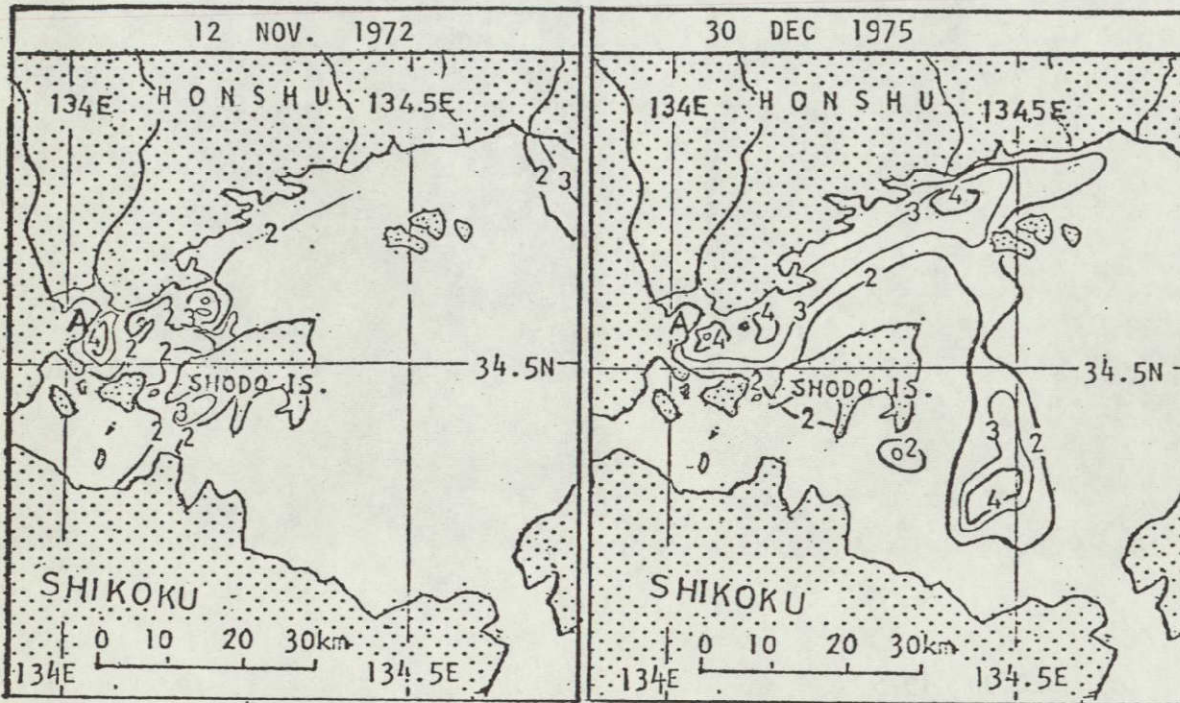


Fig. 4 Similarity to red tide in eastern Seto Inland Sea around Shodo Island. The degree of similarity is shown in 5 categories ranging from 1 to 5 with 5 the highest similarity.

### 3. A small ocean vortex as revealed by Landsat MSS image

In the image of September 11 1975 covering the coastal area of central Japan, a small ocean vortex is found off the tip of Kii Peninsula in the periphery of the Kuroshio, one of the largest warm ocean current in the world which is flowing along Japan Islands. The whole image of which is shown in Fig. 5. An attempt is made to interpret the phenomenon.

#### i) A synoptic oceanographical condition

Detailed analysis of all available data indicates the existence of a

ORIGINAL PAGE IS  
OF POOR QUALITY



ORIGINAL PAGE IS  
OF POOR QUALITY

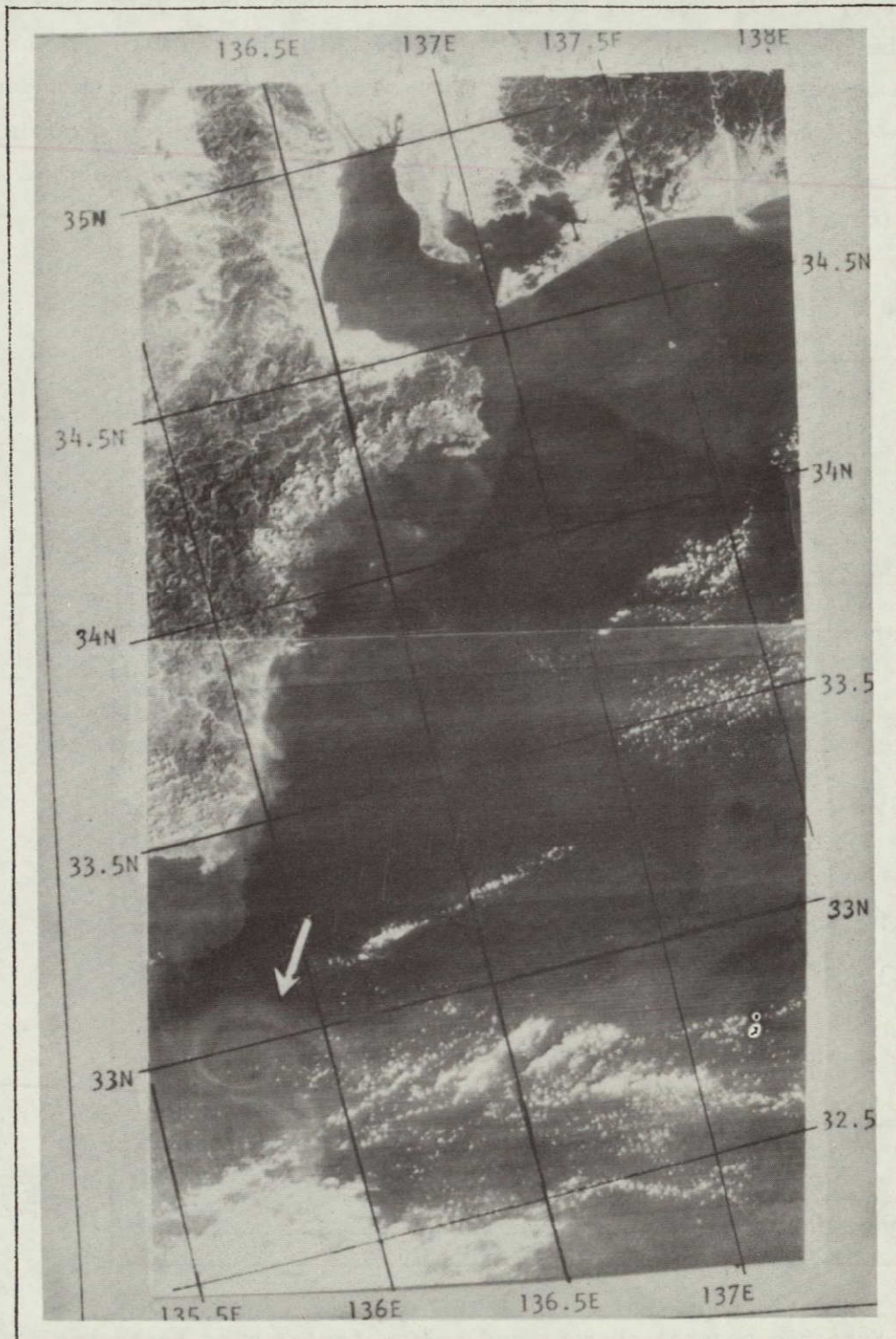


Fig.5 The image of Landsat-2 showing turbid coastal water and small ocean vortex. 0048 GMT September 11 1975



fairly large scale cold water mass to the south-eastern tip of Kii Peninsula where a large meandering of the Kuroshio was taking place as is indicated in Fig. 6. The large meandering of the Kuroshio was first found by Japanese Navy in 1934 during the maneuver. Through their large scale survey, they found a large cold water mass blocking the Kuroshio. The Kuroshio was detouring the cold water mass resulting in a large meandering. Later it was found that the cold water mass influences fishing grounds a great deal. Since then this cold water mass has been observed five times as is indicated in Table 2.

Table 2 Observation of cold water mass to the south-east of Kii Peninsula

Year of first obs.	Duration
1934	9.5 years
1953	2.5
1959	4
1969	1
1975	Still existing

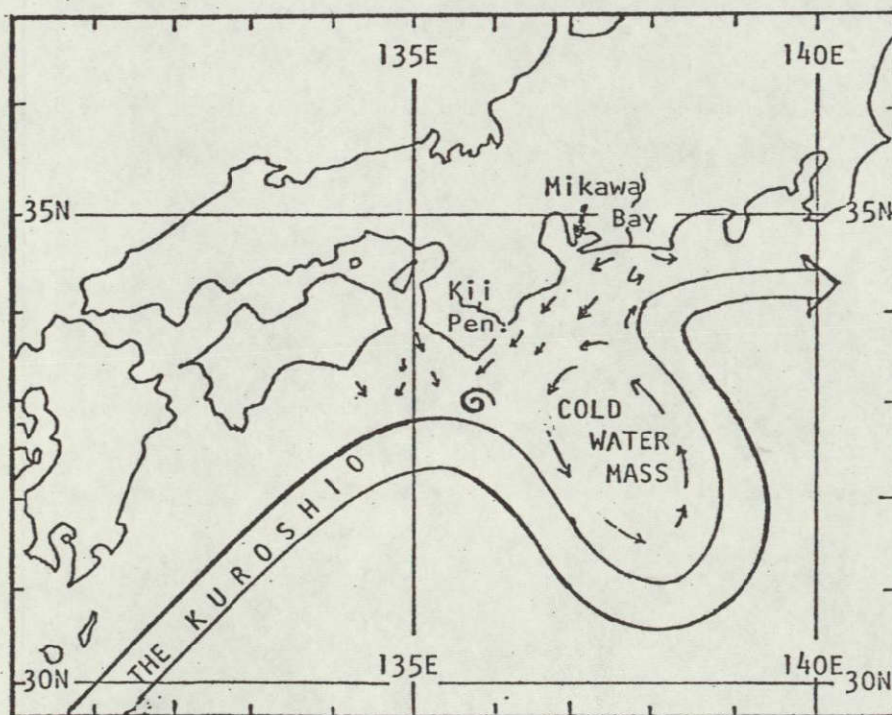


Fig. 6 Schematic representation of the synoptic condition of the Kuroshio, coastal current and cold water mass on September 11 1975.



The present cold water mass was first observed in August 1975. Its spatial dimension is oscillating. At its maximum size, the major and minor axes were as large as 280 and 220 kms respectively while at its minimum it shrunk to a circular shape of approximately 90 kms diameter. The cold water mass split into two parts in May 1977 and the meandering of the Kuroshio stopped for a while then again the meandering has started due to reformation of large cold water mass in the previous place.

At the time of observation by Landsat on September 11 1975 it is considered that the axis of the Kuroshio was slowly moving toward north or approaching Kii Peninsula. There were south-west and south-south-east ward coastal current to the east and west of Kii Peninsula respectively. It is considered that the present vortex was formed in the place where turbid coastal flows on both sides of the peninsula and the Kuroshio converge. The strong cyclonic shear may have triggered its formation and maintained it. It has a certain similarity to the plume like pattern of suspended sediments in Calorina's continental shelf revealed by Apollo pictures and studied by Mairs (1971). Both phenomena were formed on the left hand periphery of large warm ocean currents.

A similar analysis to the one made in the Seto Inland Sea is applied to the small ocean vortex using the red tide observed in Mikawa Bay (as to location see Fig. 6) the result of which is shown in Fig. 7 (a). It was found that the spiral part of the vortex has a high degree of similarity to the red tide of Mikawa Bay. Using CCT of MSS data the classification is also made with the red tide of Mikawa Bay, the water at the mouth of River Yahagi flowing into the western edge of Mikawa Bay and the water of the open sea as the sea truth. The result of analysis is shown in Fig. 7 (b).

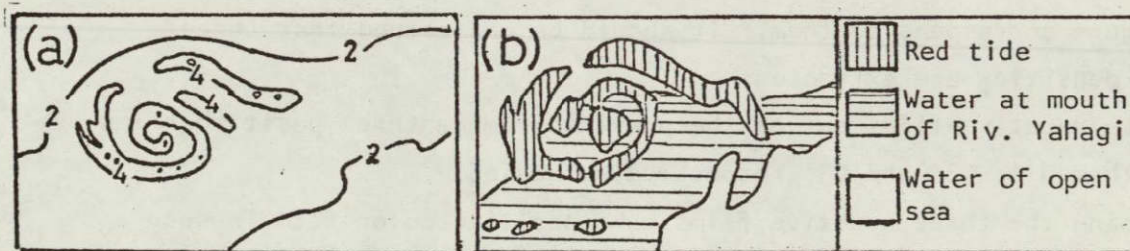


Fig. 7 (a) Similarity analysis applied to the small ocean vortex. Symbols are same as those in Fig. 4. (b) Classification of water involved in the small ocean vortex.



It is interesting to notice that the radiation characteristics of the water involved in the vortex have strong similarity to that of red tide in the spiral part and the rest of the part to the water in the mouth of the River Yahagi. There are not enough data to discuss the mechanism of the formation of the vortex in detail, however, the result of the present analysis indicates that the vortex is revealed by the water drawn into the vortex. If there is an upward motion in the spiral part like an atmospheric vortex, an upwelling nutritious water may have contributed to the generation of plankton with the result of contribution of the formation of the red tide in the spiral part.

#### 4. A simple method of photographic processing for equi-density extraction

Recently it has become easy to use false color representation method by specially made apparatus, however it is not all who can use it. The method described below may be of use who are trying to analyze a single MSS band image using only photographic processing facilities. Fig. 8 is a schematic representation of the method, the detail of which will be explained below.

i) From an original positive film make proper number of negative films giving different exposure time for simplicity make it four in this case. Assume the density of the films are:  $N_1 < N_2 < N_3 < N_4$ .

ii) Make four positive films from the four previously made negative films and name them as  $P_1$ ,  $P_2$ ,  $P_3$  and  $P_4$  respectively (same exposure time).

iii) Superpose the negative films on the positive films in such a manner:  $P_1 + N_2$ ,  $P_2 + N_3$  and  $P_3 + N_4$  then due to the difference in density of each film, equi-density part appears. In the figure, the white part corresponds to this equi-density region.

iv) Make positive films out of the superposed films. Name them as equi-density positive films;  $Q_1$ ,  $Q_2$  and  $Q_3$  respectively. Stippled areas in the figure correspond to them. It should be understood that three different densities are extracted.

v) Make negative films out of the previously made three positive films and call them  $Q_1'$ ,  $Q_2'$  and  $Q_3'$  respectively. Using

vi) Using the three negative films make positive color film in such a manner: first take  $Q_1'$  and expose it on a color paper through a blue filter, then take  $Q_2'$  and expose it through a green filter on the same paper and finally taking  $Q_3'$  expose it through a red filter on the same paper then



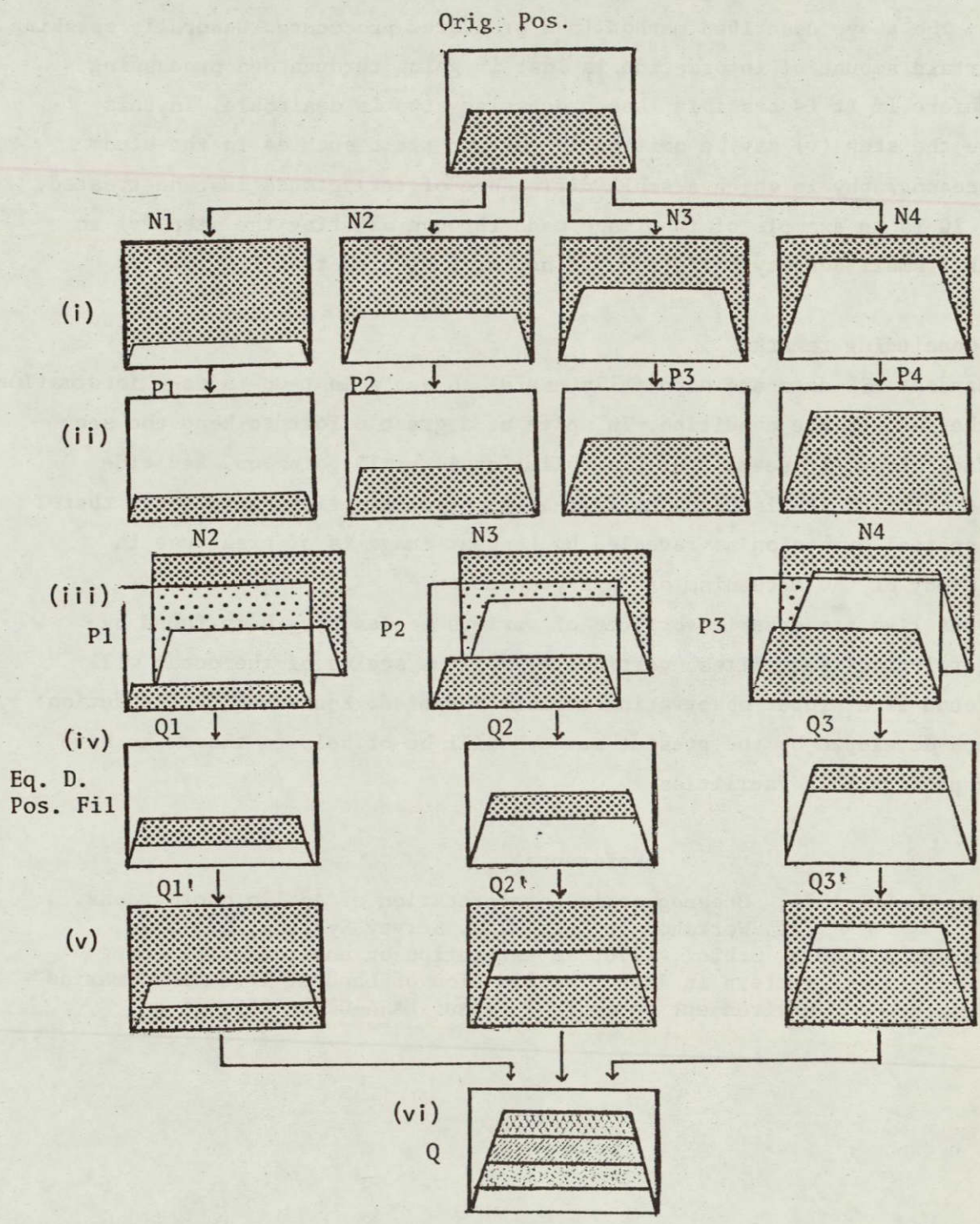


Fig. 8 Schematic representation of equi-density extraction method through manual photographic processing.



a color positive print is completed. It is not necessary to follow the combination of the color filters described above. The positive color print thus made is shown in Fig. 9 in which the turbid surface is well indicated.

The above described method is a standered procedure. Generally speaking a certain amount of information is lost in going through one processing therefore if it is possible less processing step is desirable. In this sense the step (v) may be omitted in certain field such as in the study of oceanography in which a small difference of reflectance must be treated. Fig. 10 is an example of the image made through omitting the step (v) in which a small density difference is better indicated than Fig. 9.

##### 5. Concluding remark

Landsat MSS data are especially useful to get a most-up-to date information on the sea surface condition. In spite of a great effort to keep the sea surface clean, it seems that the pollution is still going on. Red tide in Seto Inland Sea is becoming a great problem in a fishing industry there. The spatial extension as revealed by Landsat image is of great use in the study of the mechanism of this phenomenon.

Just like atmospheric vortices of various scales have been found by meteorological satellites, vortices of various scales of the ocean will be found if a proper observation tool is invented. Equi-density extraction method developed by the present authors will be of help to those who have only photographic facilities.

##### Reference

- Maris, R. L., 1971: Oceanograpjic interpretation of Apollo photographs. Int. Workshop on Earth Res. Survey Systems, 553-579.  
Maruyasu, T. and H. Ochiai, 1976: Investigation on environmental change pattern in Japan. Application of Landsat-II data to marine environment in central Japan. NASA-CR-146155, 16 pp.





space coverage of LANDSAT-2 as well as data on distribution of fishing grounds and catch statistics for the same area and season.

### 3. Accomplishment

#### 3.1. *Shirasu* fishery:

The neritic waters in the Enshu-Nada is known to be the biggest fishing ground of *shirasu*. The word *shirasu* designates a growth stage of Clupeoid fishes at the later period of postlarval stage with total length about 20 mm to 40 mm. The *shirasu* catch from the Enshu-Nada in the summer season is mostly composed of that of anchovy, *Engraulis japonica*. September 1975 (of which MSS-4 data were available) corresponds to one of the peaks of the *shirasu* catch, which was never taken so much in the same month of the previous year (Fig. 1). A heavy spawning of anchovy took place in this sea area in July 1975 (Fig. 2). Hatched larvae from this spawning were abundantly caught by *shirasu* fishery one or two months later (August to September).

The spawning and nursing areas of anchovy are usually located in the neritic waters lying coastwards the Kuroshio Current. They are easily fluctuant time and space in corresponding to the shift of the axis of the Kuroshio as well as fall and rise of neritic water. The center of spawning area of anchovy does not coincide with the major fishing ground of *shirasu* (Figs. 2 & 3). In some years there are heavy patches of *shirasu* in the neritic waters of the Enshu-Nada, while population densities of *shirasu* are very low in the other years.

In July 1975, the Kuroshio water made a pronounced intrusion into the coastal area of the Enshu-Nada because the meander of the Kuroshio caused a formation of a cold water mass offshore (Fig. 3). It is assumed that this sea condition resulted in a belt-like concentration of *shirasu* in parallel to the coastal line and thus in good catches of *shirasu* this season. This oceanographic condition was well shown in MSS-4 imagery for September 11, 1975 (Plate I).

There is a tendency that *shirasu* are frequently concentrated in a low saline area where receives a river efflux. The imagery of MSS-4 shows that there was an eastward dispersion of the effluent from the River Tenryu. This could be interpreted that an eastward current was predominant in the neritic waters then and there. As westward currents have been more frequent in usual years in this particular sea area, the existence of an eastward current was very peculiar. This might be caused by the above-mentioned oceanographical condition and resulted in a reverse pattern in shifting of *shirasu* fishing grounds in the Enshu-Nada.

Commercially exploitable stocks of *shirasu* are supplied from the spawning site towards Ise Bay-Mikawa Bay and both East and West grounds off the mouth of the River Tenryu (Figs. 2 & 3). The *shirasu* catches from either the East or the West fishing grounds off the mouth of the River Tenryu were poor in the very day of September 11, 1975. But, 3 days later (September 14), the good catch was first taken in the West ground (landed at Maisaka) and on the following day (September 15) in the East ground (landed at Fukude)(Fig. 4).

The *shirasu* catches show pronounced fluctuation day after day. Ups and downs of catch depend upon the fact whether the fishing ground is covered by neritic water with low transparency but with abundant *shirasu* population or it is predominated by offshore water with high transparency carrying poor fish population. The behavior of coastal water mass gives an important influence upon fishing condition. Therefore, MSS data which supply us with distribution pattern of water masses are very useful and important for forecasting *shirasu* fishing conditions.

### 3.2. Sardine fishery:

Sardine, *Sardinops melanosticta*, is caught in the neighborhood of Kanto District in the late July, while the major part of the stock has gone up to the coast of Hokkaido as the north-going feeding shoals (Fig. 5). The time-space changes in location of fishing grounds in this sea area are strongly influenced



by the coastward movement of the Kuroshio as well as southern intrusion of the Oyashio water.

Fig. 5 demonstrates locations of two sardine fishing grounds off Kanto District for a week from July 28 to August 2, 1976 (MSS imagery used for comparison was for July 29, 1976). One of fishing grounds was found shifted more northwardly than the previous week as fish schools were pressed towards the coast of the Kujukurihama Beach by coastward movement of the Kuroshio. Another fish school seems to be held back from north-going migration by a coastward intrusion of a warm water tongue towards the coast of the Kashima-Nada. MSS-5 imagery clearly showed locations of coastal water and Kuroshio water masses (Plates II & III).

If imageries are available successively for the major fishing season (December to May), they are most important information for foretelling distribution of fishing grounds.

### 3.3. Translocation and recruitment of fish eggs and larvae:

General speaking, eggs and larvae of many species of neritic and offshore migratory fish are translocated by the Kuroshio to the northeastern direction while they are growing. They are sometimes absorbed either in the marginal portion of the Kuroshio or in the neritic water mass in corresponding to fall and rise of these two different water masses. MSS data such as eddy-like structure in the Izu Island area (Plate III) and vortex pattern in the Kumano-Nada (Cf. Final Report by Dr. D. SHOJI) give us a clue for elucidation of mechanisms of transportation and distribution of fish eggs and larvae.

Major spawning grounds for sardine and common mackerel, *Scomber japonicus*, are located in the waters around the Izu Islands. If we can know distribution and movement of water masses in an extensive geographical coverage, we can make a rough estimate on distributional and drift areas of fish eggs and larvae. Such an information is one of the most important basis for forecasting the recruitment and consequently for managing the fisheries resources.

### 3.4. Red tide:

Fig. 6 shows distribution of water color of Atsumi Bay in September 1975 on the basis of the red tide investigation conducted by Aichi Prefectural Fisheries Experimental Station. The report from the same station said that this red tide was ceased by September 10. However, according to MSS-4 imagery for September 11,\* it made clear that the red tide was not ceased but only shifted to offshore from the inner portion of the Bay that had covered by Aichi PFES investigation. In connection with this, mass mortality of fish was reported in the area of "pale blue" in Fig. 6. (\* : Plate III)

For identification of red tide, the reader may refer the report by Dr. H. OCHIAI (this final report). If MSS data are available successively for a short period, they are very helpful for elucidating the mechanism of red tide and for forecasting the occurrence of red tide that will give a destructive effect on fisheries.

## 4. Significant Results

MSS data provide us with extensive and simultaneous information about marine environmental conditions, such as the shift of the Kuroshio, fall and rise of coastal water mass, distribution of water masses, locations of vortex and current rips, exchanges of water between embayment and open ocean, effluent of rivers, fertility of plankton, red tide, pollution etc. These information are all useful for fisheries as will be briefed below:

### 4.1. Forecast of fishing conditions:

Distribution and abundance of neritic and offshore migratory fish including sardine, anchovy, mackerels, saury, skipjack, tunas and squids are closely related to biotic and abiotic conditions of environment. It is axiomatic that environmental information obtained by LANDSAT improved accuracy of forecasting fishing conditions of these fishes.

#### 4.2. Management of fisheries resources:

From the change pattern of environment, distribution and drift patterns of fish eggs and larvae will be estimated. This gives an estimate of abundance of recruitment which is the basis of management of fisheries resources.

#### 4.3. Identification of marine pollution and eutrophication:

Data concerning exchanges of water between neritic area or embayment and oceanic area are helpful in judgement of purifying capability of sea water.

Extensive information of occurrences of red tide and oil pollution as well as other environmental worsening help to take measure against fisheries destruction.

#### 5. Problems

(1) Utilizable data were few as many scenes available were very cloudy.

(2) Data in short-term intervals, such as daily or weekly, were not available for judgement of oceanographical changes in relation to fisheries.

(3) If detection and measurement of seasonal changes of such biotic parameters as fertility of plankton and chlorophyll are successfully made in future, these information will be of great use for identifying temporal and spacial scales and changes of eutrophication and pollution as well as for management of fishing resources and fishing activities.

(4) Data of sea surface water temperature is indispensable.



## 6. Conclusions

The extensive and simultaneous coverages of MSS data obtained by LANDSAT are never incomparable with hydrographic observations made by sea-going vessels. MSS data help to make great progress in researches and methodologies concerning forecast of fishing condition, management of fisheries and identification of pollution by collating with information obtained by research ship, fishing fleet and aircraft.

To make MSS data utilizable for fisheries, development of the technique of reading environmental change pattern must be preceded. It is desirable that observation data with intervals not longer than one week (if possible, daily) could be obtainable at real time in future.

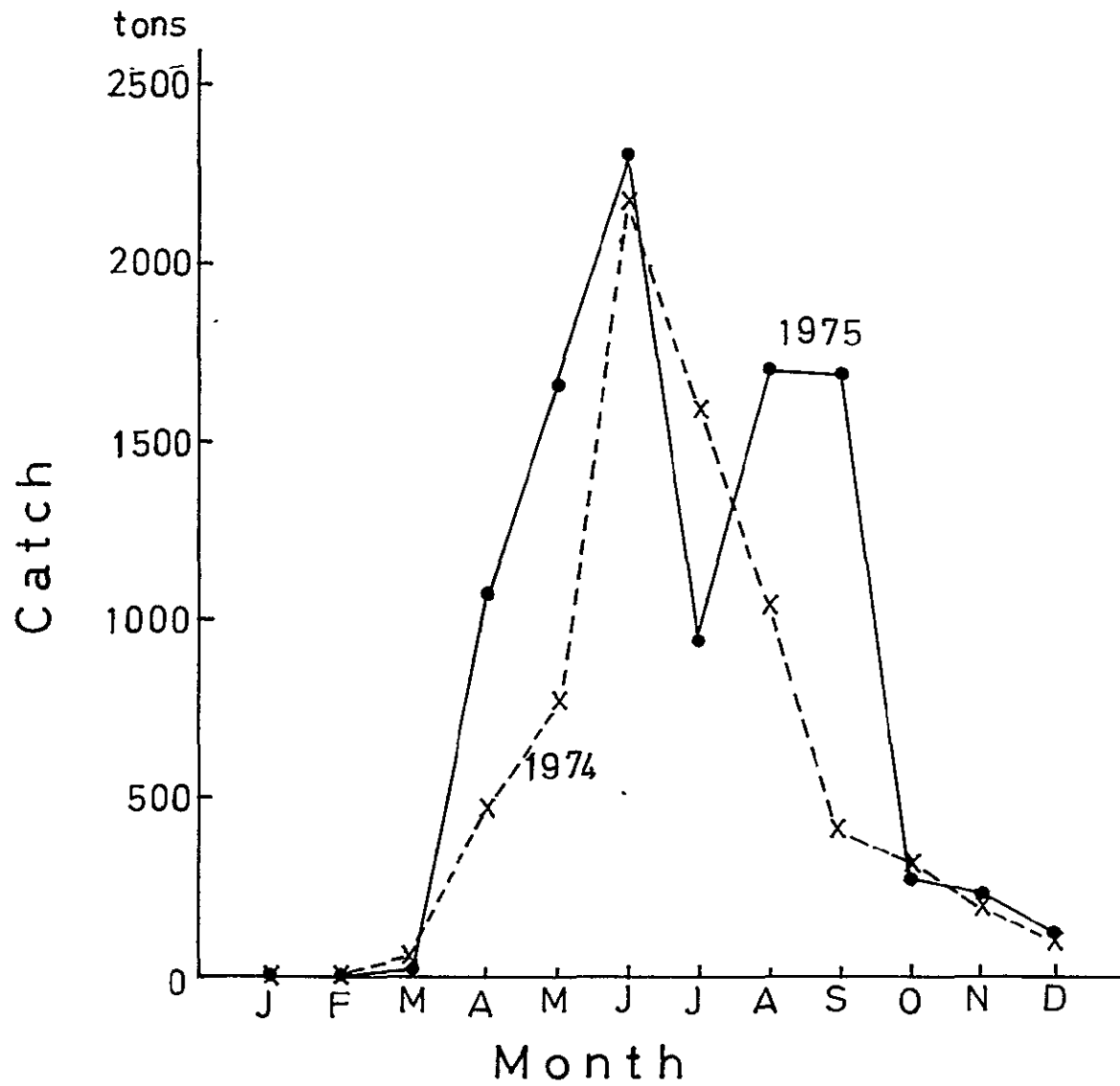


Figure 1. Monthly *shirasu* catch from the Enshu-Nada and neighborhood (statistics of Shizuoka Prefecture) 1974 and 1975

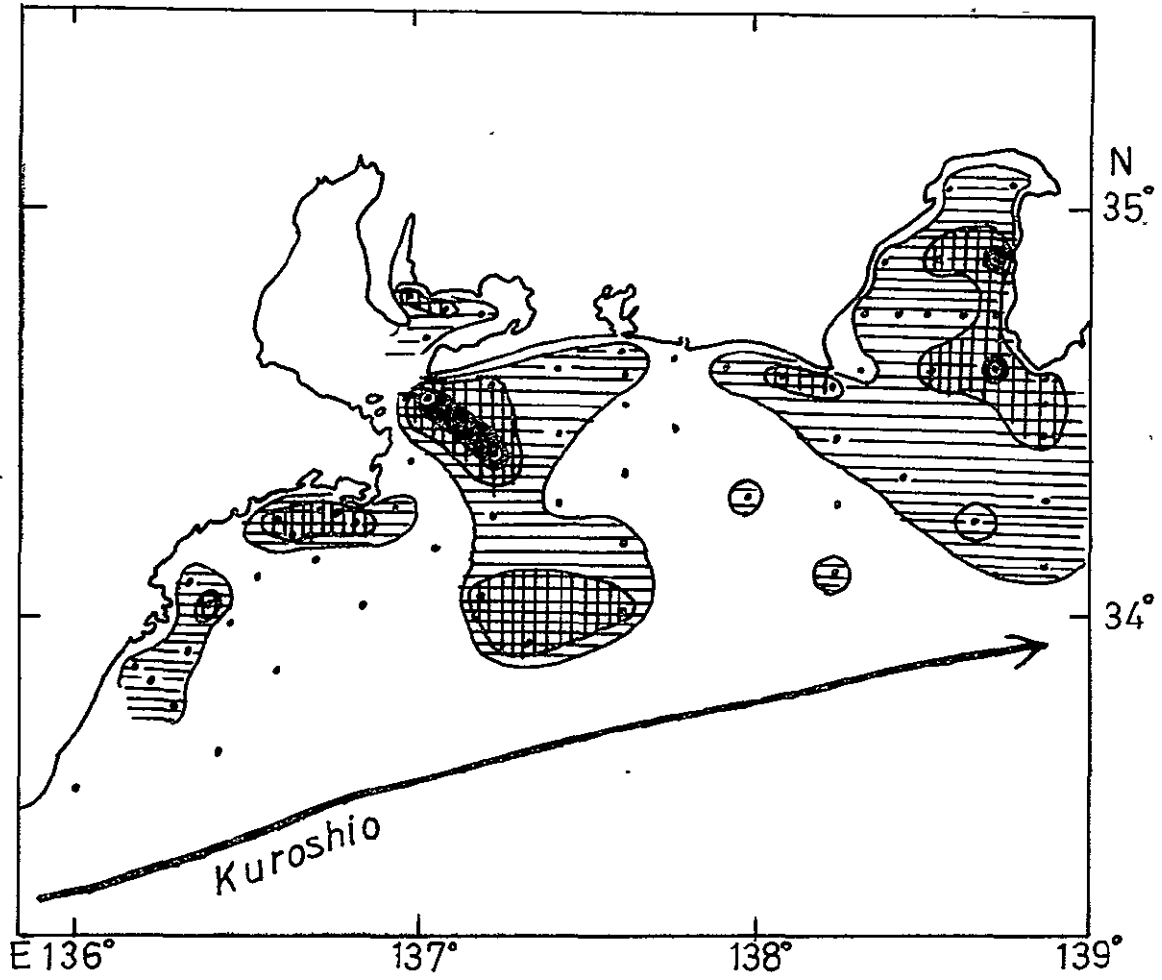


Figure 2. Density distribution of anchovy egg in July 1975  
 (After data of Shizuoka, Aichi and Mie Prefectural  
 Fisheries Experimental Stations)



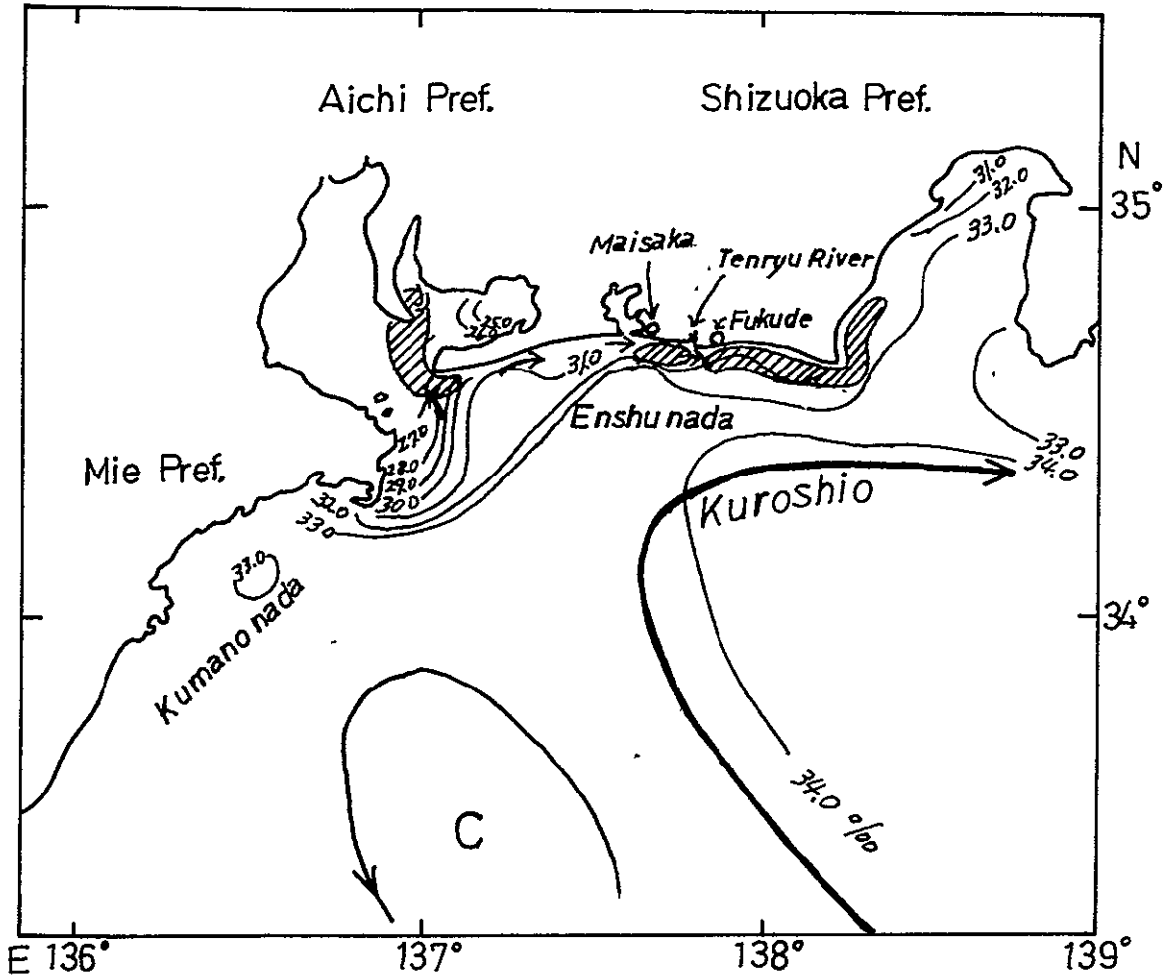


Figure 3. Locations of *shirasu* fishing grounds (hatched areas) and surface isohalines in September 1975.

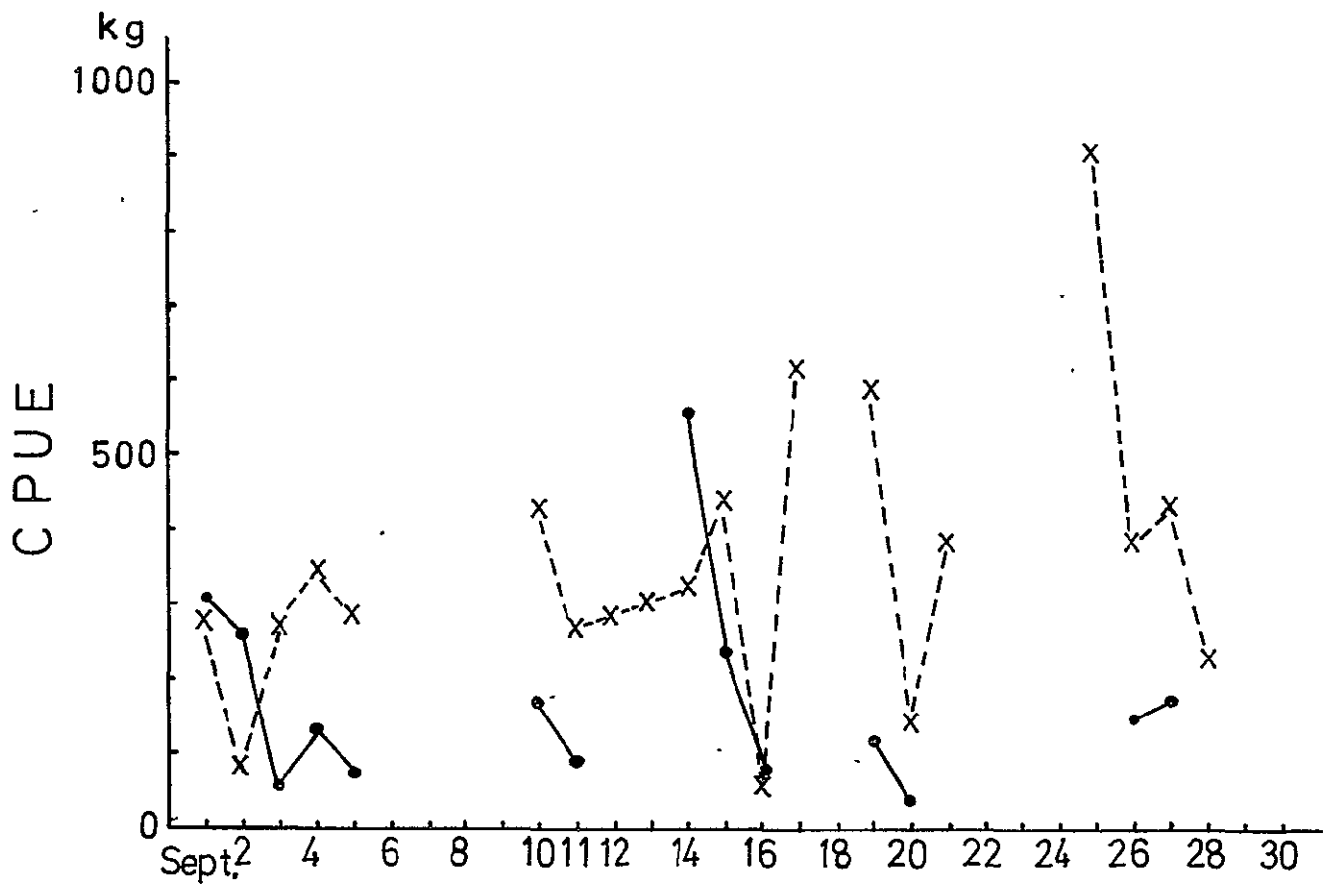


Figure 4. Daily landing of *shirasu* at Maisaka (solid line) and Fukude (broken line) in Shizuoka Prefecture, September 1975.

CPUE: Catch per day per boat.

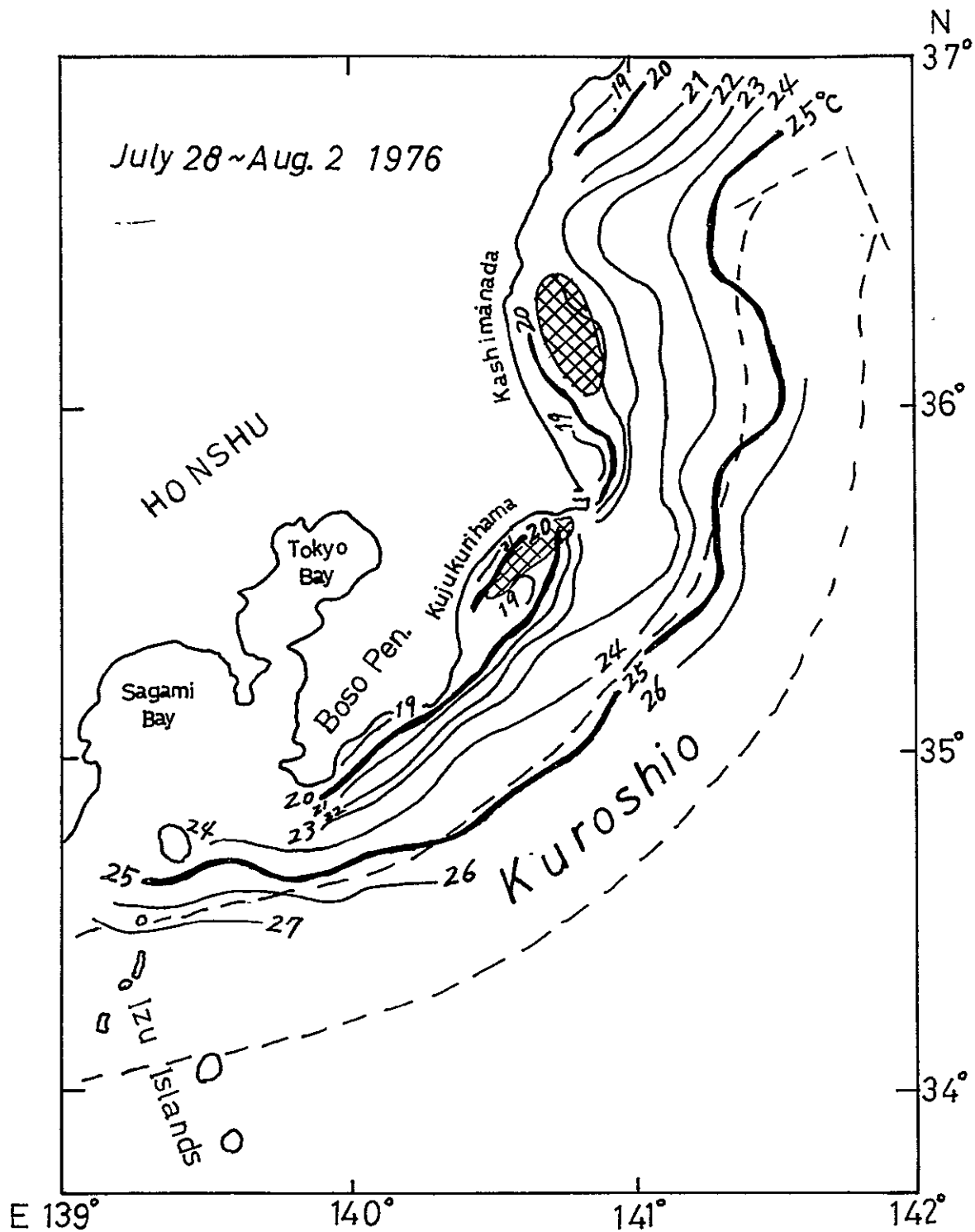


Figure 5. Locations of sardine fishing area (hatched areas) and surface isotherms during July 28 - August 2, 1976 (After data of Chiba Prefectural Fisheries Experimental Station)



ORIGINAL PAGE IS  
OF POOR QUALITY

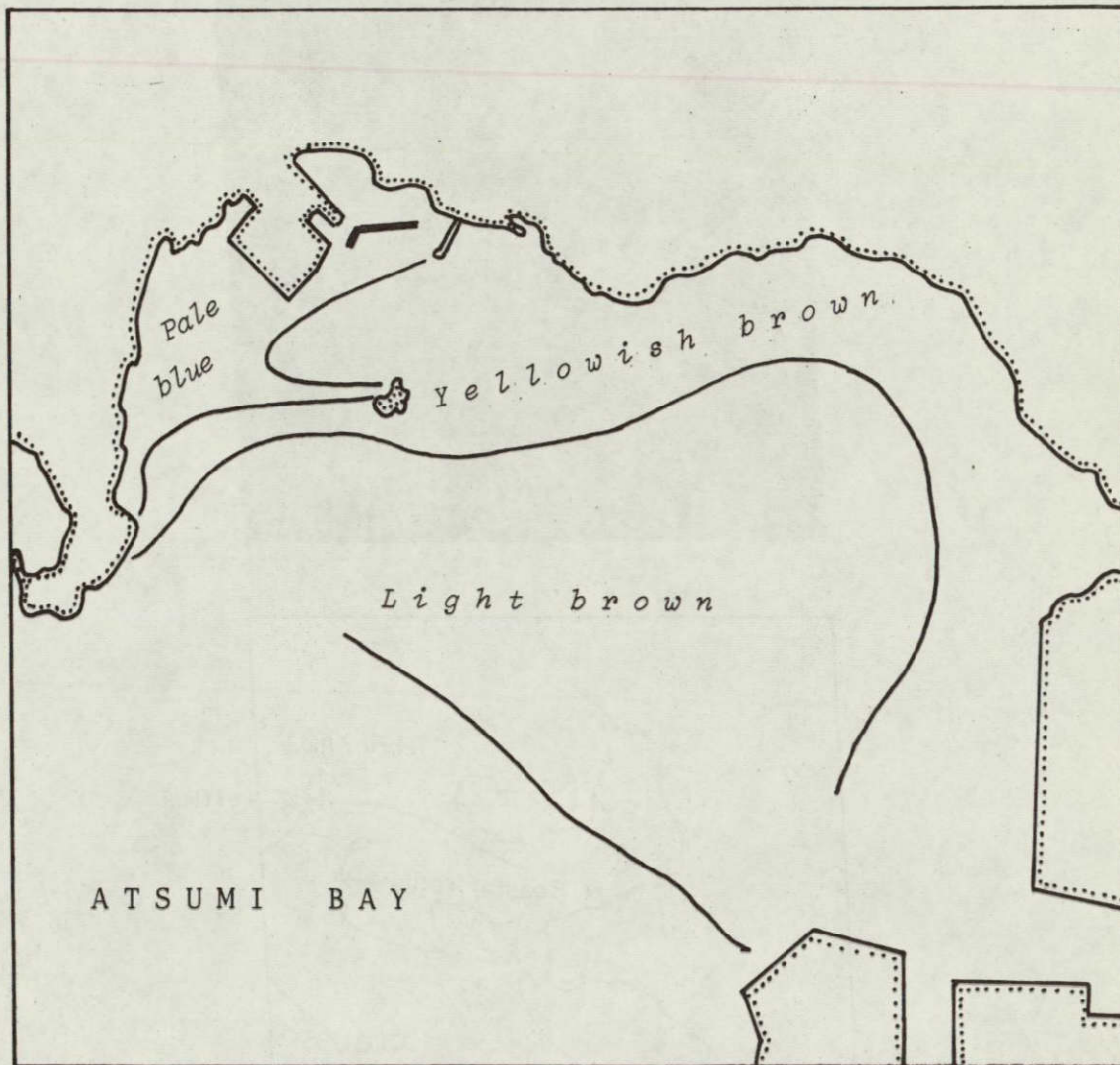


Figure 6. Water color distribution in the innermost part of Atsumi Bay in September 9 , 1976  
(After Aichi Prefectural Fisheries Experimental Station)

ORIGINAL PAGE IS  
OF POOR QUALITY

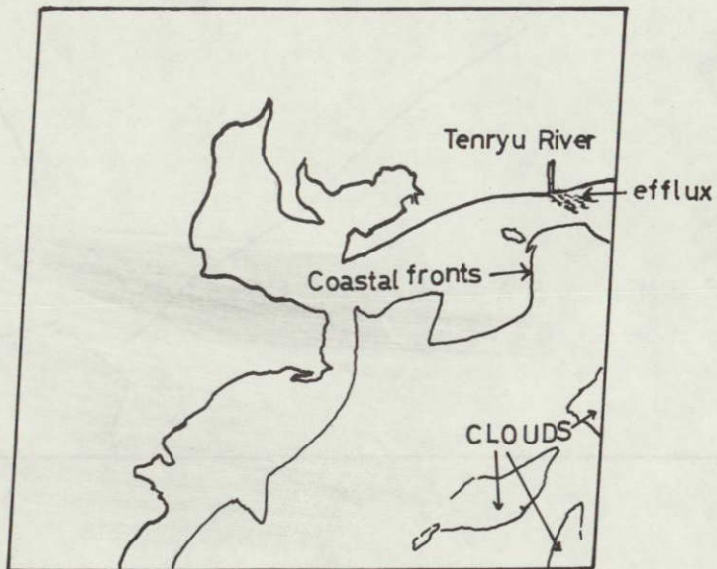


PLATE I. MSS-4 imagery of Ise Bay - Enshu-nada



ORIGINAL PAGE IS  
OF POOR QUALITY

ORIGINAL PAGE IS  
OF POOR QUALITY

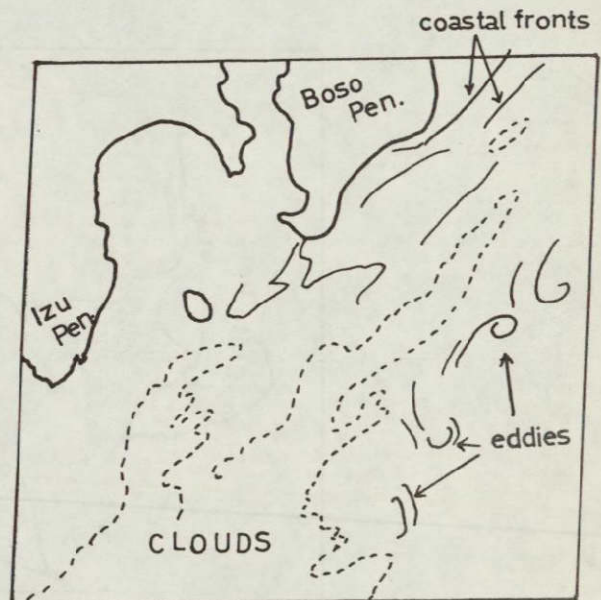
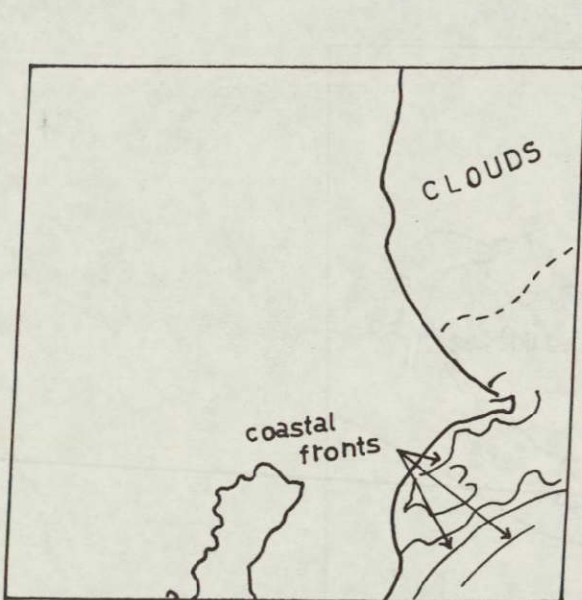
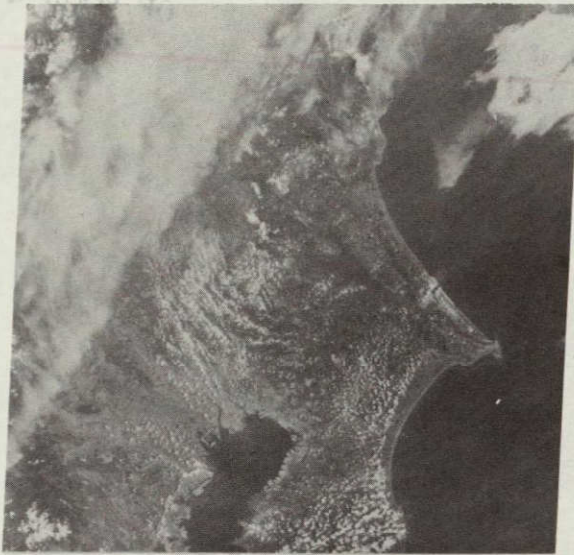


PLATE II. MSS-5 imageries of Kanto District (left) and Izu Islands (right)



ORIGINAL PAGE IS  
OF POOR QUALITY

ORIGINAL PAGE IS  
OF POOR QUALITY

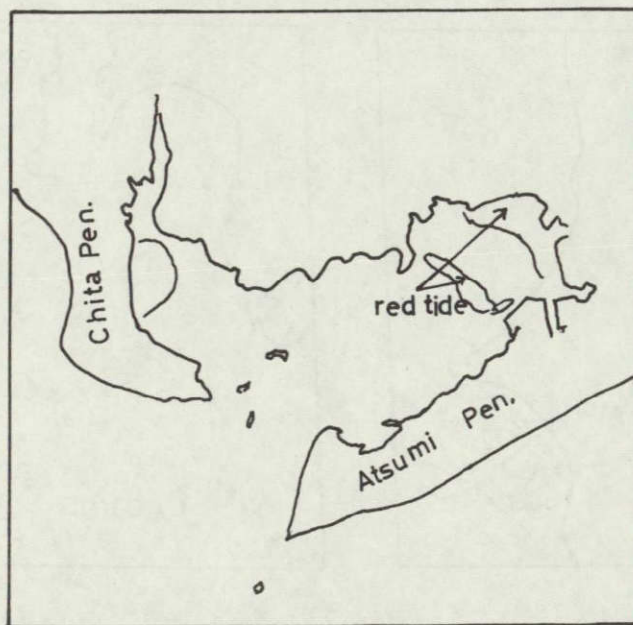
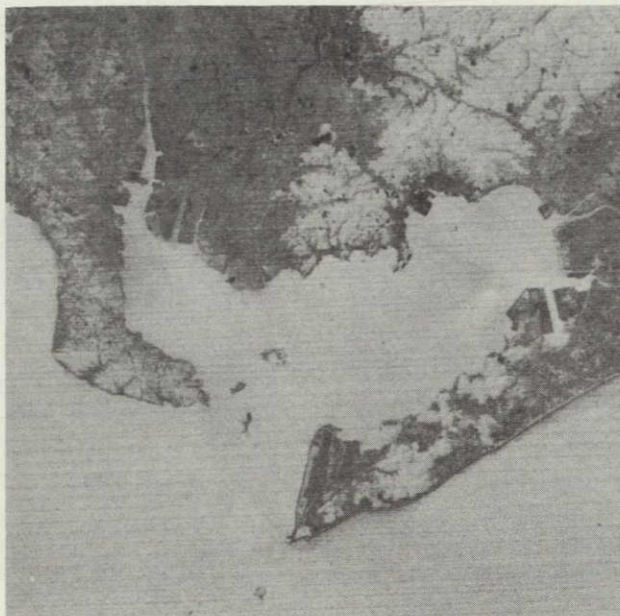


PLATE III. Enlarged part of Plate I showing red-tide area in the innermost part of Atsumi Bay